

Impact of Electroweak Corrections on Neutral Higgs Boson Decays in Extended Higgs Sectors

Marcel Krause^{1*}, Margarete Mühlleitner^{1†}

¹*Institute for Theoretical Physics, Karlsruhe Institute of Technology,
Wolfgang-Gaede-Str. 1, 76131 Karlsruhe, Germany.*

Abstract

Precision predictions play an important role in the search for indirect New Physics effects in the Higgs sector itself. For the electroweak (EW) corrections of the Higgs bosons in extended Higgs sectors several renormalization schemes have been worked out that provide gauge-parameter-independent relations between the input parameters and the computed observables. Our recently published program codes `2HDECAY` and `ewN2HDECAY` allow for the computation of the EW corrections to the Higgs decay widths and branching ratios of the Two-Higgs-Doublet Model (2HDM) and the Next-to-Minimal-2HDM (N2HDM) for different renormalization schemes of the scalar mixing angles. In this paper, we present a comprehensive and complete overview over the relative size of the EW corrections to the branching ratios of the 2HDM and N2HDM neutral Higgs bosons for different applied renormalization schemes. We quantify the size of the EW corrections of Standard Model (SM)- and non-SM-like Higgs bosons and moreover also identify renormalization schemes that are well-behaved and do not induce unnaturally large corrections. We furthermore pin down decays and parameter regions that feature large EW corrections and need further treatment in order to improve the predictions. Our study sets the scene for future work in the computation of higher-order corrections to the decays of non-minimal Higgs sectors.

*E-mail: marcel.krause@kit.edu

†E-mail: margarete.muehlleitner@kit.edu

1 Introduction

While the discovery of the Higgs boson in 2012 by the LHC experiments ATLAS [1] and CMS [2] marked a milestone for particle physics, there are still many questions left open. The Higgs boson turned out to behave very Standard-Model-like. The Standard Model (SM), however, cannot solve open problems like *e.g.* the generation of the observed baryon-antibaryon asymmetry or provide an appropriate Dark Matter candidate. This calls for New Physics extensions that usually come along with an extended Higgs sector. So far no direct sign of any New Physics manifestation has been discovered by experiments, so that the Higgs sector itself has moved into the focus of our search for New Physics. There, it might reveal itself indirectly in deviations of the Higgs properties from the SM expectations. Since experiments have pushed the exclusion limits on new particles to high mass scales, these effects are expected to be small, unless triggered by new light particles in the spectrum. These could be *e.g.* the additional light Higgs bosons of extended Higgs sectors. Still, precision is required in order to detect the indirect signs of New Physics, so that additionally the nature of the underlying model can be revealed. From the theory side this requires the inclusion of higher-order corrections to the Higgs boson observables.

Higgs sector extensions have to ensure compatibility with experimental and theoretical constraints. The extensions may be based on a weakly or strongly interacting model. Among the weakly interacting models, both supersymmetric (SUSY) and non-SUSY Higgs sectors are possible. While SUSY extensions are very well-motivated by their symmetry, non-SUSY models allow for more freedom, in particular in the Higgs boson self-couplings. In contrast to SUSY, where these coupling constants are given in terms of the gauge boson couplings, they can be sizeable in non-SUSY models, modulo the constraints stemming from the requirement of perturbativity. This may induce interesting effects not only in Higgs pair production but also in the electroweak corrections to Higgs boson observables.

In this paper, we investigate the impact of electroweak corrections on the neutral Higgs boson decays of two non-SUSY extension of the Higgs sector. These are the Two-Higgs-Doublet Model (2HDM) [3,4] and the Next-to-Minimal Two-Higgs-Doublet-Model (N2HDM) [5,6]. Both models feature an extended Higgs sector with at least three neutral Higgs bosons, inducing interesting phenomenology stemming from Higgs self-interactions. Both models allow for a strong first order phase transition and can in principle provide a Dark Matter candidate depending on the applied symmetries. While the 2HDM is the simplest Higgs doublet extension of the SM, the more complex structure of the N2HDM Higgs sector allows for more freedom in the parameter space, thus inducing additional interesting effects in the phenomenology. In both models, light Higgs bosons are still allowed in the spectrum and have an impact not only on Higgs observables but moreover, as we will show, on the size of the electroweak corrections.

The aim of this paper is to demonstrate that electroweak (EW) corrections can be important although the Higgs measurements push New Physics extensions to be very close to the SM.¹

¹Other recent works including EW corrections to non-SM Higgs decays are [7] where EW corrections to Higgs-to-Higgs decays in a singlet extension of the SM have been computed, or [8] which provides a generic calculation of the two-body partial decay widths at full one-loop level in the $\overline{\text{DR}}$ renormalization scheme. Next-to-leading order corrections to Higgs boson decays in models with non-minimal sectors have been computed in [9,10]. For the Next-to-Minimal Supersymmetric extension of the SM (NMSSM), the full one-loop renormalization and one-loop corrected two-body Higgs decay widths in the on-shell (OS) renormalization scheme have been given in [11,12]. Recent calculations of the EW corrections to the NMSSM Higgs boson decays in the CP-conserving and/or CP-violating NMSSM can be found in [13–19]. They can be computed with the public code `NMSSMCALCEW` [17] (based on the extension of `NMSSMCALC` [20]).

We furthermore aim to show the impact of different renormalization schemes. In previous papers it has been shown that care has to be taken to choose a renormalization scheme for the Higgs mixing angles that is not gauge-dependent [21–29].² Additionally, it should not lead to unnaturally large loop corrections [12, 22, 26, 32, 33]. We want to compare the results for different renormalization schemes that take into account these considerations. Lastly, we want to identify those decay channels where the relative corrections do not blow up due to an unsuitable renormalization scheme but because they have small leading-order (LO) branching ratios or because the corrections are parametrically enhanced. This serves as a starting point for future work on the reduction of these corrections by going beyond next-to-leading order (NLO) and applying resummation techniques.

The results for the loop corrected branching ratios (BRs) that we will show in this paper have been generated with the codes `2HDECAY` [34] and `N2HDECAY` [35] that are based on extensions of the `FORTRAN` codes `HDECAY` [36, 37] and `N2HDECAY` [6], respectively, to include also electroweak corrections.³ Based on `HDECAY`, the decay widths and BRs already include the state-of-the-art higher-order QCD corrections, so that the presented numbers are the most precise predictions that can be provided at present.

In Section 2 we introduce the 2HDM and N2HDM and set our notation. In Section 3, we briefly present the applied renormalization schemes. The results for the EW- and QCD-corrected BRs are given in Section 4. For the 2HDM they are presented and discussed in Subsections 4.1–4.4, and for the N2HDM in Subsections 4.5–4.8. For both models we investigate the SM-like Higgs boson decays, the non-SM-like CP-even Higgs decays and the pseudoscalar decays. We consider different mass hierarchies, where either the lighter or the heavier CP-even Higgs state represents the SM-like Higgs boson. In Section 5, we conclude with a short summary.

2 Model Introduction

In the following we introduce the two models that we consider in this work, namely the 2HDM and the N2HDM, and we set our notation.

2.1 Introduction of the 2HDM

In terms of the two complex $SU(2)_L$ Higgs doublets Φ_1 and Φ_2 with hypercharge $Y = +1$,

$$\Phi_1 = \begin{pmatrix} \phi_1^+ \\ \phi_1^0 \end{pmatrix} \quad \text{and} \quad \Phi_2 = \begin{pmatrix} \phi_2^+ \\ \phi_2^0 \end{pmatrix}, \quad (2.1)$$

the tree-level potential of a general CP-conserving 2HDM [3, 4] reads

$$\begin{aligned} V_{2\text{HDM}} = & m_{11}^2 |\Phi_1|^2 + m_{22}^2 |\Phi_2|^2 - m_{12}^2 \left(\Phi_1^\dagger \Phi_2 + h.c. \right) + \frac{\lambda_1}{2} \left(\Phi_1^\dagger \Phi_1 \right)^2 + \frac{\lambda_2}{2} \left(\Phi_2^\dagger \Phi_2 \right)^2 \\ & + \lambda_3 \left(\Phi_1^\dagger \Phi_1 \right) \left(\Phi_2^\dagger \Phi_2 \right) + \lambda_4 \left(\Phi_1^\dagger \Phi_2 \right) \left(\Phi_2^\dagger \Phi_1 \right) + \frac{\lambda_5}{2} \left[\left(\Phi_1^\dagger \Phi_2 \right)^2 + h.c. \right]. \end{aligned} \quad (2.2)$$

It is parametrized by three real mass parameters m_{11} , m_{22} and m_{12} and five dimensionless real couplings $\lambda_{1\dots 5}$. The term proportional m_{12}^2 softly breaks the global discrete \mathbb{Z}_2 symmetry

²The gauge-independent renormalization of multi-Higgs models has been discussed in [30, 31].

³A public code for the computation of loop-corrected decay widths in extended Higgs sectors, `H-COUP`, has also been provided in [38, 39]. The Higgs decay into four fermions has been implemented in the Monte Carlo generator `PROPHECY4F` 3.0 for the singlet extended SM and the 2HDM including the full QCD and EW NLO corrections [40].

under which the doublets transform as $\Phi_1 \rightarrow \Phi_1$ and $\Phi_2 \rightarrow -\Phi_2$. After electroweak symmetry breaking (EWSB), the neutral components of the Higgs doublets acquire vacuum expectation values (VEVs) v_1 and v_2 which in the CP-conserving case are real. The Higgs doublets can be expanded around their VEVs in terms of the charged complex fields ω_i^\pm and the real neutral CP-even and CP-odd fields ρ_i and η_i ($i = 1, 2$), respectively, as

$$\Phi_1 = \begin{pmatrix} \omega_1^+ \\ \frac{v_1 + \rho_1 + i\eta_1}{\sqrt{2}} \end{pmatrix} \quad \text{and} \quad \Phi_2 = \begin{pmatrix} \omega_2^+ \\ \frac{v_2 + \rho_2 + i\eta_2}{\sqrt{2}} \end{pmatrix} \quad (2.3)$$

where

$$v^2 = v_1^2 + v_2^2 \approx (246.22 \text{ GeV})^2 \quad (2.4)$$

is the squared SM VEV obtained from the Fermi constant G_F , $v = 1/\sqrt{\sqrt{2}G_F}$. We introduce the mixing angle β through

$$\tan \beta = \frac{v_2}{v_1} \quad (2.5)$$

so that

$$v_1 = v \cos \beta \quad \text{and} \quad v_2 = v \sin \beta . \quad (2.6)$$

Inserting Eq. (2.3) in the scalar potential in Eq. (2.2) yields

$$V_{2\text{HDM}} = \frac{1}{2} (\rho_1 \quad \rho_2) M_\rho^2 \begin{pmatrix} \rho_1 \\ \rho_2 \end{pmatrix} + \frac{1}{2} (\eta_1 \quad \eta_2) M_\eta^2 \begin{pmatrix} \eta_1 \\ \eta_2 \end{pmatrix} + \frac{1}{2} (\omega_1^\pm \quad \omega_2^\pm) M_\omega^2 \begin{pmatrix} \omega_1^\pm \\ \omega_2^\pm \end{pmatrix} \\ + T_1 \rho_1 + T_2 \rho_2 + \dots \quad (2.7)$$

where T_1 and T_2 denote the tadpole terms and M_ω^2 , M_ρ^2 and M_η^2 the mass matrices of the charged, neutral CP-even and CP-odd fields, respectively. Requiring the VEVs of Eq. (2.3) to represent the minimum of the potential, *i.e.*

$$\left. \frac{\partial V_{2\text{HDM}}}{\partial \Phi_i} \right|_{\langle \Phi_j \rangle} = 0 , \quad (2.8)$$

yields the tree-level tadpole conditions

$$\frac{T_1}{v_1} \equiv m_{11}^2 - m_{12}^2 \frac{v_2}{v_1} + \frac{\lambda_1}{2} v_1^2 + \frac{\lambda_{345}}{2} v_2^2 = 0 \quad (2.9)$$

$$\frac{T_2}{v_2} \equiv m_{22}^2 - m_{12}^2 \frac{v_1}{v_2} + \frac{\lambda_2}{2} v_2^2 + \frac{\lambda_{345}}{2} v_1^2 = 0 , \quad (2.10)$$

where we used the short-hand notation

$$\lambda_{345} \equiv \lambda_3 + \lambda_4 + \lambda_5 . \quad (2.11)$$

The tadpole equations can be solved for m_{11}^2 and m_{22}^2 in order to replace these two parameters by the tadpole parameters T_1 and T_2 . The mass matrices are given by

$$M_\rho^2 \equiv \begin{pmatrix} m_{12}^2 \frac{v_2}{v_1} + \lambda_1 v_1^2 & -m_{12}^2 + \lambda_{345} v_1 v_2 \\ -m_{12}^2 + \lambda_{345} v_1 v_2 & m_{12}^2 \frac{v_1}{v_2} + \lambda_2 v_2^2 \end{pmatrix} + \begin{pmatrix} \frac{T_1}{v_1} & 0 \\ 0 & \frac{T_2}{v_2} \end{pmatrix} \quad (2.12)$$

$$M_\eta^2 \equiv \begin{pmatrix} m_{12}^2 \\ v_1 v_2 \end{pmatrix} - \lambda_5 \begin{pmatrix} v_2^2 & -v_1 v_2 \\ -v_1 v_2 & v_1^2 \end{pmatrix} + \begin{pmatrix} \frac{T_1}{v_1} & 0 \\ 0 & \frac{T_2}{v_2} \end{pmatrix} \quad (2.13)$$

$$M_\omega^2 \equiv \begin{pmatrix} m_{12}^2 \\ v_1 v_2 \end{pmatrix} - \frac{\lambda_4 + \lambda_5}{2} \begin{pmatrix} v_2^2 & -v_1 v_2 \\ -v_1 v_2 & v_1^2 \end{pmatrix} + \begin{pmatrix} \frac{T_1}{v_1} & 0 \\ 0 & \frac{T_2}{v_2} \end{pmatrix} . \quad (2.14)$$

	u -type	d -type	leptons
I	Φ_2	Φ_2	Φ_2
II	Φ_2	Φ_1	Φ_1
lepton-specific	Φ_2	Φ_2	Φ_1
flipped	Φ_2	Φ_1	Φ_2

Table 1: The four Yukawa types of the \mathbb{Z}_2 -symmetric 2HDM defined by the Higgs doublet that couples to each kind of fermions.

They are diagonalized by the rotation matrices⁴

$$R(x) \equiv \begin{pmatrix} c_x & -s_x \\ s_x & c_x \end{pmatrix} \quad (2.15)$$

in terms the mixing angles α and β which rotate the field ω_i^\pm , ρ_i and η_i in the gauge basis to the mass basis as

$$\begin{pmatrix} \rho_1 \\ \rho_2 \end{pmatrix} = R(\alpha) \begin{pmatrix} H \\ h \end{pmatrix} \quad (2.16)$$

$$\begin{pmatrix} \eta_1 \\ \eta_2 \end{pmatrix} = R(\beta) \begin{pmatrix} G^0 \\ A \end{pmatrix} \quad (2.17)$$

$$\begin{pmatrix} \omega_1^\pm \\ \omega_2^\pm \end{pmatrix} = R(\beta) \begin{pmatrix} G^\pm \\ H^\pm \end{pmatrix}. \quad (2.18)$$

Here, h and H denote the CP-even Higgs bosons with masses $m_h < m_H$, respectively, A the CP-odd Higgs boson with mass m_A and H^\pm the charged Higgs bosons with masses m_{H^\pm} . The massless neutral and charged Goldstone bosons are denoted by G^0 and G^\pm , respectively. In order to avoid flavor-changing neutral currents (FCNCs) at tree level, the \mathbb{Z}_2 symmetry of the Higgs potential is extended to the Yukawa sector so that each of the up-type quarks, down-type quarks and charged leptons can only couple to one of the Higgs doublets. Depending on the \mathbb{Z}_2 charge assignments, there are four phenomenologically different types of 2HDMs that are shown in Tab. 1. We conclude by giving the set of independent parameters that parametrize the tree-level potential of the CP-conserving 2HDM. By exploiting the minimum conditions from Eqs. (2.9) and (2.10), the set of independent input parameters in the mass basis is given by

$$m_h, m_H, m_A, m_{H^\pm}, m_{12}^2, \alpha, \tan \beta, v. \quad (2.19)$$

Alternatively, the original parametrization of the scalar potential in the interaction basis can be used so that the set of independent parameters is given by

$$\lambda_1, \lambda_2, \lambda_3, \lambda_4, \lambda_5, m_{12}^2, \tan \beta, v. \quad (2.20)$$

2.2 Introduction of the N2HDM

We consider a general CP-conserving N2HDM that is obtained from the CP-conserving 2HDM with a softly broken \mathbb{Z}_2 symmetry by adding a real singlet field Φ_S . The phenomenology of this

⁴Here and in the following, we use the short-hand notation $s_x \equiv \sin(x)$, $c_x \equiv \cos(x)$, $t_x \equiv \tan(x)$ for convenience.

version of the N2HDM has been extensively discussed in [6, 41, 42].⁵ In terms of the $SU(2)_L$ Higgs doublets $\Phi_{1,2}$ and the singlet field Φ_S , the N2HDM potential reads

$$\begin{aligned}
V_{\text{N2HDM}} = & m_{11}^2 |\Phi_1|^2 + m_{22}^2 |\Phi_2|^2 - m_{12}^2 \left(\Phi_1^\dagger \Phi_2 + h.c. \right) + \frac{\lambda_1}{2} \left(\Phi_1^\dagger \Phi_1 \right)^2 + \frac{\lambda_2}{2} \left(\Phi_2^\dagger \Phi_2 \right)^2 \\
& + \lambda_3 \left(\Phi_1^\dagger \Phi_1 \right) \left(\Phi_2^\dagger \Phi_2 \right) + \lambda_4 \left(\Phi_1^\dagger \Phi_2 \right) \left(\Phi_2^\dagger \Phi_1 \right) + \frac{\lambda_5}{2} \left[\left(\Phi_1^\dagger \Phi_2 \right)^2 + h.c. \right] \\
& + \frac{1}{2} m_S^2 \Phi_S^2 + \frac{1}{8} \lambda_6 \Phi_S^4 + \frac{1}{2} \lambda_7 \left(\Phi_1^\dagger \Phi_1 \right) \Phi_S^2 + \frac{1}{2} \lambda_8 \left(\Phi_2^\dagger \Phi_2 \right) \Phi_S^2 ,
\end{aligned} \tag{2.21}$$

where the first two lines describe the 2HDM part of the N2HDM and the last line contains the contribution of the singlet field Φ_S . The potential is obtained by imposing two \mathbb{Z}_2 symmetries. The first one, called \mathbb{Z}_2 , under which the doublets and singlet transform as

$$\Phi_1 \rightarrow \Phi_1 , \quad \Phi_2 \rightarrow -\Phi_2 , \quad \Phi_S \rightarrow \Phi_S , \tag{2.22}$$

is the trivial generalization of the usual 2HDM \mathbb{Z}_2 symmetry to the N2HDM. It is softly broken by the term involving m_{12}^2 and will be extended to the Yukawa sector to avoid FCNCs at tree level. The second symmetry, called \mathbb{Z}'_2 , under which the doublets and singlet transform as

$$\Phi_1 \rightarrow \Phi_1 , \quad \Phi_2 \rightarrow \Phi_2 , \quad \Phi_S \rightarrow -\Phi_S , \tag{2.23}$$

is not explicitly broken. The N2HDM potential depends on four real mass parameters m_{11} , m_{22} , m_{12} , and m_S and eight dimensionless real coupling constants λ_i ($i = 1, \dots, 8$). After EWSB the doublet and singlet fields can be expanded around their non-negative real VEVs v_1 , v_2 and v_S as

$$\Phi_1 = \begin{pmatrix} \omega_1^\pm \\ \frac{v_1 + \rho_1 + i\eta_1}{\sqrt{2}} \end{pmatrix} , \quad \Phi_2 = \begin{pmatrix} \omega_2^\pm \\ \frac{v_2 + \rho_2 + i\eta_2}{\sqrt{2}} \end{pmatrix} , \quad \Phi_S = v_S + \rho_S , \tag{2.24}$$

where ρ_i and ρ_S represent three CP-even fields, η_i two CP-odd fields and ω_i^\pm are two charged fields ($i = 1, 2$). The two VEVs of the doublets are again related to the SM VEV v as $v^2 = v_1^2 + v_2^2$, and the mixing angle β is introduced as before through $\tan \beta = v_2/v_1$. Inserting Eq. (2.24) into the N2HDM potential Eq. (2.21) yields

$$V_{\text{N2HDM}} = \frac{1}{2} \begin{pmatrix} \rho_1 & \rho_2 & \rho_S \end{pmatrix} M_\rho^2 \begin{pmatrix} \rho_1 \\ \rho_2 \\ \rho_S \end{pmatrix} + T_1 \rho_1 + T_2 \rho_2 + T_S \rho_S + \dots , \tag{2.25}$$

where M_ρ is the 3×3 mass matrix in the CP-even scalar sector and T_k ($k = 1, 2, S$) are the three tadpole terms. We demand the three VEVs to represent the minimum of the potential by requiring ($k, l = 1, 2, S$)

$$\left. \frac{\partial V_{\text{N2HDM}}}{\partial \Phi_l} \right|_{\langle \Phi_k \rangle} = 0 , \tag{2.26}$$

⁵For the N2HDM in different phases, cf. [43]. A recent discussion of its vacuum instabilities can be found in [44].

which at tree level leads to the three tadpole conditions

$$\frac{T_1}{v_1} \equiv m_{11}^2 - m_{12}^2 \frac{v_2}{v_1} + \frac{v_1^2 \lambda_1}{2} + \frac{v_2^2 \lambda_{345}}{2} + \frac{v_S^2 \lambda_7}{2} = 0 \quad (2.27)$$

$$\frac{T_2}{v_2} \equiv m_{22}^2 - m_{12}^2 \frac{v_1}{v_2} + \frac{v_2^2 \lambda_2}{2} + \frac{v_1^2 \lambda_{345}}{2} + \frac{v_S^2 \lambda_8}{2} = 0 \quad (2.28)$$

$$\frac{T_S}{v_S} \equiv m_S^2 + \frac{v_1^2 \lambda_7}{2} + \frac{v_2^2 \lambda_8}{2} + \frac{v_S^2 \lambda_6}{2} = 0 . \quad (2.29)$$

These conditions can be used to replace m_{11}^2 , m_{22}^2 and m_S^2 in favor of the three tadpole terms. The mass matrix of the CP-even scalar fields reads

$$M_\rho^2 \equiv \begin{pmatrix} m_{12}^2 \frac{v_2}{v_1} + \lambda_1 v_1^2 & -m_{12}^2 + \lambda_{345} v_1 v_2 & \lambda_7 v_1 v_S \\ -m_{12}^2 + \lambda_{345} v_1 v_2 & m_{12}^2 \frac{v_1}{v_2} + \lambda_2 v_2^2 & \lambda_8 v_2 v_S \\ \lambda_7 v_1 v_S & \lambda_8 v_2 v_S & \lambda_6 v_S^2 \end{pmatrix} + \begin{pmatrix} \frac{T_1}{v_1} & 0 & 0 \\ 0 & \frac{T_2}{v_2} & 0 \\ 0 & 0 & \frac{T_S}{v_S} \end{pmatrix} . \quad (2.30)$$

We introduce three mixing angles α_i ($i = 1, 2, 3$) defined in the range

$$-\frac{\pi}{2} \leq \alpha_i < \frac{\pi}{2} \quad (2.31)$$

in order to diagonalize the mass matrix by means of the orthogonal matrix R , parametrized as

$$R = \begin{pmatrix} c_{\alpha_1} c_{\alpha_2} & s_{\alpha_1} c_{\alpha_2} & s_{\alpha_2} \\ -(c_{\alpha_1} s_{\alpha_2} s_{\alpha_3} + s_{\alpha_1} c_{\alpha_3}) & c_{\alpha_1} c_{\alpha_3} - s_{\alpha_1} s_{\alpha_2} s_{\alpha_3} & c_{\alpha_2} s_{\alpha_3} \\ -c_{\alpha_1} s_{\alpha_2} c_{\alpha_3} + s_{\alpha_1} s_{\alpha_3} & -(c_{\alpha_1} s_{\alpha_3} + s_{\alpha_1} s_{\alpha_2} c_{\alpha_3}) & c_{\alpha_2} c_{\alpha_3} \end{pmatrix} . \quad (2.32)$$

This matrix transforms the CP-even interaction fields ρ_i ($i = 1, 2, 3$, $\rho_3 \equiv \rho_S$) into the mass eigenstates H_i ,

$$\begin{pmatrix} H_1 \\ H_2 \\ H_3 \end{pmatrix} = R \begin{pmatrix} \rho_1 \\ \rho_2 \\ \rho_3 \end{pmatrix} . \quad (2.33)$$

This transformation yields the diagonalized mass matrix

$$D_\rho^2 \equiv R M_\rho^2 R^T \equiv \text{diag} (m_{H_1}^2, m_{H_2}^2, m_{H_3}^2) , \quad (2.34)$$

where we demand the three CP-even Higgs bosons H_i to be ordered by ascending mass,

$$m_{H_1} < m_{H_2} < m_{H_3} . \quad (2.35)$$

We do not show the CP-odd and charged mass matrices explicitly in Eq. (2.25) as they do not change with respect to the 2HDM. At tree level they are diagonalized by the mixing angle β , yielding the CP-odd and charged Higgs bosons A and H^\pm with masses m_A and m_{H^\pm} , respectively, as well as the massless neutral and charged Goldstone bosons G^0 and G^\pm .

As mentioned before, the softly broken \mathbb{Z}_2 symmetry transformation shown in Eq. (2.22) is extended to the Yukawa sector in order to avoid FCNCs at tree level. This leads to the same four types of doublet couplings to the fermion fields as in the 2HDM. At tree level, the N2HDM potential is parametrized by twelve parameters. By exploiting the minimum conditions in Eqs. (2.27) to (2.29), the set of independent parameters in the mass basis is given by

$$m_{H_1}, m_{H_2}, m_{H_3}, m_A, m_{H^\pm}, m_{12}^2, \alpha_1, \alpha_2, \alpha_3, \tan \beta, v, v_S . \quad (2.36)$$

3 Renormalization

The ultraviolet (UV) divergences that appear in the computation of the electroweak corrections to the Higgs boson decays in the 2HDM and N2HDM require the renormalization of the parameters which are involved in the calculations. The renormalization schemes that we apply are chosen such that they fulfil the following requirements as far as it is possible:

- We require physical OS renormalization conditions, where possible.
- The renormalization schemes are chosen such that they preserve gauge-parameter-independent relations between the input parameters and the computed observables.
- The NLO corrections should not become unnaturally large. Throughout the paper, we refer to this behavior of a renormalization scheme as being 'numerically stable'.
- Finally, conditions that depend on a physical process, *i.e.* so-called process-dependent renormalization schemes, are avoided, if possible.

The renormalization conditions respecting these requirements, in particular the gauge-independent renormalization, have been introduced and extensively discussed by us for the 2HDM in [21, 22] and for the N2HDM in [26]. Moreover, renormalization schemes respecting some or all of these criteria were also discussed in [23–25, 28] for the 2HDM and in [30, 31] for a generic multi-Higgs sector. In this paper we apply our renormalization conditions of Refs. [21, 22] for the 2HDM and of Ref. [26] for the N2HDM. Additionally, we apply the renormalization conditions developed for the 2HDM in [23–25, 28]. All these conditions have been implemented in the codes `2HDECAY` [34] and `N2HDECAY` [35] for the 2HDM and N2HDM, respectively, which we use to calculate the presented loop-corrected branching ratios. We refer to the given literature for the detailed introduction and description of the renormalization schemes. Here, we list them only very briefly for a convenient overview.

3.1 Renormalization of the 2HDM

The renormalization schemes for the scalar mixing angles α and β implemented in `2HDECAY` [34] for the 2HDM are summarized in Tab. 2. For details on these schemes and for the complete EW one-loop renormalization of the 2HDM, we refer to [21, 22, 34]. The first column in the table gives the identifier with which the user selects the renormalization scheme in the input file of `2HDECAY`. The second column describes the scheme and the third one the abbreviation that will be used for it in the presentation of the results. The fourth column refers to the tadpole scheme that is used and the last column lists the references where the respective renormalization scheme is introduced and described.

The standard tadpole scheme is a commonly used renormalization schemes for the tadpoles, *cf. e.g.* [47] for the SM and [33, 48] for the 2HDM. They are renormalized such that the ground state of the potential represents the minimum also at higher orders. In the standard tadpole scheme this condition is imposed on the loop-corrected potential. As the latter is in general gauge dependent, the counterterms (CTs) defined through this minimum, *e.g.* the scalar mass (matrix) CTs, become manifestly gauge-dependent themselves. In the alternative tadpole scheme, proposed by Fleischer and Jegerlehner (FJ) for the SM in [49] and applied to the 2HDM for the first time in Refs. [21, 45], the VEVs are defined through the gauge-independent tree-level potential so that they become manifestly gauge-independent quantities and hence, also the mass

2HDECAY ID	Scheme	Abbreviation	Tadpole scheme	Reference
1/2	KOSY	KOSY ^{o/c} (std)	standard	[33]
3/4	KOSY	KOSY ^{o/c}	alternative FJ	[21, 33, 45]
5/6	p_* -pinched	$p_*^{o/c}$	alternative FJ	[21, 45]
7/8	OS-pinched	pOS ^{o/c}	alternative FJ	[21, 45]
9	Process-dependent 1	proc1	alternative FJ	[21, 45, 46]
10	Process-dependent 2	proc2	alternative FJ	[46]
11	Process-dependent 3	proc3	alternative FJ	[46]
12	Physical OS 1	OS1	alternative FJ	[28]
13	Physical OS 2	OS2	alternative FJ	[28]
14	Physical OS 12	OS12	alternative FJ	[28]
15	Rigid symmetry (BFMS)	BFMS	alternative FJ	[28]
16	$\overline{\text{MS}}$	$\overline{\text{MS}}$ (std)	standard	[21, 24, 45]
17	$\overline{\text{MS}}$	$\overline{\text{MS}}$	alternative FJ	[21, 24, 45]

Table 2: Renormalization schemes of 2HDECAY [34]. For further explanations, we refer to the text.

(matrix) CTs become manifestly gauge-independent.

The KOSY scheme, introduced in [33] and named by us after the authors' initials, defines the CTs for the mixing angles α and β through off-diagonal wave-function renormalization constants. As shown in [21, 45], this not only implies a gauge-dependent definition of the mixing angle CTs but also leads to explicitly gauge-dependent decay amplitudes and partial decay widths. Nevertheless, in 2HDECAY it has been implemented as a benchmark scheme for comparison with other schemes, both in the standard and alternative tadpole scheme. Due to its intricate gauge dependence, we do not recommend to use the KOSY scheme for actual computations, however.

On the other hand, the pinched schemes lead to manifestly gauge-independent mixing angle CTs [21, 45]. In these schemes, the OS-based definition of the mixing angle counterterms for α and β of the KOSY scheme is kept, but instead of using the usual gauge-dependent off-diagonal wave function renormalization counterterms (WFRCs), the WFRCs are defined through pinched self-energies in the alternative tadpole scheme by applying the pinch technique (PT) [50–57]. We employ two different definitions that differ solely by the scale at which the self-energies are evaluated. In the p_* -pinched scheme they are evaluated at the arithmetic average of the squared masses of the external particles. In the OS-pinched scheme, OS-motivated scales are chosen for the self-energies.

The upper indices in the KOSY and pinched schemes refer to the part of the Higgs sector that is applied in the renormalization of β . The angle appears both in the charged and in the CP-odd mass matrix and its renormalization can be defined either through the charged ($'c'$) or the CP-odd ($'o'$) sector.

Process-dependent renormalization schemes have the advantage to lead to manifestly gauge-independent mixing angle CTs. However, they make the renormalization conditions dependent on a specific physical processes. In 2HDECAY, three different processes were implemented for the renormalization of the scalar mixing angles [21, 45, 46]. In the first process-dependent scheme

ewN2HDECAY ID	Scheme	Abbreviation	Tadpole scheme	Reference
1/2	Adapted KOSY	KOSY ^{o/c} (std)	standard	[26, 33, 46]
3/4	Adapted KOSY	KOSY ^{o/c}	alternative FJ	[26, 33, 46]
5/6	p_* -pinched	$p_*^{o/c}$	alternative FJ	[26, 46]
7/8	OS-pinched	pOS ^{o/c}	alternative FJ	[26, 46]
9	$\overline{\text{MS}}$	$\overline{\text{MS}}$ (std)	standard	[26, 46]
10	$\overline{\text{MS}}$	$\overline{\text{MS}}$	alternative FJ	[26, 46]

Table 3: Renormalization schemes of ewN2HDECAY [35]. For further explanations, we refer to the text.

(‘proc1’), the CT for β , $\delta\beta$ is defined through the decay of the pseudoscalar into a τ -lepton pair, $A \rightarrow \tau^+\tau^-$, and the CT for α , $\delta\alpha$, through the decay of the heavy scalar into a τ -lepton pair, $H \rightarrow \tau^+\tau^-$. In the second process-dependent scheme (‘proc2’), $\delta\beta$ is again defined through $A \rightarrow \tau^+\tau^-$, but $\delta\alpha$ is defined through the decay of the lighter CP-even Higgs boson into a τ -lepton pair, $h \rightarrow \tau^+\tau^-$. In the third process-dependent scheme (‘proc3’), $\delta\beta$ and $\delta\alpha$ are simultaneously defined through $H \rightarrow \tau^+\tau^-$ and $h \rightarrow \tau^+\tau^-$.

In the physical OS scheme proposed in [28], the mixing angles CTs are defined through ratios of processes such that they are manifestly gauge-independent, while at the same time avoiding potentially large NLO corrections that are usually present in process-dependent schemes. Solely for the purpose of renormalization, two right-handed fermion singlets ν_{1R} and ν_{2R} are introduced which transform under an additionally introduced \mathbb{Z}_2 symmetry transformation as $\nu_{1R} \rightarrow -\nu_{1R}$ and $\nu_{2R} \rightarrow \nu_{2R}$. The singlets are coupled via Yukawa couplings to left-handed lepton doublets of the 2HDM, giving rise to two massive Dirac neutrinos ν_1 and ν_2 . Denoting by \mathcal{A} the decay amplitude, the three implemented OS schemes are defined as follows. In ‘OS1’ the ratio $\mathcal{A}_{H \rightarrow \nu_1 \bar{\nu}_1} / \mathcal{A}_{h \rightarrow \nu_1 \bar{\nu}_1}$ is used to define $\delta\alpha$ while $\mathcal{A}_{A \rightarrow \nu_1 \bar{\nu}_1} / \mathcal{A}_{H \rightarrow \nu_1 \bar{\nu}_1}$ is used to define $\delta\beta$. In ‘OS2’ we have $\mathcal{A}_{H \rightarrow \nu_2 \bar{\nu}_2} / \mathcal{A}_{h \rightarrow \nu_2 \bar{\nu}_2}$ for $\delta\alpha$ and $\mathcal{A}_{A \rightarrow \nu_2 \bar{\nu}_2} / \mathcal{A}_{H \rightarrow \nu_2 \bar{\nu}_2}$ for $\delta\beta$. In ‘OS12’, again the ratio $\mathcal{A}_{H \rightarrow \nu_1 \bar{\nu}_1} / \mathcal{A}_{h \rightarrow \nu_1 \bar{\nu}_1}$ is used for $\delta\alpha$ and a specific combination of all possible decay amplitudes $\mathcal{A}_{h/H \rightarrow \nu_j \bar{\nu}_j}$ and $\mathcal{A}_{A \rightarrow \nu_j \bar{\nu}_j}$ ($i, j = 1, 2$) for $\delta\beta$.

In the rigid symmetry scheme (BFMS), the rigid symmetry of the Lagrangian is used to connect the renormalization of α and β to the renormalization of the WFRCs. In [28], this scheme was worked out and applied to derive gauge-independent counterterms for the scalar mixing angles of the 2HDM within the framework of the background field method (BFM) [58–64].

We also apply the $\overline{\text{MS}}$ scheme for $\delta\alpha$ and $\delta\beta$ [21, 23, 24, 45] for reference, both in the standard and the alternative tadpole scheme, although it can typically lead to very large corrections at NLO for many two-body decay processes [45, 65]. Note that the $\overline{\text{MS}}$ scheme induces gauge-dependent $\delta\alpha$ and $\delta\beta$ and hence gauge-dependent partial decay widths unless the alternative tadpole scheme is applied.

3.2 Renormalization of the N2HDM

In Tab. 3, we summarize the renormalization schemes that we apply for the four scalar mixing angles in the computation of the EW-corrected NLO widths of the neutral N2HDM Higgs bosons. For details on these schemes and for the complete electroweak one-loop renormalization of the N2HDM, we refer to [26, 46].

In contrast to the 2HDM, in the N2HDM three mixing angles α_i ($i = 1, 2, 3$) in the CP-even neutral Higgs sector require renormalization. Together with the mixing angle β from the CP-odd and charged Higgs sectors, in total four mixing angle CTs are required, namely $\delta\alpha_i$ and $\delta\beta$. In [26], we generalized the renormalization schemes for the mixing angles of the 2HDM developed in [21] to the more intricate Higgs sector of the N2HDM. The schemes are defined in complete analogy to the 2HDM and have been implemented in `ewN2HDECAY` [35]. The first column in Tab. 3 again gives the identifier with which the user selects the renormalization scheme in the input file of `ewN2HDECAY`. The corresponding scheme is named in the second column along with its abbreviation in the third column. The fourth column refers to the tadpole scheme that is used and the last column cites the references where the respective renormalization scheme is introduced and described.

The adapted KOSY scheme is the generalization of the KOSY scheme [33] to the N2HDM, both by applying the standard and the alternative tadpole scheme. Accordingly, the p_* -pinched and OS-pinched schemes are the extensions of the corresponding renormalization schemes introduced in the 2HDM to the case of the N2HDM. All four schemes provide the renormalization of the mixing angle β both via the charged ($'c'$) and the CP-odd ($'o'$) Higgs sector. For reference, also the renormalization of the mixing angles via the $\overline{\text{MS}}$ scheme has been implemented in both the standard and the alternative tadpole scheme.

4 Numerical Results

In the following subsections, we give in tabular format the relative sizes of the EW corrections to the BRs for the various Higgs decays in the 2HDM and in the N2HDM. In order to define them, we first have to explain what is meant when we talk about the inclusion of QCD and/or EW corrections in the BRs. Higher-order corrected BRs means that we include higher-order corrections in the partial Higgs decay widths and hence also the total widths as follows⁶.

- All decays include the state-of-the-art higher-order QCD corrections to the OS and off-shell Higgs boson decays where appropriate. Also the loop-induced decays into gluonic and photonic final states include higher-order QCD corrections. The exact description of the implemented loop-order and applied approximation in the various decays can be found in [37, 66]. The results for the SM and MSSM, respectively, have been translated to the 2HDM [67] and subsequently included in `2HDECAY`. The generalization to the N2HDM has been performed in `N2HDECAY` [6] and subsequently included in `ewN2HDECAY`.
- The codes include off-shell decays into heavy-quark pairs, massive gauge boson pairs, neutral Higgs pairs as well as Higgs and gauge boson final states. The EW corrections are included only for decays into OS final states, however. Off-shell decays are computed at LO or, where appropriate and available, with the inclusion of higher-order QCD corrections.
- The loop-induced decays into gluon and photon final states as well as into $Z\gamma$ do not include any EW corrections as they are of two-loop order.
- For the combination of the QCD and EW corrections, we assume that these corrections factorize.

⁶For further details, cf. Refs. [34, 35]

The relative size ΔBR of the higher-order corrected BRs, including QCD and EW corrections as described above, is defined as

$$\Delta\text{BR} = \frac{\text{BR}^{\text{QCD\&EW}} - \text{BR}^{\text{QCD}}}{\text{BR}^{\text{QCD}}} . \quad (4.37)$$

The superscript 'QCD&EW' means that both QCD and EW corrections have been implemented in the various partial decay widths where appropriate and/or possible as described above. The superscript 'QCD' refers to the BR where only QCD corrections are taken into account in the various Higgs decays, where appropriate. The ΔBR hence quantifies the relative importance of the EW corrections in the BRs with respect to the QCD corrected BRs.

4.1 2HDM Higgs Decays

We start with the results for the 2HDM. We consider two different kinds of parameter sets, one where the lighter of the CP-even Higgs bosons, h , is the SM-like Higgs, and another set where the heavier one, H , is SM-like. For both kinds of parameter sets, we consider all four 2HDM types. For the case that h is SM-like, the total amount of points used for the numerical analyses is as follows,

<u>h is SM-like:</u>	Type I: 373 517	Type II: 413 377	(4.38)
	Type LS: 373 000	Type FL: 431 540 ,	

where we introduced the abbreviations LS for the lepton-specific 2HDM and FL for the flipped 2HDM. In case that H is SM-like, we found less valid parameter points in our scans that could be used for our numerical analyses,

<u>H is SM-like:</u>	Type I: 747	Type II: 39	(4.39)
	Type LS: 132	Type FL: 124 .	

As can be inferred from these numbers, this case is strongly disfavored in comparison to the case that h is the SM-like Higgs. This also means that the statistics for our analyses in these scenarios is very low.

4.2 SM-Like 2HDM Higgs Decays

We start by giving our results for the 2HDM decays of the SM-like Higgs boson before moving on to the non-SM-like Higgs decays.

4.2.1 h is the SM-like Higgs Boson

In the tables of this section we list the relative size of the EW corrections ΔBR to the BRs of the SM-like Higgs boson h for the four 2HDM types I, II, LS and FL. We use subscripts for ΔBR in order to refer to the corresponding decay channel. In the computation of the EW corrections we apply various renormalization schemes presented in Tab. 2 of Section 3.1. The comparison of the results in the different renormalization schemes gives an estimate of the theoretical error on the BR due to the missing higher-order corrections that are not included. Moreover, it also shows which renormalization schemes are less suitable because they lead to very large NLO corrections. In order to keep the presentation of the higher-order EW effects computed in the

various renormalization schemes clear, we group the results into bins quantifying the size of the relative corrections to the BRs and into subsets of renormalization schemes that lead to similar results. The subsets of schemes are given as superscript of ΔBR . The following scheme sets could be defined here:

$$\begin{aligned}\mathbf{S}_1 &\equiv \{ \text{KOSY}^o, \text{KOSY}^c, \text{p}_*^o, \text{p}_*^c, \text{pOS}^o, \text{pOS}^c, \text{BFMS} \} \\ \mathbf{S}_2 &\equiv \{ \text{proc1}, \text{OS1} \} \\ \mathbf{S}_3 &\equiv \{ \text{proc2}, \text{proc3}, \text{OS12} \} \\ \mathbf{OS2} &\equiv \{ \text{OS2} \} \\ \overline{\mathbf{MS}} &\equiv \{ \overline{\mathbf{MS}} \}\end{aligned}$$

Let us clarify that in the generation of the numbers for a specific scheme the respective set of input parameters is understood to be given in this scheme. This means in particular that we did not convert an input parameter set given in one scheme to the input parameter set for a different renormalization scheme. Therefore the numbers calculated in two different schemes cannot be directly compared to each other in order to derive *e.g.* the theoretical error due to missing higher-order corrections. Our approach is instead a large-scale analysis for each scheme separately. This way, we cannot estimate the remaining theoretical errors, but we can judge if schemes or sets of schemes behave similarly with respect to their relative size of corrections.

In the tables of this section, the relative size of the corrections to the BRs are quantified via a binning as

$$\lesssim / \gtrsim a \% (b \%)\text{.} \quad (4.40)$$

This is to be read as “ $b\%$ of all used input parameter sets lead to corrections ΔBR below/above or approximately equal to $a\%$ ”. For each renormalization scheme set, we show two pairs of percentage values “ $a\%$ ” according to the format described in Eq. (4.40): a lower value where the peak of all corrections is found and a larger value where the majority of all results lies in. An exception to this is the case when all corrections are situated in the lowest bin (2.5%) in which case we only show one pair of numbers. For the $\overline{\mathbf{MS}}$ scheme (and for some other schemes and decay channels) where the corrections are typically huge, we show the following two pairs of values: one where half of the results lies in (“half” only if half of the results are actually below $\pm 100\%$, otherwise a lower appropriate value) and a second pair of values that corresponds to the largest bin (*i.e.* above $\pm 100\%$).

This means for example for the first upper left entry of Tab. 4 that in the 2HDM type I, the relative corrections $\Delta\text{BR}_{h\bar{b}\bar{b}}^{\mathbf{S}_1}$ to the BR of the SM-like Higgs boson h into the $b\bar{b}$ final state amount to less than about 2.5% for 96% of the valid parameter sets and to less than or roughly equal to 5% for all of them. This is exemplified in Fig. 1. In the plot, we present the binned percentage of parameter points for $\Delta\text{BR}_{h\bar{b}\bar{b}}$ of the electroweak corrections for the scheme sets \mathbf{S}_1 and $\overline{\mathbf{MS}}$. To that end, we computed the arithmetic average⁷ of the numerical results obtained for all renormalization schemes included in scheme set \mathbf{S}_1 and $\overline{\mathbf{MS}}$, respectively. As can be inferred from the plot, for the scheme set \mathbf{S}_1 96% of all input parameter sets lead to corrections of 2.5% or less and 100% of all input parameter sets yield corrections less than 5.0%, as stated above. For the $\overline{\mathbf{MS}}$ scheme on the other hand, roughly 50% of all parameter points yield relative

⁷We point out again that the numerical results computed for the schemes within one set are close to each other such that the arithmetic average of the results for the scheme set does not deviate much from the results computed for each scheme individually.

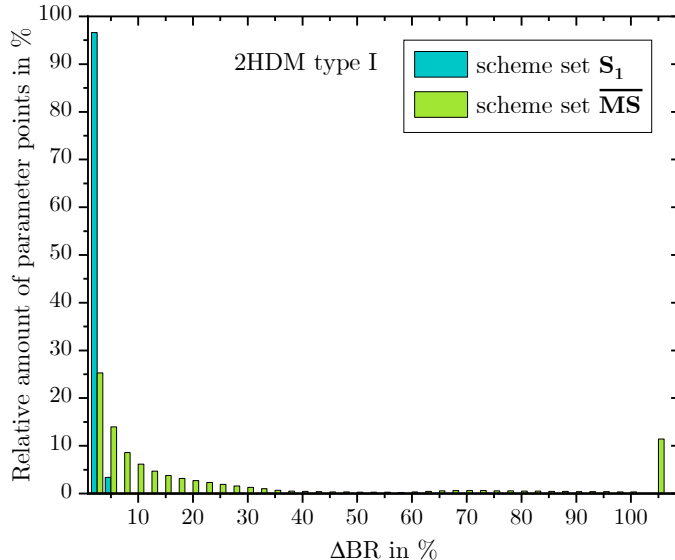


Figure 1: 2HDM type I: Binned amount of parameter points in % for the scheme sets \mathbf{S}_1 (blue) and $\overline{\mathbf{MS}}$ (green) as a function of ΔBR in % for the decay $h \rightarrow b\bar{b}$.

corrections below 10.0% while 12% of all points lead to corrections above 100.0%. The same methodology was applied for all 2HDM types and for all decays and translated into values in the tables. For example, the lower right entry of Tab. 4 tells us that in the flipped 2HDM, the relative corrections $\Delta\text{BR}_{h\tau^+\tau^-}^{\overline{\mathbf{MS}}}$ to the BR of h into $\tau^+\tau^-$ for 38% of the parameter points is as large as about 90%, with 58% leading to corrections even beyond 100%. The remaining 4% of parameter points lead to corrections between 90% and 100% and form the complement of the two preceding pairs of numbers in the table.

In Tab. 4, we show the results for the main discovery channels and the dominant down-type fermion final states, *i.e.* for the decays into $\gamma\gamma$, ZZ , $b\bar{b}$ and $\tau^+\tau^-$. We have calculated also the corrections for all other final states and provide them on demand. In order to keep the presentation of the results clear, we stick to the most important final states here, however. Note that the decay into Z boson pairs is off-shell for the 125 GeV SM-like Higgs boson, whereas the decay into photons is loop-induced already at tree level. Therefore, as described above, these decays do not include any EW corrections so that the relative corrections of their branching ratios are the same. Inspecting the numbers of the table, we make the following observations:

- The relative sizes ΔBR of the EW corrections to the BRs for the scheme set \mathbf{S}_1 for all four 2HDM types are typically very small, with the bulk of the parameter points resulting in corrections below 2.5% and 5.0%, indicating both small EW corrections as well as numerical stability of the schemes.
- For \mathbf{S}_3 , the corrections are slightly increased for the decay $h \rightarrow \tau^+\tau^-$ in the 2HDM types II, LS and FL, but for the other decays in all four types, the results are comparable to the ones in set \mathbf{S}_1 .
- For \mathbf{S}_2 , the corrections for the decays in all 2HDM types are increased compared to \mathbf{S}_1 and \mathbf{S}_3 and in particular in the 2HDM types LS and FL, the corrections to the decay $h \rightarrow \tau^+\tau^-$ can be considerably larger.

Type	$\Delta\text{BR}_{hbb}^{\mathbf{S}_1}$	$\Delta\text{BR}_{hbb}^{\mathbf{S}_2}$	$\Delta\text{BR}_{hbb}^{\mathbf{S}_3}$	$\Delta\text{BR}_{hbb}^{\text{OS2}}$	$\Delta\text{BR}_{hbb}^{\overline{\text{MS}}}$
I	$\gtrsim 2.5\%$ (96%)	$\gtrsim 5.0\%$ (98%)	$\gtrsim 2.5\%$ (90%)	$\gtrsim 2.5\%$ (94%)	$\gtrsim 10.0\%$ (50%)
	$\gtrsim 5.0\%$ (100%)	$\gtrsim 7.5\%$ (99%)	$\gtrsim 5.0\%$ (99%)	$\gtrsim 5.0\%$ (99%)	$\gtrsim 100.0\%$ (12%)
II	$\gtrsim 2.5\%$ (99%)	$\gtrsim 2.5\%$ (54%)	$\gtrsim 2.5\%$ (98%)	$\gtrsim 2.5\%$ (81%)	$\gtrsim 40.0\%$ (50%)
	$\gtrsim 5.0\%$ (100%)	$\gtrsim 7.5\%$ (96%)	$\gtrsim 5.0\%$ (99%)	$\gtrsim 5.0\%$ (99%)	$\gtrsim 100.0\%$ (36%)
LS	$\gtrsim 2.5\%$ (96%)	$\gtrsim 2.5\%$ (54%)	$\gtrsim 2.5\%$ (75%)	$\gtrsim 2.5\%$ (94%)	$\gtrsim 17.5\%$ (50%)
	$\gtrsim 5.0\%$ (99%)	$\gtrsim 5.0\%$ (97%)	$\gtrsim 5.0\%$ (99%)	$\gtrsim 5.0\%$ (99%)	$\gtrsim 100.0\%$ (14%)
FL	$\gtrsim 2.5\%$ (96%)	$\gtrsim 2.5\%$ (54%)	$\gtrsim 2.5\%$ (75%)	$\gtrsim 2.5\%$ (94%)	$\gtrsim 17.5\%$ (50%)
	$\gtrsim 5.0\%$ (99%)	$\gtrsim 5.0\%$ (97%)	$\gtrsim 5.0\%$ (99%)	$\gtrsim 5.0\%$ (99%)	$\gtrsim 100.0\%$ (12%)

Type	$\Delta\text{BR}_{h\gamma\gamma/hZZ}^{\mathbf{S}_1}$	$\Delta\text{BR}_{h\gamma\gamma/hZZ}^{\mathbf{S}_2}$	$\Delta\text{BR}_{h\gamma\gamma/hZZ}^{\mathbf{S}_3}$	$\Delta\text{BR}_{h\gamma\gamma/hZZ}^{\text{OS2}}$	$\Delta\text{BR}_{h\gamma\gamma/hZZ}^{\overline{\text{MS}}}$
I	$\gtrsim 5.0\%$ (97%)	$\gtrsim 5.0\%$ (90%)	$\gtrsim 5.0\%$ (90%)	$\gtrsim 5.0\%$ (94%)	$\gtrsim 20.0\%$ (50%)
	$\gtrsim 7.5\%$ (99%)	$\gtrsim 10.0\%$ (98%)	$\gtrsim 7.5\%$ (99%)	$\gtrsim 7.5\%$ (99%)	$\gtrsim 100.0\%$ (21%)
II	$\gtrsim 5.0\%$ (99%)	$\gtrsim 5.0\%$ (60%)	$\gtrsim 2.5\%$ (96%)	$\gtrsim 5.0\%$ (82%)	$\gtrsim 62.0\%$ (50%)
	$\gtrsim 7.5\%$ (99%)	$\gtrsim 12.5\%$ (96%)	$\gtrsim 5.0\%$ (99%)	$\gtrsim 7.5\%$ (97%)	$\gtrsim 100.0\%$ (47%)
LS	$\gtrsim 5.0\%$ (97%)	$\gtrsim 5.0\%$ (75%)	$\gtrsim 2.5\%$ (88%)	$\gtrsim 5.0\%$ (95%)	$\gtrsim 12.5\%$ (50%)
	$\gtrsim 7.5\%$ (99%)	$\gtrsim 10.0\%$ (99%)	$\gtrsim 5.0\%$ (99%)	$\gtrsim 7.5\%$ (99%)	$\gtrsim 100.0\%$ (13%)
FL	$\gtrsim 5.0\%$ (97%)	$\gtrsim 5.0\%$ (75%)	$\gtrsim 2.5\%$ (88%)	$\gtrsim 5.0\%$ (95%)	$\gtrsim 15.0\%$ (50%)
	$\gtrsim 7.5\%$ (99%)	$\gtrsim 10.0\%$ (99%)	$\gtrsim 5.0\%$ (99%)	$\gtrsim 7.5\%$ (99%)	$\gtrsim 100.0\%$ (11%)

Type	$\Delta\text{BR}_{h\tau^+\tau^-}^{\mathbf{S}_1}$	$\Delta\text{BR}_{h\tau^+\tau^-}^{\mathbf{S}_2}$	$\Delta\text{BR}_{h\tau^+\tau^-}^{\mathbf{S}_3}$	$\Delta\text{BR}_{h\tau^+\tau^-}^{\text{OS2}}$	$\Delta\text{BR}_{h\tau^+\tau^-}^{\overline{\text{MS}}}$
I	$\gtrsim 2.5\%$ (98%)	$\gtrsim 2.5\%$ (88%)	$\gtrsim 2.5\%$ (97%)	$\gtrsim 2.5\%$ (98%)	$\gtrsim 7.5\%$ (50%)
	$\gtrsim 5.0\%$ (99%)	$\gtrsim 5.0\%$ (99%)	$\gtrsim 5.0\%$ (99%)	$\gtrsim 5.0\%$ (99%)	$\gtrsim 100.0\%$ (12%)
II	$\gtrsim 5.0\%$ (98%)	$\gtrsim 5.0\%$ (85%)	$\gtrsim 5.0\%$ (96%)	$\gtrsim 2.5\%$ (57%)	$\gtrsim 35.0\%$ (50%)
	$\gtrsim 7.5\%$ (99%)	$\gtrsim 10.0\%$ (97%)	$\gtrsim 10.0\%$ (99%)	$\gtrsim 5.0\%$ (96%)	$\gtrsim 100.0\%$ (34%)
LS	$\gtrsim 5.0\%$ (94%)	$\gtrsim 7.5\%$ (42%)	$\gtrsim 5.0\%$ (95%)	$\gtrsim 5.0\%$ (70%)	$\gtrsim 90.0\%$ (37%)
	$\gtrsim 7.5\%$ (99%)	$\gtrsim 25.0\%$ (96%)	$\gtrsim 7.5\%$ (99%)	$\gtrsim 10.0\%$ (98%)	$\gtrsim 100.0\%$ (58%)
FL	$\gtrsim 5.0\%$ (94%)	$\gtrsim 7.5\%$ (42%)	$\gtrsim 5.0\%$ (95%)	$\gtrsim 5.0\%$ (70%)	$\gtrsim 90.0\%$ (38%)
	$\gtrsim 7.5\%$ (99%)	$\gtrsim 25.0\%$ (96%)	$\gtrsim 7.5\%$ (99%)	$\gtrsim 10.0\%$ (98%)	$\gtrsim 100.0\%$ (58%)

Table 4: Relative size of the EW corrections to the BRs of the 2HDM SM-like Higgs boson h in the four 2HDM types I, II, LS and FL. For details, we refer to the text.

- The results for the OS2 scheme are similar to the ones for the scheme set \mathbf{S}_1 , but depending on the decay and 2HDM type, the majority of corrections are sometimes shifted towards lower/higher bins. Nevertheless, the corrections are moderate and the scheme is numerically stable.
- The results for the $\overline{\text{MS}}$ scheme are typically very large for all decays and 2HDM types and hence clearly demonstrate numerical instability of the renormalization scheme. We find that this is the case throughout all decay channels and mass hierarchies as presented in the following subsections, both for the 2HDM and N2HDM and for all types of the two models. We do not remark this explicitly any more when discussing the various decays and models but only present the corresponding results in the tables.

Overall, with the exception of the $\overline{\text{MS}}$ scheme, the corrections to the SM-like decays are of the typical size of EW corrections with values ranging between below 2.5% up to about 25% depending on the decay, the renormalization scheme and the type of the 2HDM.

4.2.2 H is the SM-like Higgs Boson

In Tab. 5 we show the relative corrections ΔBR for the 2HDM parameter sets where the heavier of the two CP-even Higgs bosons, H , is the SM-like Higgs boson. We want to mention again that in contrast to the case where h is SM-like, we found much less valid parameter points in

Type	$\Delta\text{BR}_{Hb\bar{b}}^{\mathbf{S}_1}$	$\Delta\text{BR}_{Hb\bar{b}}^{\mathbf{S}_2}$	$\Delta\text{BR}_{Hb\bar{b}}^{\mathbf{S}_3}$	$\Delta\text{BR}_{Hb\bar{b}}^{\mathbf{S}_4}$	$\Delta\text{BR}_{Hb\bar{b}}^{\overline{\mathbf{MS}}}$
I	$\gtrsim 2.5\%$ (95%)	$\lesssim 2.5\%$ (100%)	$\gtrsim 2.5\%$ (87%)	$\gtrsim 2.5\%$ (97%)	$\gtrsim 7.5\%$ (50%)
	$\gtrsim 5.0\%$ (100%)		$\gtrsim 5.0\%$ (98%)	$\gtrsim 5.0\%$ (100%)	$\gtrsim 100.0\%$ (4%)
II	$\gtrsim 2.5\%$ (75%)	$\lesssim 2.5\%$ (100%)	$\gtrsim 15.0\%$ (51%)	$\gtrsim 5.0\%$ (74%)	$\gtrsim 75.0\%$ (50%)
	$\gtrsim 5.0\%$ (99%)		$\gtrsim 30.0\%$ (89%)	$\gtrsim 10.0\%$ (99%)	$\gtrsim 100.0\%$ (13%)
LS	$\gtrsim 2.5\%$ (94%)	$\lesssim 2.5\%$ (62%)	$\gtrsim 7.5\%$ (57%)	$\gtrsim 2.5\%$ (96%)	$\gtrsim 90.0\%$ (34%)
	$\gtrsim 5.0\%$ (100%)	$\lesssim 5.0\%$ (100%)	$\gtrsim 20.0\%$ (93%)	$\gtrsim 5.0\%$ (100%)	$\gtrsim 100.0\%$ (63%)
FL	$\gtrsim 2.5\%$ (62%)	$\lesssim 40.0\%$ (50%)	$\gtrsim 10.0\%$ (50%)	$\lesssim 5.0\%$ (50%)	$\lesssim 90.0\%$ (17%)
	$\gtrsim 7.5\%$ (98%)	$\gtrsim 100.0\%$ (23%)	$\lesssim 35.0\%$ (91%)	$\lesssim 15.0\%$ (97%)	$\gtrsim 100.0\%$ (58%)

Type	$\Delta\text{BR}_{H\gamma\gamma/HZZ}^{\mathbf{S}_1}$	$\Delta\text{BR}_{H\gamma\gamma/HZZ}^{\mathbf{S}_2}$	$\Delta\text{BR}_{H\gamma\gamma/HZZ}^{\mathbf{S}_3}$	$\Delta\text{BR}_{H\gamma\gamma/HZZ}^{\mathbf{S}_4}$	$\Delta\text{BR}_{H\gamma\gamma/HZZ}^{\overline{\mathbf{MS}}}$
I	$\lesssim 5.0\%$ (95%)	$\lesssim 2.5\%$ (100%)	$\lesssim 5.0\%$ (86%)	$\lesssim 5.0\%$ (97%)	$\lesssim 17.5\%$ (50%)
	$\gtrsim 100.0\%$ (100%)		$\gtrsim 10.0\%$ (98%)	$\gtrsim 7.5\%$ (100%)	$\gtrsim 100.0\%$ (6%)
II	$\gtrsim 5.0\%$ (82%)	$\lesssim 2.5\%$ (100%)	$\gtrsim 22.5\%$ (55%)	$\gtrsim 7.5\%$ (56%)	$\gtrsim 90.0\%$ (3%)
	$\gtrsim 7.5\%$ (99%)		$\gtrsim 50.0\%$ (92%)	$\gtrsim 15.0\%$ (99%)	$\gtrsim 100.0\%$ (96%)
LS	$\gtrsim 5.0\%$ (77%)	$\lesssim 5.0\%$ (80%)	$\gtrsim 5.0\%$ (48%)	$\gtrsim 5.0\%$ (66%)	$\gtrsim 90.0\%$ (48%)
	$\gtrsim 7.5\%$ (100%)	$\gtrsim 7.5\%$ (100%)	$\gtrsim 20.0\%$ (94%)	$\gtrsim 7.5\%$ (99%)	$\gtrsim 100.0\%$ (51%)
FL	$\gtrsim 5.0\%$ (79%)	$\gtrsim 50.0\%$ (50%)	$\gtrsim 10.0\%$ (44%)	$\gtrsim 7.5\%$ (52%)	$\lesssim 90.0\%$ (1%)
	$\gtrsim 7.5\%$ (98%)	$\gtrsim 100.0\%$ (26%)	$\lesssim 40.0\%$ (90%)	$\lesssim 15.0\%$ (98%)	$\gtrsim 100.0\%$ (98%)

Type	$\Delta\text{BR}_{H\tau^+\tau^-}^{\mathbf{S}_1}$	$\Delta\text{BR}_{H\tau^+\tau^-}^{\mathbf{S}_2}$	$\Delta\text{BR}_{H\tau^+\tau^-}^{\mathbf{S}_3}$	$\Delta\text{BR}_{H\tau^+\tau^-}^{\mathbf{S}_4}$	$\Delta\text{BR}_{H\tau^+\tau^-}^{\overline{\mathbf{MS}}}$
I	$\gtrsim 2.5\%$ (99%)	$\lesssim 2.5\%$ (100%)	$\gtrsim 2.5\%$ (89%)	$\gtrsim 2.5\%$ (99%)	$\lesssim 7.5\%$ (50%)
	$\gtrsim 5.0\%$ (100%)		$\gtrsim 5.0\%$ (99%)	$\gtrsim 5.0\%$ (100%)	$\gtrsim 100.0\%$ (4%)
II	$\gtrsim 2.5\%$ (64%)	$\lesssim 2.5\%$ (100%)	$\gtrsim 10.0\%$ (32%)	$\gtrsim 7.5\%$ (59%)	$\gtrsim 77.5\%$ (50%)
	$\gtrsim 7.5\%$ (99%)		$\gtrsim 30.0\%$ (90%)	$\gtrsim 12.5\%$ (99%)	$\gtrsim 100.0\%$ (13%)
LS	$\gtrsim 5.0\%$ (72%)	$\lesssim 2.5\%$ (88%)	$\gtrsim 62.5\%$ (50%)	$\gtrsim 10.0\%$ (43%)	$\lesssim 90.0\%$ (1%)
	$\gtrsim 15.0\%$ (98%)	$\lesssim 5.0\%$ (100%)	$\gtrsim 100.0\%$ (36%)	$\gtrsim 25.0\%$ (98%)	$\gtrsim 100.0\%$ (98%)
FL	$\gtrsim 5.0\%$ (99%)	$\gtrsim 45.0\%$ (50%)	$\gtrsim 5.0\%$ (48%)	$\lesssim 5.0\%$ (95%)	$\lesssim 90.0\%$ (1%)
	$\gtrsim 7.5\%$ (100%)	$\gtrsim 100.0\%$ (25%)	$\lesssim 50.0\%$ (92%)	$\lesssim 10.0\%$ (98%)	$\gtrsim 100.0\%$ (98%)

Table 5: Relative size of the EW corrections to the BRs of the 2HDM SM-like H in the four 2HDM types I, II, LS and FL. For details, we refer to the text.

the case that H is SM-like and hence, the statistics of the analysis is rather low. For a clear presentation of the results, we grouped renormalization schemes to the following sets:

$$\begin{aligned}
\mathbf{S}_1 &\equiv \{ \text{KOSY}^o, \text{KOSY}^c, p_*^o, p_*^c, \text{pOS}^o, \text{pOS}^c, \text{BFMS} \} \\
\mathbf{S}_2 &\equiv \{ \text{proc1}, \text{proc3} \} \\
\mathbf{S}_3 &\equiv \{ \text{proc2}, \text{OS1} \} \\
\mathbf{S}_4 &\equiv \{ \text{OS2}, \text{OS12} \} \\
\overline{\mathbf{MS}} &\equiv \{ \overline{\mathbf{MS}} \}
\end{aligned}$$

As before, we show results for the decays into $\gamma\gamma$, ZZ , $b\bar{b}$ and $\tau^+\tau^-$. The data in the table allows us to make the following observations:

- The scheme set \mathbf{S}_1 , comprising the KOSY, the pinched and the BFMS schemes, induces the smallest EW corrections for all decays and 2HDM types.
- The process-dependent schemes, collected in the scheme sets \mathbf{S}_2 to \mathbf{S}_4 , induce moderate corrections but for some decays and 2HDM types, they can also lead to very large corrections.

In principle, also decays $H \rightarrow hh$ are possible, with the heavier Higgs boson H being SM-like. Since we did not find enough valid parameter points to reach significant statistics, we do

ΔBR	$b\bar{b}$	$\tau^+\tau^-$	$\mu^+\mu^-$	$s\bar{s}$	$c\bar{c}$	gg	$\gamma\gamma$	$Z\gamma$	W^+W^-	ZZ
	-1.76%	-1.59%	-3.52%	2.24%	-3.81%	4.34%	-2.29%	-0.71%	3.68%	1.61%

Table 6: Relative size of the EW corrections to the BRs of the SM Higgs boson H_{SM} with mass $m_{H_{\text{SM}}} = 125.09$ GeV.

not show results here for this final state, however. In our scan, did not find any parameter points that allow for the OS decay $H \rightarrow ZA$.

4.2.3 Comparison with the SM

We compare our results for the 2HDM with the size of the EW corrections to the decays of the SM Higgs boson H_{SM} with mass $m_{H_{\text{SM}}} = 125.09$ GeV [68]. The decays with and without the EW corrections on top of the QCD corrections (where applicable) have been calculated with HDECAY version 6.52 [36, 37]. By setting the flag 'OMIT ELW' in the input file equal to 0 (1), the EW corrections are computed (omitted). They have been implemented for the decay into gluons [69–71], into the fermion final states $b\bar{b}$, $\tau^+\tau^-$, $\mu^+\mu^-$, $s\bar{s}$, and $c\bar{c}$ [66, 72], into $\gamma\gamma$ [70, 73–75] and into the massive gauge boson final states W^+W^- and ZZ [76–78]. Hence, in the SM also the EW corrections to the loop-induced decays into gg and $\gamma\gamma$ and into the off-shell final states of massive gauge bosons are included. For the decay width into $Z\gamma$ no EW corrections are implemented. Still the BR changes because of the EW-corrected total decay width entering the BR.

The results for the relative corrections ΔBR into the various final states are given in Tab. 6. As can be inferred from the table the relative size of the EW corrections is always small, ranging below 5%, with the maximum value given by 4.34% for the decay into a pair of gluons. The comparison of these results with the relative EW corrections to the 2HDM SM-like Higgs BRs (computed with the renormalization scheme set \mathbf{S}_1 , which delivers the most moderate corrections) shows that in the 2HDM the EW corrections are in general somewhat more important.

4.3 Non-SM-Like CP-even 2HDM Higgs Decays

Next, we consider the decays of the non-SM-like CP-even Higgs bosons, again for the two possible Higgs hierarchies, with the total amount of points that have been used for the analysis as given in Sec. 4.1.

4.3.1 h is the SM-like Higgs boson

With h being SM-like, the non-SM-like CP-even Higgs boson corresponds to the heavier Higgs boson H . Its important decay channels are those into $t\bar{t}$, but also decays into mixed Higgs plus gauge boson final states, *i.e.* ZA and $W^\pm H^\mp$, can become important if they are kinematically allowed. In contrast to the SM-like decays presented above, for the relative corrections ΔBR of individual final states we now consider only the parameter points for which the decays are OS and not loop-induced. This reduces the number of points available for the analysis as shown in Tab. 7 where we list the numbers for the individual final states that are left over with the additional requirement of the decays being OS. The relative corrections ΔBR for the decays into $b\bar{b}$, $t\bar{t}$, $\tau^+\tau^-$, ZA and $W^\pm H^\mp$ are given in Tab. 8, and those for the decays into ZZ and into two light Higgs bosons hh in Tab. 9. For simplicity, we do not list the relative corrections to the

Type	$H \rightarrow t\bar{t}$	$H \rightarrow ZA$	$H \rightarrow W^\pm H^\mp$	$H \rightarrow ZZ$	$H \rightarrow hh$
I	166 444	10 406	7600	186 474	179 777
II	239 747	19 464	12 569	239 759	239 755
LS	365 299	14 506	10 898	369 448	168 129
FL	419 079	12 388	8472	419 149	289 146

Table 7: Number of parameter points available for the analysis in the individual OS decay channels of H (h is SM-like).

WW final state separately here, as they behave similarly to those of the ZZ final state.

The scheme sets with comparable sizes in the EW corrections, shown in the table, are defined as follows:

$$\begin{aligned}
\mathbf{S}_1 &\equiv \{ \text{KOSY}^o, \text{KOSY}^c, \text{pOS}^o, \text{pOS}^c, \text{BFMS} \} \\
\mathbf{S}_2 &\equiv \{ \text{p}_*^o, \text{p}_*^c \} \\
\mathbf{S}_3 &\equiv \{ \text{proc1}, \text{proc2}, \text{proc3}, \text{OS1} \} \\
\mathbf{S}_4 &\equiv \{ \text{OS2}, \text{OS12} \} \\
\overline{\mathbf{MS}} &\equiv \{ \overline{\mathbf{MS}} \}
\end{aligned}$$

From the tables, we deduce the following:

- For all renormalization schemes apart from the $\overline{\mathbf{MS}}$ scheme, the corrections to the decays into the fermionic final states as well as to into ZA and $H^\pm W^\mp$ are mostly of moderate size. Depending on the scheme and 2HDM type they can become also significant, however, with relative corrections of up to 40%. The process-dependent schemes summarized in the sets \mathbf{S}_3 and \mathbf{S}_4 have larger maximal correction values than the schemes of \mathbf{S}_1 and \mathbf{S}_2 which exploit the symmetries of the model.
- The corrections to the (typically dominant) decay $H \rightarrow t\bar{t}$ are the most moderate ones which is due to the relatively large BR already at tree level.
- The decays $H \rightarrow ZZ$ and $H \rightarrow hh$ typically feature huge EW corrections. For the decay into ZZ , this is mostly due to the smallness of the tree-level width which is proportional to $c_{\beta-\alpha}^2$. As h behaves SM-like, its coupling to massive gauge bosons, proportional to $s_{\beta-\alpha}^2$, is close to one, so that the branching ratio for the decay of H into ZZ/WW is almost zero.⁸ Therefore, the relative EW corrections become large. Another reason for the large corrections can be parametrically enhanced counterterm contributions that arise due to small coupling constants (due to the sum rules) in the denominator that are multiplied by the counterterms, or the counterterms themselves become large.

For the decay into hh , the dominant effect that enhances the EW corrections are non-decoupling effects, inducing parametrically enhanced EW corrections to the Higgs-to-Higgs decays. This has been discussed in detail in [22, 26, 33]. Such enhanced corrections call for the resummation of all orders of perturbation theory, which is beyond the phenomenological investigation performed here. Recently, the two-loop corrections to the Higgs trilinear

⁸We note that in the computation of the EW-corrected decay width we only include one-loop terms proportional to the product of the tree-level and the one-loop amplitude. We do not include terms proportional to the squared one-loop amplitude, as might be considered if the tree-level decay width is small. These terms are formally of two-loop order so that we chose not to include them.

Type	$\Delta\text{BR}_{Hb\bar{b}}^{S_1}$	$\Delta\text{BR}_{Hb\bar{b}}^{S_2}$	$\Delta\text{BR}_{Hb\bar{b}}^{S_3}$	$\Delta\text{BR}_{Hb\bar{b}}^{S_4}$	$\Delta\text{BR}_{Hb\bar{b}}^{\text{MS}}$
I	\lesssim 15.0% (48%)	\lesssim 12.5% (52%)	\lesssim 12.5% (48%)	\lesssim 10.0% (45%)	\lesssim 60.0% (50%)
	\gtrsim 27.5% (93%)	\gtrsim 35.0% (89%)	\gtrsim 40.0% (80%)	\gtrsim 35.0% (89%)	\gtrsim 100.0% (40%)
II	\lesssim 10.0% (52%)	\lesssim 20.0% (48%)	\lesssim 10.0% (52%)	\lesssim 25.0% (44%)	\lesssim 90.0% (14%)
	\gtrsim 25.0% (92%)	\gtrsim 32.5% (93%)	\gtrsim 35.0% (91%)	\gtrsim 42.5% (88%)	\gtrsim 100.0% (85%)
LS	\lesssim 10.0% (52%)	\lesssim 10.0% (52%)	\lesssim 10.0% (46%)	\lesssim 7.5% (42%)	\lesssim 45.0% (50%)
	\gtrsim 25.0% (92%)	\gtrsim 25.0% (92%)	\gtrsim 30.0% (90%)	\gtrsim 22.5% (90%)	\gtrsim 100.0% (36%)
FL	\lesssim 12.5% (52%)	\lesssim 10.0% (52%)	\lesssim 10.0% (46%)	\lesssim 7.5% (42%)	\lesssim 45.0% (50%)
	\gtrsim 32.5% (88%)	\gtrsim 25.0% (92%)	\gtrsim 30.0% (90%)	\gtrsim 22.5% (90%)	\gtrsim 100.0% (36%)
Type	$\Delta\text{BR}_{Ht\bar{t}}^{S_1}$	$\Delta\text{BR}_{Ht\bar{t}}^{S_2}$	$\Delta\text{BR}_{Ht\bar{t}}^{S_3}$	$\Delta\text{BR}_{Ht\bar{t}}^{S_4}$	$\Delta\text{BR}_{Ht\bar{t}}^{\text{MS}}$
I	\lesssim 5.0% (48%)	\lesssim 7.5% (58%)	\lesssim 7.5% (54%)	\lesssim 5.0% (50%)	\lesssim 52.5% (50%)
	\gtrsim 22.5% (85%)	\gtrsim 22.5% (85%)	\gtrsim 25.0% (80%)	\gtrsim 25.0% (88%)	\gtrsim 100.0% (36%)
II	\lesssim 2.5% (60%)	\lesssim 2.5% (60%)	\lesssim 2.5% (55%)	\lesssim 2.5% (61%)	\lesssim 37.5% (50%)
	\gtrsim 10.0% (86%)	\gtrsim 10.0% (86%)	\gtrsim 12.5% (87%)	\gtrsim 10.0% (87%)	\gtrsim 100.0% (33%)
LS	\lesssim 5.0% (61%)	\lesssim 2.5% (46%)	\lesssim 5.0% (54%)	\lesssim 2.5% (47%)	\lesssim 45.0% (50%)
	\gtrsim 15.0% (88%)	\gtrsim 15.0% (87%)	\gtrsim 20.0% (88%)	\gtrsim 15.0% (88%)	\gtrsim 100.0% (35%)
FL	\lesssim 5.0% (68%)	\lesssim 5.0% (68%)	\lesssim 5.0% (56%)	\lesssim 2.5% (54%)	\lesssim 50.0% (50%)
	\gtrsim 12.5% (87%)	\gtrsim 12.5% (87%)	\gtrsim 20.0% (87%)	\gtrsim 12.5% (87%)	\gtrsim 100.0% (39%)
Type	$\Delta\text{BR}_{H\tau^+\tau^-}^{S_1}$	$\Delta\text{BR}_{H\tau^+\tau^-}^{S_2}$	$\Delta\text{BR}_{H\tau^+\tau^-}^{S_3}$	$\Delta\text{BR}_{H\tau^+\tau^-}^{S_4}$	$\Delta\text{BR}_{H\tau^+\tau^-}^{\text{MS}}$
I	\lesssim 15.0% (49%)	\lesssim 15.0% (51%)	\lesssim 15.0% (48%)	\lesssim 15.0% (55%)	\lesssim 60.0% (50%)
	\gtrsim 35.0% (88%)	\gtrsim 35.0% (88%)	\gtrsim 35.0% (77%)	\gtrsim 35.0% (88%)	\gtrsim 100.0% (40%)
II	\lesssim 15.0% (54%)	\lesssim 20.0% (53%)	\lesssim 10.0% (51%)	\lesssim 25.0% (47%)	\lesssim 85.0% (14%)
	\gtrsim 25.0% (91%)	\gtrsim 30.0% (90%)	\gtrsim 35.0% (90%)	\gtrsim 40.0% (86%)	\gtrsim 100.0% (84%)
LS	\lesssim 15.0% (54%)	\lesssim 17.5% (48%)	\lesssim 7.5% (46%)	\lesssim 25.0% (46%)	\lesssim 77.5% (15%)
	\gtrsim 27.5% (90%)	\gtrsim 30.0% (88%)	\gtrsim 30.0% (88%)	\gtrsim 40.0% (85%)	\gtrsim 100.0% (81%)
FL	\lesssim 15.0% (55%)	\lesssim 17.5% (48%)	\lesssim 7.5% (46%)	\lesssim 25.0% (46%)	\lesssim 77.5% (15%)
	\gtrsim 27.5% (90%)	\gtrsim 30.0% (88%)	\gtrsim 30.0% (88%)	\gtrsim 40.0% (85%)	\gtrsim 100.0% (81%)
Type	$\Delta\text{BR}_{HZA}^{S_1}$	$\Delta\text{BR}_{HZA}^{S_2}$	$\Delta\text{BR}_{HZA}^{S_3}$	$\Delta\text{BR}_{HZA}^{S_4}$	$\Delta\text{BR}_{HZA}^{\text{MS}}$
I	\lesssim 5.0% (51%)	\lesssim 5.0% (51%)	\lesssim 10.0% (46%)	\lesssim 10.0% (53%)	\lesssim 80.0% (26%)
	\gtrsim 15.0% (80%)	\gtrsim 15.0% (80%)	\gtrsim 30.0% (80%)	\gtrsim 22.5% (83%)	\gtrsim 100.0% (52%)
II	\lesssim 5.0% (68%)	\lesssim 5.0% (69%)	\lesssim 10.0% (50%)	\lesssim 7.5% (73%)	\lesssim 85.0% (20%)
	\gtrsim 10.0% (91%)	\gtrsim 12.5% (94%)	\gtrsim 25.0% (81%)	\gtrsim 10.0% (90%)	\gtrsim 100.0% (56%)
LS	\lesssim 5.0% (65%)	\lesssim 5.0% (65%)	\lesssim 10.0% (48%)	\lesssim 7.5% (41%)	\lesssim 85.0% (29%)
	\gtrsim 10.0% (86%)	\gtrsim 10.0% (86%)	\gtrsim 27.5% (80%)	\gtrsim 15.0% (90%)	\gtrsim 100.0% (44%)
FL	\lesssim 5.0% (65%)	\lesssim 5.0% (63%)	\lesssim 10.0% (53%)	\lesssim 7.5% (51%)	\lesssim 82.5% (20%)
	\gtrsim 10.0% (88%)	\gtrsim 10.0% (88%)	\gtrsim 15.0% (83%)	\gtrsim 10.0% (84%)	\gtrsim 100.0% (30%)
Type	$\Delta\text{BR}_{HW^\pm H^\mp}^{S_1}$	$\Delta\text{BR}_{HW^\pm H^\mp}^{S_2}$	$\Delta\text{BR}_{HW^\pm H^\mp}^{S_3}$	$\Delta\text{BR}_{HW^\pm H^\mp}^{S_4}$	$\Delta\text{BR}_{HW^\pm H^\mp}^{\text{MS}}$
I	\lesssim 5.0% (56%)	\lesssim 5.0% (55%)	\lesssim 10.0% (49%)	\lesssim 10.0% (57%)	\lesssim 70.0% (25%)
	\gtrsim 17.5% (81%)	\gtrsim 17.5% (81%)	\gtrsim 30.0% (78%)	\gtrsim 25.0% (82%)	\gtrsim 100.0% (52%)
II	\lesssim 5.0% (60%)	\lesssim 5.0% (59%)	\lesssim 12.5% (49%)	\lesssim 5.0% (55%)	\lesssim 82.5% (18%)
	\gtrsim 10.0% (87%)	\gtrsim 10.0% (85%)	\gtrsim 30.0% (81%)	\gtrsim 10.0% (94%)	\gtrsim 100.0% (50%)
LS	\lesssim 5.0% (71%)	\lesssim 5.0% (70%)	\lesssim 12.5% (52%)	\lesssim 7.5% (57%)	\lesssim 75.0% (26%)
	\gtrsim 7.5% (84%)	\gtrsim 7.5% (84%)	\gtrsim 27.5% (81%)	\gtrsim 12.5% (85%)	\gtrsim 100.0% (45%)
FL	\lesssim 5.0% (67%)	\lesssim 5.0% (62%)	\lesssim 7.5% (48%)	\lesssim 5.0% (53%)	\lesssim 82.5% (19%)
	\gtrsim 7.5% (85%)	\gtrsim 7.5% (84%)	\gtrsim 15.0% (87%)	\gtrsim 10.0% (95%)	\gtrsim 100.0% (36%)

Table 8: Relative size of the EW corrections to the BRs for the non-SM-like 2HDM Higgs boson H decays into $b\bar{b}$, $t\bar{t}$, $\tau^+\tau^-$, ZA , $W^\pm H^\mp$, in the four 2HDM types I, II, LS and FL (h is SM-like).

Type	$\Delta\text{BR}_{HZZ}^{\mathcal{S}_1}$	$\Delta\text{BR}_{HZZ}^{\mathcal{S}_2}$	$\Delta\text{BR}_{HZZ}^{\mathcal{S}_3}$	$\Delta\text{BR}_{HZZ}^{\mathcal{S}_4}$	$\Delta\text{BR}_{HZZ}^{\overline{\text{MS}}}$
I	$\gtrsim 47.5\%$ (50%)	$\gtrsim 45.0\%$ (50%)	$\gtrsim 90.0\%$ (48%)	$\gtrsim 52.5\%$ (50%)	$\gtrsim 80.0\%$ (44%)
	$\gtrsim 100.0\%$ (29%)	$\gtrsim 100.0\%$ (29%)	$\gtrsim 100.0\%$ (49%)	$\gtrsim 100.0\%$ (32%)	$\gtrsim 100.0\%$ (50%)
II	$\gtrsim 62.5\%$ (50%)	$\gtrsim 60.0\%$ (50%)	$\gtrsim 90.0\%$ (22%)	$\gtrsim 82.5\%$ (35%)	$\gtrsim 82.5\%$ (34%)
	$\gtrsim 100.0\%$ (39%)	$\gtrsim 100.0\%$ (39%)	$\gtrsim 100.0\%$ (76%)	$\gtrsim 100.0\%$ (59%)	$\gtrsim 100.0\%$ (61%)
LS	$\gtrsim 67.5\%$ (50%)	$\gtrsim 65.0\%$ (50%)	$\gtrsim 90.0\%$ (30%)	$\gtrsim 80.0\%$ (50%)	$\gtrsim 80.0\%$ (38%)
	$\gtrsim 100.0\%$ (38%)	$\gtrsim 100.0\%$ (37%)	$\gtrsim 100.0\%$ (68%)	$\gtrsim 100.0\%$ (43%)	$\gtrsim 100.0\%$ (56%)
FL	$\gtrsim 90.0\%$ (40%)	$\gtrsim 90.0\%$ (40%)	$\gtrsim 90.0\%$ (30%)	$\gtrsim 82.5\%$ (35%)	$\gtrsim 80.0\%$ (38%)
	$\gtrsim 100.0\%$ (57%)	$\gtrsim 100.0\%$ (57%)	$\gtrsim 100.0\%$ (68%)	$\gtrsim 100.0\%$ (60%)	$\gtrsim 100.0\%$ (56%)

Type	$\Delta\text{BR}_{Hhh}^{\mathcal{S}_1}$	$\Delta\text{BR}_{Hhh}^{\mathcal{S}_2}$	$\Delta\text{BR}_{Hhh}^{\mathcal{S}_3}$	$\Delta\text{BR}_{Hhh}^{\mathcal{S}_4}$	$\Delta\text{BR}_{Hhh}^{\overline{\text{MS}}}$
I	$\gtrsim 90.0\%$ (28%)	$\gtrsim 90.0\%$ (28%)	$\gtrsim 90.0\%$ (25%)	$\gtrsim 82.5\%$ (27%)	$\gtrsim 85.0\%$ (44%)
	$\gtrsim 100.0\%$ (70%)	$\gtrsim 100.0\%$ (70%)	$\gtrsim 100.0\%$ (73%)	$\gtrsim 100.0\%$ (69%)	$\gtrsim 100.0\%$ (53%)
II	$\gtrsim 90.0\%$ (10%)	$\gtrsim 90.0\%$ (10%)	$\gtrsim 90.0\%$ (8%)	$\gtrsim 85.0\%$ (10%)	$\gtrsim 87.5\%$ (35%)
	$\gtrsim 100.0\%$ (89%)	$\gtrsim 100.0\%$ (89%)	$\gtrsim 100.0\%$ (91%)	$\gtrsim 100.0\%$ (88%)	$\gtrsim 100.0\%$ (63%)
LS	$\gtrsim 90.0\%$ (20%)	$\gtrsim 90.0\%$ (21%)	$\gtrsim 85.0\%$ (15%)	$\gtrsim 85.0\%$ (20%)	$\gtrsim 85.0\%$ (40%)
	$\gtrsim 100.0\%$ (78%)	$\gtrsim 100.0\%$ (78%)	$\gtrsim 100.0\%$ (83%)	$\gtrsim 100.0\%$ (77%)	$\gtrsim 100.0\%$ (57%)
FL	$\gtrsim 90.0\%$ (14%)	$\gtrsim 90.0\%$ (14%)	$\gtrsim 85.0\%$ (8%)	$\gtrsim 90.0\%$ (14%)	$\gtrsim 85.0\%$ (38%)
	$\gtrsim 100.0\%$ (84%)	$\gtrsim 100.0\%$ (85%)	$\gtrsim 100.0\%$ (90%)	$\gtrsim 100.0\%$ (84%)	$\gtrsim 100.0\%$ (59%)

Table 9: Relative size of the EW corrections to the BRs for the non-SM-like 2HDM Higgs boson H decays into ZZ , and hh , in the four 2HDM types I, II, LS and FL (h is SM-like).

couplings in extended scalar sectors have been calculated in [79,80]. The authors find that they remain smaller than the one-loop corrections so that the large deviations predicted at one-loop level do not change significantly. In [22] where we investigated in detail the non-decoupling effects in the EW corrections to the Higgs-to-Higgs decays we also provided parameter scenarios where we are truly in the decoupling limit and find decent EW corrections. Finding such scenarios required a dedicated scan. On the other hand, for this work we performed a scan without demanding special parameter features and hence our sample of valid points does not contain such specific parameter configurations. For an exemplary analysis in the decoupling regime, we therefore refer to Ref. [22].

Note, finally, that these huge corrections also indirectly affect the ΔBR of the other decay channels through the total width, namely the decays with smaller BRs. This also explains their larger values of ΔBR in some cases.

4.3.2 H is the SM-like Higgs boson

In case that the lighter CP-even Higgs boson h is the non-SM-like Higgs boson many decay channels are kinematically closed. In Tab. 10 we show the relative corrections ΔBR for the OS decays into $b\bar{b}$ and $\tau^+\tau^-$. The schemes that are grouped together in scheme sets are as follows:

$$\begin{aligned}
\mathcal{S}_1 &\equiv \{ \text{KOSY}^o, \text{KOSY}^c, \text{p}_*^o, \text{p}_*^c, \text{pOS}^o, \text{pOS}^c, \text{BFMS} \} \\
\mathcal{S}_2 &\equiv \{ \text{proc1}, \text{proc3} \} \\
\mathcal{S}_3 &\equiv \{ \text{proc2}, \text{OS1} \} \\
\mathcal{S}_4 &\equiv \{ \text{OS2}, \text{OS12} \} \\
\overline{\text{MS}} &\equiv \{ \overline{\text{MS}} \}
\end{aligned}$$

From the table, we read off:

Type	$\Delta\text{BR}_{h\bar{b}\bar{b}}^{\mathbf{S}_1}$	$\Delta\text{BR}_{h\bar{b}\bar{b}}^{\mathbf{S}_2}$	$\Delta\text{BR}_{h\bar{b}\bar{b}}^{\mathbf{S}_3}$	$\Delta\text{BR}_{h\bar{b}\bar{b}}^{\mathbf{S}_4}$	$\Delta\text{BR}_{h\bar{b}\bar{b}}^{\overline{\mathbf{MS}}}$
I	$\gtrsim 2.5\%$ (91%) $\gtrsim 10.0\%$ (96%)	$\gtrsim 5.0\%$ (61%) $\gtrsim 40.0\%$ (90%)	$\gtrsim 2.5\%$ (91%) $\gtrsim 15.0\%$ (97%)	$\gtrsim 2.5\%$ (91%) $\gtrsim 15.0\%$ (98%)	$\gtrsim 10.0\%$ (50%) $\gtrsim 100.0\%$ (12%)
II	$\gtrsim 2.5\%$ (100%)	$\gtrsim 2.5\%$ (100%)	$\gtrsim 2.5\%$ (100%)	$\gtrsim 2.5\%$ (100%)	$\gtrsim 2.5\%$ (77%) $\gtrsim 100.0\%$ (3%)
LS	$\gtrsim 10.0\%$ (67%) $\gtrsim 20.0\%$ (99%)	$\gtrsim 7.5\%$ (63%) $\gtrsim 20.0\%$ (98%)	$\gtrsim 50.0\%$ (50%) $\gtrsim 90.0\%$ (69%)	$\gtrsim 17.5\%$ (49%) $\gtrsim 30.0\%$ (97%)	$\gtrsim 90.0\%$ (18%) $\gtrsim 100.0\%$ (79%)
FL	$\gtrsim 2.5\%$ (100%)	$\gtrsim 2.5\%$ (96%) $\gtrsim 7.5\%$ (99%)	$\gtrsim 2.5\%$ (100%)	$\gtrsim 2.5\%$ (100%)	$\gtrsim 2.5\%$ (73%) $\gtrsim 100.0\%$ (3%)

Type	$\Delta\text{BR}_{h\tau^+\tau^-}^{\mathbf{S}_1}$	$\Delta\text{BR}_{h\tau^+\tau^-}^{\mathbf{S}_2}$	$\Delta\text{BR}_{h\tau^+\tau^-}^{\mathbf{S}_3}$	$\Delta\text{BR}_{h\tau^+\tau^-}^{\mathbf{S}_4}$	$\Delta\text{BR}_{h\tau^+\tau^-}^{\overline{\mathbf{MS}}}$
I	$\gtrsim 7.5\%$ (93%) $\gtrsim 20.0\%$ (98%)	$\gtrsim 5.0\%$ (51%) $\gtrsim 35.0\%$ (87%)	$\gtrsim 5.0\%$ (83%) $\gtrsim 15.0\%$ (98%)	$\gtrsim 5.0\%$ (86%) $\gtrsim 10.0\%$ (97%)	$\gtrsim 12.5\%$ (63%) $\gtrsim 100.0\%$ (12%)
II	$\gtrsim 2.5\%$ (100%)	$\gtrsim 2.5\%$ (100%)	$\gtrsim 2.5\%$ (100%)	$\gtrsim 2.5\%$ (96%) $\gtrsim 5.0\%$ (100%)	$\gtrsim 2.5\%$ (74%) $\gtrsim 100.0\%$ (3%)
LS	$\gtrsim 2.5\%$ (94%) $\gtrsim 7.5\%$ (100%)	$\gtrsim 2.5\%$ (91%) $\gtrsim 10.0\%$ (98%)	$\gtrsim 2.5\%$ (83%) $\gtrsim 15.0\%$ (97%)	$\gtrsim 2.5\%$ (88%) $\gtrsim 10.0\%$ (97%)	$\gtrsim 2.5\%$ (64%) $\gtrsim 100.0\%$ (13%)
FL	$\gtrsim 5.0\%$ (96%) $\gtrsim 10.0\%$ (98%)	$\gtrsim 77.5\%$ (50%) $\gtrsim 100.0\%$ (43%)	$\gtrsim 35.0\%$ (52%) $\gtrsim 60.0\%$ (98%)	$\gtrsim 15.0\%$ (49%) $\gtrsim 30.0\%$ (100%)	$\gtrsim 90.0\%$ (24%) $\gtrsim 100.0\%$ (73%)

Table 10: Relative size of the EW corrections to the BRs for the non-SM-like 2HDM Higgs boson h decays into $b\bar{b}$ and $\tau^+\tau^-$, in the four 2HDM types I, II, LS and FL (H is SM-like).

Type	$A \rightarrow t\bar{t}$	$A \rightarrow Zh$	$A \rightarrow ZH$
I	176 057	183 927	101 561
II	239 750	239 756	87 004
LS	238 520	239 122	95 863
FL	219 123	219 146	108 082

Table 11: Number of parameter points available for the analysis in the individual OS decay channels of the pseudoscalar Higgs boson A (h is SM-like).

- For the renormalization schemes exploiting the symmetries of the Lagrangian, grouped together in \mathbf{S}_1 , the EW corrections are of moderate size, not exceeding 20%.
- The process-dependent renormalization schemes, *cf.* sets \mathbf{S}_2 , \mathbf{S}_3 , and \mathbf{S}_4 , in general also lead to moderate corrections. For some decays and 2HDM types, however, the corrections become very large. Note, however, that these claims are based on the very low statistics stemming from the low amount of input parameter sets used.

4.4 Pseudoscalar 2HDM Decays

4.4.1 h is the SM-like Higgs boson

We turn to the decays of the pseudoscalar Higgs boson A for the input parameter sets where h is SM-like. Besides the usual fermionic decays, A can also decay into a mixed gauge boson plus Higgs boson final state. Electroweak corrections are computed only for OS decays so that the number of available parameter points reduces as shown in Tab. 11. In Tab. 12, the relative corrections ΔBR for the pseudoscalar decays into $b\bar{b}$, $\tau^+\tau^-$ and $t\bar{t}$ as well as in the gauge boson plus Higgs boson final states Zh and ZH are given for the case that h is SM-like, for all four 2HDM types. The scheme sets shown in the table are defined as follows:

$$\mathbf{S}_1 \equiv \{ \text{KOSY}^o, \text{KOSY}^c, \text{pOS}^o, \text{pOS}^c \}$$

$$\begin{aligned}
\mathbf{S}_2 &\equiv \{ p_*^o, p_*^c \} \\
\mathbf{S}_3 &\equiv \{ \text{proc1}, \text{proc2}, \text{proc3}, \text{OS1}, \text{OS2} \} \\
\mathbf{OS12} &\equiv \{ \text{OS12} \} \\
\mathbf{BFMS} &\equiv \{ \text{BFMS} \} \\
\overline{\mathbf{MS}} &\equiv \{ \overline{\text{MS}} \}
\end{aligned}$$

With A being above the $t\bar{t}$ threshold, the decay $A \rightarrow t\bar{t}$ is in general the dominant decay channel and consequently also the EW corrections are the most moderate ones compared to the other final states. The corrections to $b\bar{b}$ and $\tau^+\tau^-$ are larger, but still of moderate size for the renormalization scheme sets \mathbf{S}_1 and \mathbf{BFMS} . These two scheme sets show the smallest corrections throughout all decays and 2HDM types. This implies a good numerical stability through large parts of the parameter space and for all considered decay channels.

The decay $A \rightarrow Zh$ features relatively large electroweak corrections for all 2HDM types and scheme sets, with a lot of points leading to corrections above $\pm 100\%$. Again, several effects may be responsible for this behaviour. The decay width is proportional to $c_{\beta-\alpha}^2$ which is very small in case that h is SM-like since then, $s_{\beta-\alpha}$ is close to 1. The tree-level BR of $A \rightarrow Zh$ is hence very small, so that the relative EW corrections blow up. Moreover, the corrections can also be parametrically enhanced in this corner of the parameter space and the counterterms themselves can become large. The BR of the decay $A \rightarrow ZH$ on the other hand can become important so that here the EW corrections are of moderate size.

4.4.2 H is the SM-like Higgs boson

As mentioned before, the amount of parameter points available reduces considerably in case that the SM-like Higgs boson corresponds to H , *cf.* Eq. (4.39), and hence the statistics for these scenarios is rather low. The amount of available parameter points is even further reduced by the requirement of the decays to be OS. The corresponding number of scenarios that we can use in the individual channels are listed in Tab. 13. The relative corrections ΔBR are given in Tab. 14. The scheme sets shown in the table have been combined according to:

$$\begin{aligned}
\mathbf{S}_1 &\equiv \{ \text{KOSY}^o, \text{KOSY}^c, \text{pOS}^o, \text{pOS}^c, p_*^o, p_*^c, \text{BFMS} \} \\
\mathbf{S}_2 &\equiv \{ \text{proc1}, \text{proc2} \} \\
\mathbf{S}_3 &\equiv \{ \text{OS2}, \text{OS12} \} \\
\mathbf{proc3} &\equiv \{ \text{proc3} \} \\
\mathbf{OS1} &\equiv \{ \text{OS1} \} \\
\overline{\mathbf{MS}} &\equiv \{ \overline{\text{MS}} \}
\end{aligned}$$

As can be inferred from Tab. 14, the results for the *proc3* and *OS1* schemes are typically very large for all decays and hence indicate numerical instability of these renormalization schemes and for the considered decay channels. The results computed within the other schemes are typically of medium size in the fermionic final states. The BRs into Zh are more important now. Since H is SM-like, we typically have $c_{\beta-\alpha}$ close to 1 so that the decay into Zh , whose EW corrections are proportional to $c_{\beta-\alpha}^2$, is not suppressed, while the BR for the decay into ZH is typically very small. This is reflected in the relative corrections of the BRs which for the Zh final state are the smallest among all decays whereas for the decay into ZH , they become very large. In

Type	$\Delta\text{BR}_{Abb}^{S_1}$	$\Delta\text{BR}_{Abb}^{S_2}$	$\Delta\text{BR}_{Abb}^{S_3}$	$\Delta\text{BR}_{Abb}^{\text{OS12}}$	$\Delta\text{BR}_{Abb}^{\text{BFMS}}$	$\Delta\text{BR}_{Abb}^{\text{MS}}$
I	$\gtrsim 7.5\%$ (53%)	$\gtrsim 7.5\%$ (55%)	$\gtrsim 5.0\%$ (40%)	$\gtrsim 5.0\%$ (40%)	$\gtrsim 7.5\%$ (46%)	$\gtrsim 37.5\%$ (50%)
	$\gtrsim 17.5\%$ (95%)	$\gtrsim 17.5\%$ (94%)	$\gtrsim 17.5\%$ (86%)	$\gtrsim 17.5\%$ (86%)	$\gtrsim 20.0\%$ (96%)	$\gtrsim 100.0\%$ (36%)
II	$\gtrsim 10.0\%$ (45%)	$\gtrsim 17.5\%$ (50%)	$\gtrsim 12.5\%$ (47%)	$\gtrsim 15.0\%$ (44%)	$\gtrsim 7.5\%$ (37%)	$\gtrsim 50.0\%$ (2%)
	$\gtrsim 22.5\%$ (96%)	$\gtrsim 30.0\%$ (94%)	$\gtrsim 30.0\%$ (82%)	$\gtrsim 27.5\%$ (89%)	$\gtrsim 25.0\%$ (97%)	$\gtrsim 100.0\%$ (95%)
LS	$\gtrsim 7.5\%$ (49%)	$\gtrsim 7.5\%$ (54%)	$\gtrsim 7.5\%$ (48%)	$\gtrsim 7.5\%$ (48%)	$\gtrsim 7.5\%$ (46%)	$\gtrsim 32.5\%$ (50%)
	$\gtrsim 17.5\%$ (94%)	$\gtrsim 17.5\%$ (95%)	$\gtrsim 25.0\%$ (95%)	$\gtrsim 25.0\%$ (95%)	$\gtrsim 20.0\%$ (96%)	$\gtrsim 100.0\%$ (30%)
FL	$\gtrsim 10.0\%$ (45%)	$\gtrsim 17.5\%$ (50%)	$\gtrsim 30.0\%$ (50%)	$\gtrsim 17.5\%$ (44%)	$\gtrsim 7.5\%$ (50%)	$\gtrsim 55.0\%$ (2%)
	$\gtrsim 22.5\%$ (96%)	$\gtrsim 30.0\%$ (94%)	$\gtrsim 50.0\%$ (89%)	$\gtrsim 30.0\%$ (94%)	$\gtrsim 20.0\%$ (98%)	$\gtrsim 100.0\%$ (94%)
Type	$\Delta\text{BR}_{At\bar{t}}^{S_1}$	$\Delta\text{BR}_{At\bar{t}}^{S_2}$	$\Delta\text{BR}_{At\bar{t}}^{S_3}$	$\Delta\text{BR}_{At\bar{t}}^{\text{OS12}}$	$\Delta\text{BR}_{At\bar{t}}^{\text{BFMS}}$	$\Delta\text{BR}_{At\bar{t}}^{\text{MS}}$
I	$\gtrsim 2.5\%$ (87%)	$\gtrsim 2.5\%$ (90%)	$\gtrsim 2.5\%$ (60%)	$\gtrsim 2.5\%$ (83%)	$\gtrsim 2.5\%$ (83%)	$\gtrsim 45.0\%$ (50%)
	$\gtrsim 5.0\%$ (95%)	$\gtrsim 5.0\%$ (95%)	$\gtrsim 10.0\%$ (85%)	$\gtrsim 5.0\%$ (92%)	$\gtrsim 5.0\%$ (90%)	$\gtrsim 100.0\%$ (35%)
II	$\gtrsim 2.5\%$ (96%)	$\gtrsim 2.5\%$ (97%)	$\gtrsim 2.5\%$ (82%)	$\gtrsim 2.5\%$ (94%)	$\gtrsim 2.5\%$ (95%)	$\gtrsim 17.5\%$ (50%)
	$\gtrsim 5.0\%$ (99%)	$\gtrsim 5.0\%$ (99%)	$\gtrsim 7.5\%$ (93%)	$\gtrsim 2.5\%$ (98%)	$\gtrsim 5.0\%$ (98%)	$\gtrsim 100.0\%$ (20%)
LS	$\gtrsim 2.5\%$ (93%)	$\gtrsim 2.5\%$ (95%)	$\gtrsim 2.5\%$ (72%)	$\gtrsim 2.5\%$ (92%)	$\gtrsim 2.5\%$ (91%)	$\gtrsim 35.0\%$ (50%)
	$\gtrsim 5.0\%$ (98%)	$\gtrsim 5.0\%$ (98%)	$\gtrsim 10.0\%$ (90%)	$\gtrsim 5.0\%$ (97%)	$\gtrsim 5.0\%$ (96%)	$\gtrsim 100.0\%$ (30%)
FL	$\gtrsim 2.5\%$ (93%)	$\gtrsim 2.5\%$ (95%)	$\gtrsim 2.5\%$ (76%)	$\gtrsim 2.5\%$ (92%)	$\gtrsim 2.5\%$ (91%)	$\gtrsim 40.0\%$ (50%)
	$\gtrsim 5.0\%$ (98%)	$\gtrsim 5.0\%$ (98%)	$\gtrsim 7.5\%$ (90%)	$\gtrsim 5.0\%$ (96%)	$\gtrsim 5.0\%$ (96%)	$\gtrsim 100.0\%$ (31%)
Type	$\Delta\text{BR}_{A\tau^+\tau^-}^{S_1}$	$\Delta\text{BR}_{A\tau^+\tau^-}^{S_2}$	$\Delta\text{BR}_{A\tau^+\tau^-}^{S_3}$	$\Delta\text{BR}_{A\tau^+\tau^-}^{\text{OS12}}$	$\Delta\text{BR}_{A\tau^+\tau^-}^{\text{BFMS}}$	$\Delta\text{BR}_{A\tau^+\tau^-}^{\text{MS}}$
I	$\gtrsim 10.0\%$ (50%)	$\gtrsim 10.0\%$ (55%)	$\gtrsim 7.5\%$ (45%)	$\gtrsim 10.0\%$ (64%)	$\gtrsim 10.0\%$ (45%)	$\gtrsim 47.5\%$ (50%)
	$\gtrsim 20.0\%$ (97%)	$\gtrsim 20.0\%$ (97%)	$\gtrsim 17.5\%$ (93%)	$\gtrsim 17.5\%$ (93%)	$\gtrsim 25.0\%$ (97%)	$\gtrsim 100.0\%$ (36%)
II	$\gtrsim 10.0\%$ (45%)	$\gtrsim 17.5\%$ (56%)	$\gtrsim 12.5\%$ (38%)	$\gtrsim 15.0\%$ (50%)	$\gtrsim 7.5\%$ (40%)	$\gtrsim 50.0\%$ (3%)
	$\gtrsim 20.0\%$ (97%)	$\gtrsim 30.0\%$ (97%)	$\gtrsim 30.0\%$ (87%)	$\gtrsim 27.5\%$ (95%)	$\gtrsim 25.0\%$ (97%)	$\gtrsim 100.0\%$ (95%)
LS	$\gtrsim 10.0\%$ (53%)	$\gtrsim 15.0\%$ (55%)	$\gtrsim 10.0\%$ (40%)	$\gtrsim 17.5\%$ (46%)	$\gtrsim 7.5\%$ (55%)	$\gtrsim 50.0\%$ (5%)
	$\gtrsim 20.0\%$ (97%)	$\gtrsim 27.5\%$ (98%)	$\gtrsim 27.5\%$ (93%)	$\gtrsim 30.0\%$ (96%)	$\gtrsim 20.0\%$ (98%)	$\gtrsim 100.0\%$ (85%)
FL	$\gtrsim 10.0\%$ (51%)	$\gtrsim 10.0\%$ (53%)	$\gtrsim 10.0\%$ (70%)	$\gtrsim 10.0\%$ (61%)	$\gtrsim 10.0\%$ (49%)	$\gtrsim 40.0\%$ (50%)
	$\gtrsim 20.0\%$ (97%)	$\gtrsim 20.0\%$ (98%)	$\gtrsim 17.5\%$ (97%)	$\gtrsim 17.5\%$ (96%)	$\gtrsim 25.0\%$ (97%)	$\gtrsim 100.0\%$ (31%)
Type	$\Delta\text{BR}_{AZh}^{S_1}$	$\Delta\text{BR}_{AZh}^{S_2}$	$\Delta\text{BR}_{AZh}^{S_3}$	$\Delta\text{BR}_{AZh}^{\text{OS12}}$	$\Delta\text{BR}_{AZh}^{\text{BFMS}}$	$\Delta\text{BR}_{AZh}^{\text{MS}}$
I	$\gtrsim 15.0\%$ (51%)	$\gtrsim 17.5\%$ (51%)	$\gtrsim 85.0\%$ (45%)	$\gtrsim 30.0\%$ (50%)	$\gtrsim 10.0\%$ (46%)	$\gtrsim 90.0\%$ (38%)
	$\gtrsim 100.0\%$ (12%)	$\gtrsim 100.0\%$ (13%)	$\gtrsim 100.0\%$ (50%)	$\gtrsim 100.0\%$ (22%)	$\gtrsim 100.0\%$ (8%)	$\gtrsim 100.0\%$ (60%)
II	$\gtrsim 30.0\%$ (51%)	$\gtrsim 27.5\%$ (51%)	$\gtrsim 80.0\%$ (27%)	$\gtrsim 90.0\%$ (42%)	$\gtrsim 10.0\%$ (46%)	$\gtrsim 90.0\%$ (27%)
	$\gtrsim 100.0\%$ (22%)	$\gtrsim 100.0\%$ (21%)	$\gtrsim 100.0\%$ (67%)	$\gtrsim 100.0\%$ (55%)	$\gtrsim 100.0\%$ (10%)	$\gtrsim 100.0\%$ (70%)
LS	$\gtrsim 22.5\%$ (50%)	$\gtrsim 25.0\%$ (50%)	$\gtrsim 90.0\%$ (40%)	$\gtrsim 50.0\%$ (50%)	$\gtrsim 12.5\%$ (49%)	$\gtrsim 90.0\%$ (36%)
	$\gtrsim 100.0\%$ (17%)	$\gtrsim 100.0\%$ (18%)	$\gtrsim 100.0\%$ (57%)	$\gtrsim 100.0\%$ (32%)	$\gtrsim 100.0\%$ (10%)	$\gtrsim 100.0\%$ (64%)
FL	$\gtrsim 35.0\%$ (50%)	$\gtrsim 37.5\%$ (50%)	$\gtrsim 90.0\%$ (25%)	$\gtrsim 77.5\%$ (50%)	$\gtrsim 12.5\%$ (51%)	$\gtrsim 90.0\%$ (30%)
	$\gtrsim 100.0\%$ (28%)	$\gtrsim 100.0\%$ (28%)	$\gtrsim 100.0\%$ (73%)	$\gtrsim 100.0\%$ (43%)	$\gtrsim 100.0\%$ (9%)	$\gtrsim 100.0\%$ (67%)
Type	$\Delta\text{BR}_{AZH}^{S_1}$	$\Delta\text{BR}_{AZH}^{S_2}$	$\Delta\text{BR}_{AZH}^{S_3}$	$\Delta\text{BR}_{AZH}^{\text{OS12}}$	$\Delta\text{BR}_{AZH}^{\text{BFMS}}$	$\Delta\text{BR}_{AZH}^{\text{MS}}$
I	$\gtrsim 2.5\%$ (61%)	$\gtrsim 2.5\%$ (69%)	$\gtrsim 7.5\%$ (55%)	$\gtrsim 2.5\%$ (69%)	$\gtrsim 2.5\%$ (49%)	$\gtrsim 90.0\%$ (37%)
	$\gtrsim 7.5\%$ (84%)	$\gtrsim 5.0\%$ (82%)	$\gtrsim 17.5\%$ (83%)	$\gtrsim 5.0\%$ (85%)	$\gtrsim 12.5\%$ (87%)	$\gtrsim 100.0\%$ (50%)
II	$\gtrsim 5.0\%$ (59%)	$\gtrsim 2.5\%$ (54%)	$\gtrsim 15.0\%$ (40%)	$\gtrsim 5.0\%$ (65%)	$\gtrsim 5.0\%$ (55%)	$\gtrsim 90.0\%$ (22%)
	$\gtrsim 10.0\%$ (82%)	$\gtrsim 7.5\%$ (83%)	$\gtrsim 32.5\%$ (70%)	$\gtrsim 10.0\%$ (84%)	$\gtrsim 12.5\%$ (83%)	$\gtrsim 100.0\%$ (52%)
LS	$\gtrsim 2.5\%$ (52%)	$\gtrsim 2.5\%$ (66%)	$\gtrsim 15.0\%$ (56%)	$\gtrsim 5.0\%$ (82%)	$\gtrsim 5.0\%$ (61%)	$\gtrsim 90.0\%$ (33%)
	$\gtrsim 7.5\%$ (81%)	$\gtrsim 7.5\%$ (87%)	$\gtrsim 32.5\%$ (80%)	$\gtrsim 7.5\%$ (89%)	$\gtrsim 12.5\%$ (86%)	$\gtrsim 100.0\%$ (49%)
FL	$\gtrsim 5.0\%$ (62%)	$\gtrsim 2.5\%$ (57%)	$\gtrsim 10.0\%$ (48%)	$\gtrsim 2.5\%$ (56%)	$\gtrsim 5.0\%$ (50%)	$\gtrsim 90.0\%$ (23%)
	$\gtrsim 10.0\%$ (84%)	$\gtrsim 7.5\%$ (83%)	$\gtrsim 20.0\%$ (81%)	$\gtrsim 7.5\%$ (86%)	$\gtrsim 15.0\%$ (86%)	$\gtrsim 100.0\%$ (52%)

Table 12: Relative size of the EW corrections to the BRs for the pseudoscalar 2HDM Higgs boson A decays into $b\bar{b}$, $\tau^+\tau^-$, $t\bar{t}$, Zh , and ZH , in the four 2HDM types I, II, LS and FL (h is SM-like).

case that the decay into Zh is the dominant one, the LO branching ratio into $t\bar{t}$ is reduced so that the relative corrections here can become more important than in the previous case where h is SM-like.

Type	$A \rightarrow t\bar{t}$	$A \rightarrow Zh$	$A \rightarrow ZH$
I	291	558	124
II	39	14	12
LS	84	114	107
FL	124	124	114

Table 13: Number of parameter points available for the analysis in the individual OS decay channels of the pseudoscalar Higgs boson A (H is SM-like).

4.5 N2HDM Higgs Decays

In the N2HDM, all three CP-even Higgs bosons can in principle be SM-like. Although the case where the heaviest one, H_3 , is SM-like is not completely excluded yet, it is strongly disfavored. For type I we only found 25 valid parameter points, and for the other three types none.⁹ As the statistics would be very low, we decided not to present the results for this case. Instead, we focus on the scenarios where H_1 or H_2 are SM-like. In the former case the number of valid scenarios are as follows:

$$\begin{aligned}
\text{Type I:} & \quad 262\,332 & \text{Type II:} & \quad 299\,959 \\
\text{Type LS:} & \quad 283\,234 & \text{Type FL:} & \quad 292\,634 .
\end{aligned} \tag{4.41}$$

In case that H_2 is SM-like, the total amount of points that can be used for the analysis is given by:

$$\begin{aligned}
\text{Type I:} & \quad 8540 & \text{Type II:} & \quad 2381 \\
\text{Type LS:} & \quad 3303 & \text{Type FL:} & \quad 1562 .
\end{aligned} \tag{4.42}$$

The scheme sets shown in the following in all tables for the N2HDM are defined as:

$$\mathbf{S}_1 \equiv \{ \text{KOSY}^o, \text{KOSY}^c, \text{pOS}^o, \text{pOS}^c \} \tag{4.43}$$

$$\mathbf{S}_2 \equiv \{ \text{p}_*^o, \text{p}_*^c \} \tag{4.44}$$

$$\overline{\mathbf{MS}} \equiv \{ \overline{\mathbf{MS}} \} \tag{4.45}$$

4.6 SM-like N2HDM Higgs Decays

We again start with the presentation of the SM-like Higgs boson results before moving on to the corrections to the BRs of the non-SM-like CP-even and CP-odd Higgs bosons.

4.6.1 H_1 is the SM-like Higgs Boson

In Tab. 15, the relative corrections ΔBR for the decays of the SM-like Higgs boson H_1 into $b\bar{b}$, $\tau^+\tau^-$, $\gamma\gamma$ and ZZ final states are shown. The number of points used for the analysis has been given in Eq. (4.41). Note, however, that the decays into ZZ are always off-shell while the process $H_1 \rightarrow \gamma\gamma$ is loop-induced already at tree level. Therefore, as in the 2HDM, no EW corrections to $H_1 \rightarrow ZZ$ and $H_1 \rightarrow \gamma\gamma$ are included and the relative corrections to the BRs are the same for both decay channels.

From the table we read off that the ΔBR for both scheme sets \mathbf{S}_1 and \mathbf{S}_2 for all four N2HDM types are typically very small, with the bulk of points resulting in corrections below 2.5% and 5.0%, indicating both small EW corrections as well as numerical stability of the schemes.

⁹This does not necessarily mean that this case is excluded, but it would require a dedicated scan to find valid scenarios.

Type	$\Delta\text{BR}_{Abb}^{S_1}$	$\Delta\text{BR}_{Abb}^{S_2}$	$\Delta\text{BR}_{Abb}^{S_3}$	$\Delta\text{BR}_{Abb}^{\text{proc3}}$	$\Delta\text{BR}_{Abb}^{\text{OS1}}$	$\Delta\text{BR}_{Abb}^{\text{MS}}$
I	$\gtrsim 7.5\%$ (73%)	$\gtrsim 7.5\%$ (93%)	$\gtrsim 5.0\%$ (97%)	$\gtrsim 90.0\%$ (39%)	$\gtrsim 50.0\%$ (50%)	$\gtrsim 90.0\%$ (22%)
	$\gtrsim 17.5\%$ (98%)	$\gtrsim 10.0\%$ (99%)	$\gtrsim 10.0\%$ (100%)	$\gtrsim 100.0\%$ (58%)	$\gtrsim 100.0\%$ (29%)	$\gtrsim 100.0\%$ (77%)
II	$\gtrsim 12.5\%$ (76%)	$\gtrsim 7.5\%$ (59%)	$\gtrsim 20.0\%$ (46%)	$\gtrsim 2.5\%$ (82%)	$\gtrsim 62.5\%$ (50%)	$\gtrsim 90.0\%$ (2%)
	$\gtrsim 15.0\%$ (98%)	$\gtrsim 10.0\%$ (100%)	$\gtrsim 30.0\%$ (96%)	$\gtrsim 7.5\%$ (100%)	$\gtrsim 100.0\%$ (31%)	$\gtrsim 100.0\%$ (97%)
LS	$\gtrsim 7.5\%$ (57%)	$\gtrsim 20.0\%$ (58%)	$\gtrsim 5.0\%$ (76%)	$\gtrsim 20.0\%$ (67%)	$\gtrsim 77.5\%$ (50%)	$\gtrsim 90.0\%$ (2%)
	$\gtrsim 17.5\%$ (98%)	$\gtrsim 30.0\%$ (98%)	$\gtrsim 15.0\%$ (100%)	$\gtrsim 25.0\%$ (98%)	$\gtrsim 100.0\%$ (42%)	$\gtrsim 100.0\%$ (97%)
FL	$\gtrsim 12.5\%$ (76%)	$\gtrsim 30.0\%$ (60%)	$\gtrsim 22.5\%$ (54%)	$\gtrsim 75.0\%$ (50%)	$\gtrsim 77.5\%$ (50%)	$\gtrsim 90.0\%$ (2%)
	$\gtrsim 15.0\%$ (98%)	$\gtrsim 35.0\%$ (98%)	$\gtrsim 32.5\%$ (99%)	$\gtrsim 100.0\%$ (27%)	$\gtrsim 100.0\%$ (32%)	$\gtrsim 100.0\%$ (97%)

Type	$\Delta\text{BR}_{At\bar{t}}^{S_1}$	$\Delta\text{BR}_{At\bar{t}}^{S_2}$	$\Delta\text{BR}_{At\bar{t}}^{S_3}$	$\Delta\text{BR}_{At\bar{t}}^{\text{proc3}}$	$\Delta\text{BR}_{At\bar{t}}^{\text{OS1}}$	$\Delta\text{BR}_{At\bar{t}}^{\text{MS}}$
I	$\gtrsim 7.5\%$ (82%)	$\gtrsim 15.0\%$ (46%)	$\gtrsim 12.5\%$ (54%)	$\gtrsim 90.0\%$ (50%)	$\gtrsim 37.5\%$ (50%)	$\gtrsim 90.0\%$ (17%)
	$\gtrsim 12.5\%$ (99%)	$\gtrsim 27.5\%$ (97%)	$\gtrsim 22.5\%$ (97%)	$\gtrsim 100.0\%$ (47%)	$\gtrsim 100.0\%$ (24%)	$\gtrsim 100.0\%$ (82%)
II	$\gtrsim 10.0\%$ (84%)	$\gtrsim 10.0\%$ (87%)	$\gtrsim 17.5\%$ (51%)	$\gtrsim 5.0\%$ (82%)	$\gtrsim 60.0\%$ (50%)	$\gtrsim 90.0\%$ (12%)
	$\gtrsim 12.5\%$ (99%)	$\gtrsim 12.5\%$ (100%)	$\gtrsim 25.0\%$ (97%)	$\gtrsim 10.0\%$ (100%)	$\gtrsim 100.0\%$ (31%)	$\gtrsim 100.0\%$ (87%)
LS	$\gtrsim 10.0\%$ (91%)	$\gtrsim 10.0\%$ (85%)	$\gtrsim 15.0\%$ (65%)	$\gtrsim 5.0\%$ (55%)	$\gtrsim 60.0\%$ (50%)	$\gtrsim 95.0\%$ (7%)
	$\gtrsim 12.5\%$ (99%)	$\gtrsim 15.0\%$ (97%)	$\gtrsim 25.0\%$ (98%)	$\gtrsim 15.0\%$ (98%)	$\gtrsim 100.0\%$ (29%)	$\gtrsim 100.0\%$ (89%)
FL	$\gtrsim 10.0\%$ (86%)	$\gtrsim 25.0\%$ (49%)	$\gtrsim 20.0\%$ (61%)	$\gtrsim 67.5\%$ (50%)	$\gtrsim 75.0\%$ (50%)	$\gtrsim 90.0\%$ (7%)
	$\gtrsim 12.5\%$ (99%)	$\gtrsim 30.0\%$ (98%)	$\gtrsim 25.0\%$ (97%)	$\gtrsim 100.0\%$ (25%)	$\gtrsim 100.0\%$ (31%)	$\gtrsim 100.0\%$ (92%)

Type	$\Delta\text{BR}_{A\tau^+\tau^-}^{S_1}$	$\Delta\text{BR}_{A\tau^+\tau^-}^{S_2}$	$\Delta\text{BR}_{A\tau^+\tau^-}^{S_3}$	$\Delta\text{BR}_{A\tau^+\tau^-}^{\text{proc3}}$	$\Delta\text{BR}_{A\tau^+\tau^-}^{\text{OS1}}$	$\Delta\text{BR}_{A\tau^+\tau^-}^{\text{MS}}$
I	$\gtrsim 10.0\%$ (62%)	$\gtrsim 5.0\%$ (94%)	$\gtrsim 5.0\%$ (92%)	$\gtrsim 90.0\%$ (40%)	$\gtrsim 50.0\%$ (50%)	$\gtrsim 90.0\%$ (22%)
	$\gtrsim 25.0\%$ (99%)	$\gtrsim 7.5\%$ (99%)	$\gtrsim 12.5\%$ (100%)	$\gtrsim 100.0\%$ (57%)	$\gtrsim 100.0\%$ (29%)	$\gtrsim 100.0\%$ (77%)
II	$\gtrsim 12.5\%$ (71%)	$\gtrsim 7.5\%$ (83%)	$\gtrsim 22.5\%$ (53%)	$\gtrsim 2.5\%$ (82%)	$\gtrsim 62.5\%$ (50%)	$\gtrsim 90.0\%$ (2%)
	$\gtrsim 17.5\%$ (100%)	$\gtrsim 10.0\%$ (100%)	$\gtrsim 35.0\%$ (100%)	$\gtrsim 5.0\%$ (100%)	$\gtrsim 100.0\%$ (31%)	$\gtrsim 100.0\%$ (97%)
LS	$\gtrsim 10.0\%$ (53%)	$\gtrsim 5.0\%$ (74%)	$\gtrsim 17.5\%$ (50%)	$\gtrsim 2.5\%$ (82%)	$\gtrsim 60.0\%$ (50%)	$\gtrsim 90.0\%$ (21%)
	$\gtrsim 17.5\%$ (100%)	$\gtrsim 12.5\%$ (100%)	$\gtrsim 30.0\%$ (97%)	$\gtrsim 7.5\%$ (99%)	$\gtrsim 100.0\%$ (34%)	$\gtrsim 100.0\%$ (78%)
FL	$\gtrsim 12.5\%$ (67%)	$\gtrsim 5.0\%$ (50%)	$\gtrsim 5.0\%$ (64%)	$\gtrsim 90.0\%$ (77%)	$\gtrsim 90.0\%$ (46%)	$\gtrsim 90.0\%$ (8%)
	$\gtrsim 20.0\%$ (98%)	$\gtrsim 12.5\%$ (100%)	$\gtrsim 10.0\%$ (100%)	$\gtrsim 100.0\%$ (22%)	$\gtrsim 100.0\%$ (44%)	$\gtrsim 100.0\%$ (91%)

Type	$\Delta\text{BR}_{AZh}^{S_1}$	$\Delta\text{BR}_{AZh}^{S_2}$	$\Delta\text{BR}_{AZh}^{S_3}$	$\Delta\text{BR}_{AZh}^{\text{proc3}}$	$\Delta\text{BR}_{AZh}^{\text{OS1}}$	$\Delta\text{BR}_{AZh}^{\text{MS}}$
I	$\gtrsim 2.5\%$ (100%)	$\gtrsim 2.5\%$ (95%)	$\gtrsim 2.5\%$ (99%)	$\gtrsim 2.5\%$ (79%)	$\gtrsim 2.5\%$ (95%)	$\gtrsim 90.0\%$ (33%)
		$\gtrsim 5.0\%$ (97%)	$\gtrsim 5.0\%$ (100%)	$\gtrsim 5.0\%$ (97%)	$\gtrsim 5.0\%$ (100%)	$\gtrsim 100.0\%$ (65%)
II	$\gtrsim 2.5\%$ (100%)	$\gtrsim 2.5\%$ (100%)	$\gtrsim 2.5\%$ (95%)	$\gtrsim 2.5\%$ (100%)	$\gtrsim 2.5\%$ (37%)	$\gtrsim 90.0\%$ (4%)
			$\gtrsim 5.0\%$ (100%)		$\gtrsim 5.0\%$ (100%)	$\gtrsim 100.0\%$ (95%)
LS	$\gtrsim 2.5\%$ (96%)	$\gtrsim 2.5\%$ (100%)	$\gtrsim 2.5\%$ (92%)	$\gtrsim 2.5\%$ (100%)	$\gtrsim 2.5\%$ (50%)	$\gtrsim 90.0\%$ (10%)
	$\gtrsim 5.0\%$ (98%)		$\gtrsim 5.0\%$ (97%)		$\gtrsim 10.0\%$ (90%)	$\gtrsim 100.0\%$ (83%)
FL	$\gtrsim 2.5\%$ (100%)	$\gtrsim 2.5\%$ (92%)	$\gtrsim 2.5\%$ (97%)	$\gtrsim 2.5\%$ (48%)	$\gtrsim 2.5\%$ (40%)	$\gtrsim 90.0\%$ (6%)
		$\gtrsim 5.0\%$ (99%)	$\gtrsim 5.0\%$ (100%)	$\gtrsim 5.0\%$ (98%)	$\gtrsim 5.0\%$ (98%)	$\gtrsim 100.0\%$ (92%)

Type	$\Delta\text{BR}_{AZH}^{S_1}$	$\Delta\text{BR}_{AZH}^{S_2}$	$\Delta\text{BR}_{AZH}^{S_3}$	$\Delta\text{BR}_{AZH}^{\text{proc3}}$	$\Delta\text{BR}_{AZH}^{\text{OS1}}$	$\Delta\text{BR}_{AZH}^{\text{MS}}$
I	$\gtrsim 10.0\%$ (53%)	$\gtrsim 35.0\%$ (30%)	$\gtrsim 27.5\%$ (48%)	$\gtrsim 82.5\%$ (3%)	$\gtrsim 47.5\%$ (20%)	$\gtrsim 90.0\%$ (5%)
	$\gtrsim 100.0\%$ (6%)	$\gtrsim 100.0\%$ (54%)	$\gtrsim 100.0\%$ (15%)	$\gtrsim 100.0\%$ (96%)	$\gtrsim 100.0\%$ (68%)	$\gtrsim 100.0\%$ (94%)
II	$\gtrsim 25.0\%$ (51%)	$\gtrsim 57.5\%$ (10%)	$\gtrsim 22.5\%$ (10%)	$\gtrsim 72.5\%$ (40%)	$\gtrsim 100.0\%$ (100%)	$\gtrsim 90.0\%$ (10%)
	$\gtrsim 100.0\%$ (22%)	$\gtrsim 100.0\%$ (74%)	$\gtrsim 100.0\%$ (52%)	$\gtrsim 100.0\%$ (48%)		$\gtrsim 100.0\%$ (89%)
LS	$\gtrsim 30.0\%$ (36%)	$\gtrsim 67.5\%$ (10%)	$\gtrsim 70.0\%$ (21%)	$\gtrsim 57.5\%$ (12%)	$\gtrsim 95.0\%$ (5%)	$\gtrsim 90.0\%$ (1%)
	$\gtrsim 100.0\%$ (34%)	$\gtrsim 100.0\%$ (79%)	$\gtrsim 100.0\%$ (69%)	$\gtrsim 100.0\%$ (61%)	$\gtrsim 100.0\%$ (94%)	$\gtrsim 100.0\%$ (98%)
FL	$\gtrsim 27.5\%$ (49%)	$\gtrsim 75.0\%$ (2%)	$\gtrsim 72.5\%$ (30%)	$\gtrsim 100.0\%$ (100%)	$\gtrsim 100.0\%$ (100%)	$\gtrsim 92.5\%$ (7%)
	$\gtrsim 100.0\%$ (16%)	$\gtrsim 100.0\%$ (94%)	$\gtrsim 100.0\%$ (62%)			$\gtrsim 100.0\%$ (92%)

Table 14: Relative size of the EW corrections to the BRs for the pseudoscalar 2HDM Higgs boson A decays into $b\bar{b}$, $\tau^+\tau^-$, $t\bar{t}$, Zh , and ZH , in the four 2HDM types I, II, LS and FL (H is SM-like).

4.6.2 H_2 is the SM-like Higgs Boson

For the case that H_2 is SM-like, we display in Tab. 16 the relative EW corrections to the BRs into $b\bar{b}$, $\tau^+\tau^-$, $\gamma\gamma$, ZZ as well as into H_1H_1 since this channel can be OS in these scenarios.

Type	$\Delta\text{BR}_{H_1 b\bar{b}}^{\mathcal{S}_1}$	$\Delta\text{BR}_{H_1 b\bar{b}}^{\mathcal{S}_2}$	$\Delta\text{BR}_{H_1 b\bar{b}}^{\text{MS}}$
I	$\lesssim 2.5\%$ (99%)	$\lesssim 2.5\%$ (99%)	$\lesssim 17.5\%$ (50%)
II	$\lesssim 2.5\%$ (99%)	$\lesssim 2.5\%$ (99%)	$\gtrsim 100.0\%$ (21%)
LS	$\lesssim 2.5\%$ (99%)	$\lesssim 2.5\%$ (99%)	$\gtrsim 90.0\%$ (50%)
FL	$\lesssim 2.5\%$ (99%)	$\lesssim 2.5\%$ (99%)	$\gtrsim 100.0\%$ (42%)
			$\gtrsim 25.0\%$ (22%)
			$\gtrsim 100.0\%$ (%)
			$\gtrsim 90.0\%$ (45%)
			$\gtrsim 100.0\%$ (52%)

Type	$\Delta\text{BR}_{H_1\gamma\gamma/H_1ZZ}^{\mathcal{S}_1}$	$\Delta\text{BR}_{H_1\gamma\gamma/H_1ZZ}^{\mathcal{S}_2}$	$\Delta\text{BR}_{H_1\gamma\gamma/H_1ZZ}^{\text{MS}}$
I	$\lesssim 2.5\%$ (1%)	$\lesssim 2.5\%$ (3%)	$\lesssim 35.0\%$ (50%)
II	$\lesssim 5.0\%$ (99%)	$\lesssim 5.0\%$ (99%)	$\gtrsim 100.0\%$ (33%)
LS	$\lesssim 2.5\%$ (66%)	$\lesssim 2.5\%$ (46%)	$\gtrsim 90.0\%$ (34%)
FL	$\lesssim 5.0\%$ (99%)	$\lesssim 5.0\%$ (99%)	$\gtrsim 100.0\%$ (65%)
	$\lesssim 2.5\%$ (1%)	$\lesssim 2.5\%$ (1%)	$\gtrsim 32.5\%$ (50%)
	$\lesssim 5.0\%$ (99%)	$\lesssim 5.0\%$ (99%)	$\gtrsim 100.0\%$ (30%)
	$\lesssim 2.5\%$ (60%)	$\lesssim 2.5\%$ (40%)	$\gtrsim 90.0\%$ (38%)
	$\lesssim 5.0\%$ (99%)	$\lesssim 5.0\%$ (99%)	$\gtrsim 100.0\%$ (61%)

Type	$\Delta\text{BR}_{H_1\tau^+\tau^-}^{\mathcal{S}_1}$	$\Delta\text{BR}_{H_1\tau^+\tau^-}^{\mathcal{S}_2}$	$\Delta\text{BR}_{H_1\tau^+\tau^-}^{\text{MS}}$
I	$\lesssim 2.5\%$ (99%)	$\lesssim 2.5\%$ (99%)	$\lesssim 17.5\%$ (50%)
II	$\lesssim 2.5\%$ (98%)	$\lesssim 2.5\%$ (93%)	$\gtrsim 100.0\%$ (21%)
LS	$\lesssim 5.0\%$ (99%)	$\lesssim 2.5\%$ (99%)	$\gtrsim 90.0\%$ (50%)
FL	$\lesssim 2.5\%$ (94%)	$\lesssim 2.5\%$ (73%)	$\gtrsim 100.0\%$ (45%)
	$\lesssim 5.0\%$ (99%)	$\lesssim 7.5\%$ (99%)	$\gtrsim 90.0\%$ (37%)
	$\lesssim 2.5\%$ (82%)	$\lesssim 2.5\%$ (93%)	$\gtrsim 100.0\%$ (61%)
	$\lesssim 5.0\%$ (99%)	$\lesssim 5.0\%$ (99%)	$\gtrsim 90.0\%$ (47%)
			$\gtrsim 100.0\%$ (49%)

Table 15: Relative size of the EW corrections to the BRs of the N2HDM SM-like H_1 in the four N2HDM types I, II, LS and FL.

However, the additional OS condition $m_{H_2} \geq 2m_{H_1}$ reduces the number of parameters points available for this particular channel as follows:

$$\begin{aligned}
\text{Type I:} & \quad 204 & \text{Type II:} & \quad 146 \\
\text{Type LS:} & \quad 181 & \text{Type FL:} & \quad 133 .
\end{aligned}$$

From the table, we conclude the following:

- The ΔBR for $H_2\gamma\gamma$ and H_2ZZ are again the same as they do not receive EW corrections, since the former is loop-induced and the latter off-shell.
- The ΔBR for both scheme sets \mathcal{S}_1 and \mathcal{S}_2 for the fermionic decays for all four N2HDM types are typically very small, with the bulk of points resulting in corrections below 2.5% and 5.0%, indicating both small electroweak corrections as well as numerical stability of the schemes.
- For \mathcal{S}_2 , the corrections are slightly increased compared to \mathcal{S}_1 , *i.e.* the bulk of points is slightly shifted towards larger corrections. Overall, the corrections are still very moderate, however.

Type	$\Delta\text{BR}_{H_2 b\bar{b}}^{S_1}$	$\Delta\text{BR}_{H_2 b\bar{b}}^{S_2}$	$\Delta\text{BR}_{H_2 b\bar{b}}^{\text{MS}}$	$\Delta\text{BR}_{H_2 \gamma\gamma/H_2 ZZ}^{S_1}$	$\Delta\text{BR}_{H_2 \gamma\gamma/H_2 ZZ}^{S_2}$	$\Delta\text{BR}_{H_2 \gamma\gamma/H_2 ZZ}^{\text{MS}}$
I	$\lesssim 2.5\%$ (97%) $\gtrsim 5.0\%$ (99%)	$\lesssim 2.5\%$ (98%) $\gtrsim 5.0\%$ (99%)	$\lesssim 32.5\%$ (50%) $\gtrsim 100.0\%$ (7%)	$\lesssim 5.0\%$ (97%) $\lesssim 7.5\%$ (99%)	$\lesssim 5.0\%$ (98%) $\lesssim 7.5\%$ (99%)	$\lesssim 70.0\%$ (50%) $\gtrsim 100.0\%$ (26%)
II	$\lesssim 2.5\%$ (97%) $\gtrsim 7.5\%$ (99%)	$\lesssim 2.5\%$ (97%) $\gtrsim 7.5\%$ (99%)	$\lesssim 37.5\%$ (50%) $\gtrsim 100.0\%$ (10%)	$\lesssim 2.5\%$ (65%) $\lesssim 7.5\%$ (99%)	$\lesssim 2.5\%$ (42%) $\lesssim 7.5\%$ (99%)	$\lesssim 75.0\%$ (50%) $\gtrsim 100.0\%$ (14%)
LS	$\lesssim 2.5\%$ (97%) $\gtrsim 7.5\%$ (99%)	$\lesssim 2.5\%$ (96%) $\gtrsim 5.0\%$ (98%)	$\lesssim 27.5\%$ (51%) $\gtrsim 100.0\%$ (18%)	$\lesssim 5.0\%$ (96%) $\lesssim 7.5\%$ (98%)	$\lesssim 5.0\%$ (96%) $\lesssim 10.0\%$ (98%)	$\lesssim 47.5\%$ (50%) $\gtrsim 100.0\%$ (13%)
FL	$\lesssim 2.5\%$ (95%) $\gtrsim 7.5\%$ (98%)	$\lesssim 2.5\%$ (95%) $\gtrsim 7.5\%$ (98%)	$\lesssim 37.5\%$ (51%) $\gtrsim 100.0\%$ (10%)	$\lesssim 2.5\%$ (61%) $\lesssim 5.0\%$ (97%)	$\lesssim 2.5\%$ (31%) $\lesssim 5.0\%$ (97%)	$\lesssim 72.5\%$ (49%) $\gtrsim 100.0\%$ (10%)

Type	$\Delta\text{BR}_{H_2 \tau^+\tau^-}^{S_1}$	$\Delta\text{BR}_{H_2 \tau^+\tau^-}^{S_2}$	$\Delta\text{BR}_{H_2 \tau^+\tau^-}^{\text{MS}}$	$\Delta\text{BR}_{H_2 H_1 H_1}^{S_1}$	$\Delta\text{BR}_{H_2 H_1 H_1}^{S_2}$	$\Delta\text{BR}_{H_2 H_1 H_1}^{\text{MS}}$
I	$\lesssim 2.5\%$ (98%) $\gtrsim 5.0\%$ (99%)	$\lesssim 2.5\%$ (98%) $\gtrsim 5.0\%$ (99%)	$\lesssim 32.5\%$ (50%) $\gtrsim 100.0\%$ (7%)	$\lesssim 82.5\%$ (39%) $\gtrsim 100.0\%$ (60%)	$\lesssim 77.5\%$ (40%) $\gtrsim 100.0\%$ (59%)	$\lesssim 85.0\%$ (4%) $\gtrsim 100.0\%$ (95%)
II	$\lesssim 2.5\%$ (93%) $\gtrsim 5.0\%$ (98%)	$\lesssim 2.5\%$ (83%) $\gtrsim 5.0\%$ (98%)	$\lesssim 37.5\%$ (50%) $\gtrsim 100.0\%$ (10%)	$\lesssim 85.0\%$ (35%) $\gtrsim 100.0\%$ (64%)	$\lesssim 90.0\%$ (35%) $\gtrsim 100.0\%$ (64%)	$\lesssim 90.0\%$ (1%) $\gtrsim 100.0\%$ (98%)
LS	$\lesssim 2.5\%$ (67%) $\gtrsim 7.5\%$ (94%)	$\lesssim 5.0\%$ (79%) $\gtrsim 10.0\%$ (94%)	$\lesssim 92.5\%$ (50%) $\gtrsim 100.0\%$ (48%)	$\lesssim 87.5\%$ (40%) $\gtrsim 100.0\%$ (57%)	$\lesssim 77.5\%$ (40%) $\gtrsim 100.0\%$ (54%)	$\lesssim 87.5\%$ (2%) $\gtrsim 100.0\%$ (97%)
FL	$\lesssim 2.5\%$ (67%) $\gtrsim 7.5\%$ (98%)	$\lesssim 2.5\%$ (86%) $\gtrsim 5.0\%$ (97%)	$\lesssim 50.0\%$ (50%) $\gtrsim 100.0\%$ (26%)	$\lesssim 85.0\%$ (35%) $\gtrsim 100.0\%$ (60%)	$\lesssim 87.5\%$ (37%) $\gtrsim 100.0\%$ (60%)	$\lesssim 100.0\%$ (100%)

Table 16: Relative size of the EW corrections to the BRs of the N2HDM SM-like H_2 in the four N2HDM types I, II, LS and FL.

- For the decays into $\gamma\gamma$ and ZZ , the relative corrections are slightly increased compared to the case where H_1 is SM-like. But since they do not receive electroweak corrections, this is an indirect effect through the corrections of the other decay channels.
- The relative corrections to the Higgs-to-Higgs decay $H_2 \rightarrow H_1 H_1$ are very large. On the one hand this is due to non-decoupling effects in scenarios where the quartic couplings of the potential and hence the trilinear Higgs self-couplings become large. For a detailed discussion, see [22, 26, 32, 33, 79, 80]. The other reason for the large relative corrections are very small tree-level BRs. Due to the LHC constraints on the SM Higgs rates $\text{BR}(H_2 \rightarrow H_1 H_1)$ must be small so that the H_2 BRs into the other SM final states remain SM-like.

4.7 Non-SM-Like CP-even N2HDM Higgs Decays

We continue with the analysis of the relative EW corrections to the BRs of the N2HDM non-SM-like CP-even Higgs bosons. Due to the extended Higgs sector we now have two non-SM-like CP-even Higgs bosons to be analysed in contrast to just one as in the 2HDM.

4.7.1 H_1 is the SM-like Higgs Boson

We start with the case where H_1 is SM-like and investigate the decays of the non-SM-like Higgs bosons H_2 and H_3 .

H_2 Decays: We only show results for OS decays as only for these the EW corrections are computed. Additional OS conditions reduce the number of available parameter points, *cf.* Eq. (4.41), in the individual decay channels as shown in Tab. 17. The relative corrections ΔBR for the non-SM-like CP-even H_2 are displayed in Tab. 18. From the table, we observe:

Type	$H_2 \rightarrow t\bar{t}$	$H_2 \rightarrow ZA$	$H_2 \rightarrow W^\pm H^\mp$	$H_2 \rightarrow ZZ$	$H_2 \rightarrow H_1 H_1$	$H_2 \rightarrow AA$
I	210 527	1970	2558	250 074	237 558	488
II	280 113	942	893	296 615	292 134	33 420
LS	255 075	498	592	277 968	271 130	134
FL	278 944	211	452	290 381	287 446	0

Table 17: Number of parameter points available for the analysis in the individual OS decay channels of the non-SM-like Higgs boson H_2 (H_1 is SM-like).

Type	$\Delta\text{BR}_{H_2 b\bar{b}}^{\mathcal{S}_1}$	$\Delta\text{BR}_{H_2 b\bar{b}}^{\mathcal{S}_2}$	$\Delta\text{BR}_{H_2 b\bar{b}}^{\overline{\text{MS}}}$	$\Delta\text{BR}_{H_2 t\bar{t}}^{\mathcal{S}_1}$	$\Delta\text{BR}_{H_2 t\bar{t}}^{\mathcal{S}_2}$	$\Delta\text{BR}_{H_2 t\bar{t}}^{\overline{\text{MS}}}$
I	$\lesssim 7.5\%$ (48%)	$\lesssim 7.5\%$ (49%)	$\lesssim 90.0\%$ (50%)	$\lesssim 5.0\%$ (48%)	$\lesssim 7.5\%$ (59%)	$\lesssim 90.0\%$ (50%)
	$\gtrsim 30.0\%$ (87%)	$\lesssim 35.0\%$ (89%)	$\gtrsim 100.0\%$ (48%)	$\lesssim 25.0\%$ (86%)	$\lesssim 25.0\%$ (86%)	$\gtrsim 100.0\%$ (48%)
II	$\lesssim 7.5\%$ (46%)	$\lesssim 12.5\%$ (51%)	$\lesssim 90.0\%$ (29%)	$\lesssim 5.0\%$ (57%)	$\gtrsim 5.0\%$ (57%)	$\lesssim 95.0\%$ (50%)
	$\gtrsim 25.0\%$ (90%)	$\lesssim 27.5\%$ (90%)	$\gtrsim 100.0\%$ (69%)	$\gtrsim 25.0\%$ (89%)	$\lesssim 27.5\%$ (90%)	$\gtrsim 100.0\%$ (49%)
LS	$\gtrsim 5.0\%$ (45%)	$\gtrsim 7.5\%$ (59%)	$\gtrsim 80.0\%$ (50%)	$\gtrsim 5.0\%$ (57%)	$\gtrsim 5.0\%$ (57%)	$\gtrsim 85.0\%$ (50%)
	$\gtrsim 22.5\%$ (90%)	$\gtrsim 22.5\%$ (90%)	$\gtrsim 100.0\%$ (46%)	$\gtrsim 20.0\%$ (90%)	$\gtrsim 20.0\%$ (90%)	$\gtrsim 100.0\%$ (47%)
FL	$\gtrsim 7.5\%$ (50%)	$\gtrsim 12.5\%$ (60%)	$\gtrsim 90.0\%$ (25%)	$\gtrsim 5.0\%$ (52%)	$\gtrsim 5.0\%$ (52%)	$\gtrsim 95.0\%$ (50%)
	$\gtrsim 30.0\%$ (90%)	$\gtrsim 30.0\%$ (90%)	$\gtrsim 100.0\%$ (72%)	$\gtrsim 30.0\%$ (89%)	$\gtrsim 25.0\%$ (87%)	$\gtrsim 100.0\%$ (49%)
Type	$\Delta\text{BR}_{H_2 \tau^+ \tau^-}^{\mathcal{S}_1}$	$\Delta\text{BR}_{H_2 \tau^+ \tau^-}^{\mathcal{S}_2}$	$\Delta\text{BR}_{H_2 \tau^+ \tau^-}^{\overline{\text{MS}}}$	$\Delta\text{BR}_{H_2 ZA}^{\mathcal{S}_1}$	$\Delta\text{BR}_{H_2 ZA}^{\mathcal{S}_2}$	$\Delta\text{BR}_{H_2 ZA}^{\overline{\text{MS}}}$
I	$\lesssim 10.0\%$ (51%)	$\lesssim 10.0\%$ (52%)	$\lesssim 92.5\%$ (50%)	$\lesssim 12.5\%$ (50%)	$\lesssim 12.5\%$ (50%)	$\lesssim 90.0\%$ (41%)
	$\gtrsim 35.0\%$ (87%)	$\lesssim 32.5\%$ (86%)	$\gtrsim 100.0\%$ (48%)	$\gtrsim 100.0\%$ (25%)	$\gtrsim 100.0\%$ (25%)	$\gtrsim 100.0\%$ (47%)
II	$\lesssim 7.5\%$ (50%)	$\lesssim 12.5\%$ (55%)	$\lesssim 90.0\%$ (28%)	$\lesssim 5.0\%$ (71%)	$\lesssim 5.0\%$ (46%)	$\lesssim 90.0\%$ (20%)
	$\gtrsim 25.0\%$ (90%)	$\lesssim 27.5\%$ (90%)	$\gtrsim 100.0\%$ (69%)	$\lesssim 15.0\%$ (94%)	$\lesssim 17.5\%$ (95%)	$\gtrsim 100.0\%$ (57%)
LS	$\gtrsim 10.0\%$ (62%)	$\lesssim 10.0\%$ (44%)	$\lesssim 90.0\%$ (31%)	$\lesssim 5.0\%$ (57%)	$\lesssim 5.0\%$ (54%)	$\lesssim 90.0\%$ (38%)
	$\gtrsim 22.5\%$ (90%)	$\lesssim 25.0\%$ (90%)	$\gtrsim 100.0\%$ (65%)	$\lesssim 20.0\%$ (83%)	$\lesssim 25.0\%$ (85%)	$\gtrsim 100.0\%$ (47%)
FL	$\gtrsim 10.0\%$ (58%)	$\lesssim 7.5\%$ (47%)	$\lesssim 92.5\%$ (50%)	$\lesssim 10.0\%$ (55%)	$\lesssim 7.5\%$ (52%)	$\lesssim 90.0\%$ (20%)
	$\gtrsim 30.0\%$ (86%)	$\gtrsim 30.0\%$ (86%)	$\gtrsim 100.0\%$ (48%)	$\gtrsim 100.0\%$ (16%)	$\gtrsim 100.0\%$ (16%)	$\gtrsim 100.0\%$ (45%)
Type	$\Delta\text{BR}_{H_2 W^\pm H^\mp}^{\mathcal{S}_1}$	$\Delta\text{BR}_{H_2 W^\pm H^\mp}^{\mathcal{S}_2}$	$\Delta\text{BR}_{H_2 W^\pm H^\mp}^{\overline{\text{MS}}}$	$\Delta\text{BR}_{H_2 ZZ}^{\mathcal{S}_1}$	$\Delta\text{BR}_{H_2 ZZ}^{\mathcal{S}_2}$	$\Delta\text{BR}_{H_2 ZZ}^{\overline{\text{MS}}}$
I	$\lesssim 12.5\%$ (41%)	$\lesssim 10.0\%$ (38%)	$\lesssim 90.0\%$ (34%)	$\lesssim 7.5\%$ (42%)	$\lesssim 10.0\%$ (43%)	$\lesssim 50.0\%$ (62.5%)
	$\gtrsim 100.0\%$ (33%)	$\gtrsim 100.0\%$ (33%)	$\gtrsim 100.0\%$ (57%)	$\lesssim 22.5\%$ (71%)	$\lesssim 30.0\%$ (72%)	$\gtrsim 100.0\%$ (42%)
II	$\lesssim 7.5\%$ (59%)	$\lesssim 5.0\%$ (58%)	$\lesssim 90.0\%$ (27%)	$\lesssim 7.5\%$ (47%)	$\lesssim 10.0\%$ (48%)	$\lesssim 75.0\%$ (50%)
	$\gtrsim 100.0\%$ (19%)	$\gtrsim 100.0\%$ (18%)	$\gtrsim 100.0\%$ (49%)	$\lesssim 25.0\%$ (81%)	$\lesssim 30.0\%$ (80%)	$\gtrsim 100.0\%$ (45%)
LS	$\lesssim 5.0\%$ (51%)	$\lesssim 5.0\%$ (57%)	$\lesssim 90.0\%$ (41%)	$\lesssim 7.5\%$ (47%)	$\lesssim 10.0\%$ (48%)	$\lesssim 70.0\%$ (50%)
	$\gtrsim 20.0\%$ (83%)	$\lesssim 15.0\%$ (80%)	$\gtrsim 100.0\%$ (50%)	$\lesssim 27.5\%$ (81%)	$\lesssim 35.0\%$ (79%)	$\gtrsim 100.0\%$ (44%)
FL	$\gtrsim 15.0\%$ (21%)	$\lesssim 15.0\%$ (23%)	$\lesssim 90.0\%$ (18%)	$\lesssim 7.5\%$ (48%)	$\lesssim 7.5\%$ (44%)	$\lesssim 57.5\%$ (50%)
	$\gtrsim 100.0\%$ (55%)	$\gtrsim 100.0\%$ (54%)	$\gtrsim 100.0\%$ (63%)	$\lesssim 25.0\%$ (81%)	$\lesssim 30.0\%$ (81%)	$\gtrsim 100.0\%$ (40%)
Type	$\Delta\text{BR}_{H_2 H_1 H_1}^{\mathcal{S}_1}$	$\Delta\text{BR}_{H_2 H_1 H_1}^{\mathcal{S}_2}$	$\Delta\text{BR}_{H_2 H_1 H_1}^{\overline{\text{MS}}}$	$\Delta\text{BR}_{H_2 AA}^{\mathcal{S}_1}$	$\Delta\text{BR}_{H_2 AA}^{\mathcal{S}_2}$	$\Delta\text{BR}_{H_2 AA}^{\overline{\text{MS}}}$
I	$\lesssim 50.0\%$ (50%)	$\lesssim 47.5\%$ (50%)	$\lesssim 90.0\%$ (41%)	$\lesssim 12.5\%$ (52%)	$\lesssim 12.5\%$ (52%)	$\lesssim 25.0\%$ (50%)
	$\gtrsim 100.0\%$ (37%)	$\gtrsim 100.0\%$ (34%)	$\gtrsim 100.0\%$ (57%)	$\gtrsim 100.0\%$ (25%)	$\gtrsim 100.0\%$ (25%)	$\gtrsim 100.0\%$ (28%)
II	$\lesssim 40.0\%$ (50%)	$\lesssim 40.0\%$ (51%)	$\lesssim 90.0\%$ (31%)	$\lesssim 5.0\%$ (64%)	$\lesssim 5.0\%$ (67%)	$\lesssim 90.0\%$ (21%)
	$\gtrsim 100.0\%$ (31%)	$\gtrsim 100.0\%$ (30%)	$\gtrsim 100.0\%$ (67%)	$\lesssim 20.0\%$ (87%)	$\lesssim 20.0\%$ (88%)	$\gtrsim 100.0\%$ (40%)
LS	$\lesssim 45.0\%$ (50%)	$\lesssim 45.0\%$ (50%)	$\lesssim 90.0\%$ (35%)	$\lesssim 7.5\%$ (56%)	$\lesssim 7.5\%$ (58%)	$\lesssim 15.0\%$ (52%)
	$\gtrsim 100.0\%$ (32%)	$\gtrsim 100.0\%$ (32%)	$\gtrsim 100.0\%$ (63%)	$\gtrsim 100.0\%$ (17%)	$\gtrsim 100.0\%$ (17%)	$\gtrsim 100.0\%$ (19%)
FL	$\lesssim 37.5\%$ (50%)	$\lesssim 37.5\%$ (50%)	$\lesssim 90.0\%$ (34%)	-	-	-
	$\gtrsim 100.0\%$ (29%)	$\gtrsim 100.0\%$ (29%)	$\gtrsim 100.0\%$ (64%)	-	-	-

Table 18: Relative size of the EW corrections to the BRs of the non-SM-like N2HDM Higgs boson H_2 into $b\bar{b}$, $\tau^+ \tau^-$, ZA , $W^\pm H^\mp$, ZZ , $H_1 H_1$, and AA for the four N2HDM types I, II, LS and FL (H_1 is SM-like).

- The ΔBR for the scheme sets \mathcal{S}_1 and \mathcal{S}_2 for all four N2HDM types typically range between moderate and significant corrections of up to 35%. However, they can also become very

Type	$H_3 \rightarrow t\bar{t}$	$H_3 \rightarrow ZA$	$H_3 \rightarrow W^\pm H^\mp$	$H_3 \rightarrow ZZ$	$H_3 \rightarrow H_1 H_1$	$H_3 \rightarrow H_1 H_2$	$H_3 \rightarrow H_2 H_2$	$H_3 \rightarrow AA$
I	254 113	120 280	137 260	262 051	260 531	185 847	53 558	25 033
II	299 959	118 359	133 277	299 959	299 959	215 367	31 552	4055
LS	281 975	121 501	138 894	283 221	283 037	202 202	44 160	15 533
FL	292 634	116 923	133 182	292 634	292 634	208 005	24 927	4519

Table 19: Number of parameter points available for the analysis in the individual OS decay channels of the non-SM-like Higgs boson H_3 (H_1 is SM-like).

large in the Higgs plus gauge boson and di-Higgs final states. For most of the channels and types, the scheme set \mathcal{S}_1 produces smaller corrections than \mathcal{S}_2 .

- The enhanced relative EW corrections to the BRs of the decay channels $H_2 \rightarrow ZA$ and $H_2 \rightarrow W^\pm H^\mp$ computed with the scheme sets \mathcal{S}_1 and \mathcal{S}_2 are due to a very small BR at leading order which is due to a small phase space. Hence, this does not indicate the numerical instability of the two scheme sets but rather demonstrates artificially large electroweak corrections due to the small LO BRs.
- For the Higgs-to-Higgs decays $H_2 \rightarrow H_1 H_1$ and $H_2 \rightarrow AA$, the corrections are typically large for all schemes. This is either due to very small LO BRs or due to parametrically enhanced Higgs-to-Higgs decays in certain regions of the N2HDM parameter space.
- We remark that the huge corrections indirectly affect through the total width the other decay channels into fermion and ZZ^{10} final states so that their corrections can become significant in particular if the LO BR is not large.

H_3 Decays: As before, we restrict the analysis to OS decays which reduces the number of available parameter points in the individual channels as shown in Tab. 19¹¹. The relative corrections ΔBR are given in Tab. 20 from which we conclude the following:

- The corrections for the renormalization scheme sets \mathcal{S}_1 and \mathcal{S}_2 are of similar size.
- Considering the decay channels, the smallest corrections are found for the decays into $t\bar{t}$, $W^\pm H^\mp$, ZA , and ZZ^{12} and range from below 7.5% up to 40% at most. Note that a heavy non-SM-like Higgs boson H_3 can have important BRs not only into $t\bar{t}$ but also into gauge plus Higgs final states. The relative corrections to the BRs into $b\bar{b}$ and $\tau^+\tau^-$ are slightly larger.
- The relative corrections to the Higgs-to-Higgs decays $H_3 \rightarrow H_i H_j$ ($i, j = 1, 2$) and $H_3 \rightarrow AA$ on the other hand can become again very large which is due to either small LO BRs (see next item) or parametrically enhanced corrections. This again indirectly affects through

¹⁰Note, that although H_1 behaves SM-like, the couplings of H_2 to ZZ need not necessarily be suppressed, as we would expect from sum rules. The N2HDM with its larger number of parameters allows for a Higgs boson that behaves SM-like although its individual couplings to SM particles are not very close to the SM values. Since it is the rates that decide about the SM-like behaviour, the interplay of production and decay can still lead to very SM-like signatures. This leaves room for the couplings of the other Higgs bosons to the ZZ bosons to be non-zero. Additionally, the singlet admixture influences the Higgs couplings.

¹¹A comparison with Eq. (4.41) shows that the amount of available parameter points is not reduced for all N2HDM types and final states, actually.

¹²The same argument as given in footnote 10 for H_2 also applies here for H_3 .

Type	$\Delta\text{BR}_{H_3 b\bar{b}}^{S_1}$	$\Delta\text{BR}_{H_3 b\bar{b}}^{S_2}$	$\Delta\text{BR}_{H_3 b\bar{b}}^{\text{MS}}$	$\Delta\text{BR}_{H_3 t\bar{t}}^{S_1}$	$\Delta\text{BR}_{H_3 t\bar{t}}^{S_2}$	$\Delta\text{BR}_{H_3 t\bar{t}}^{\text{MS}}$
I	$\lesssim 12.5\%$ (53%)	$\lesssim 12.5\%$ (53%)	$\lesssim 70.0\%$ (50%)	$\lesssim 7.5\%$ (45%)	$\lesssim 7.5\%$ (45%)	$\lesssim 67.5\%$ (50%)
	$\gtrsim 40.0\%$ (80%)	$\gtrsim 40.0\%$ (80%)	$\gtrsim 100.0\%$ (42%)	$\gtrsim 25.0\%$ (72%)	$\gtrsim 30.0\%$ (75%)	$\gtrsim 100.0\%$ (41%)
II	$\lesssim 12.5\%$ (51%)	$\lesssim 17.5\%$ (55%)	$\gtrsim 90.0\%$ (28%)	$\lesssim 5.0\%$ (46%)	$\gtrsim 7.5\%$ (54%)	$\gtrsim 75.0\%$ (50%)
	$\gtrsim 35.0\%$ (81%)	$\gtrsim 32.5\%$ (80%)	$\gtrsim 100.0\%$ (69%)	$\gtrsim 30.0\%$ (78%)	$\gtrsim 35.0\%$ (79%)	$\gtrsim 100.0\%$ (44%)
LS	$\lesssim 10.0\%$ (49%)	$\lesssim 10.0\%$ (49%)	$\gtrsim 65.0\%$ (50%)	$\gtrsim 7.5\%$ (49%)	$\gtrsim 7.5\%$ (49%)	$\gtrsim 65.0\%$ (50%)
	$\gtrsim 37.5\%$ (80%)	$\gtrsim 37.5\%$ (80%)	$\gtrsim 100.0\%$ (41%)	$\gtrsim 35.0\%$ (78%)	$\gtrsim 30.0\%$ (76%)	$\gtrsim 100.0\%$ (41%)
FL	$\lesssim 12.5\%$ (50%)	$\lesssim 15.0\%$ (50%)	$\gtrsim 90.0\%$ (27%)	$\gtrsim 7.5\%$ (51%)	$\gtrsim 7.5\%$ (50%)	$\gtrsim 77.5\%$ (50%)
	$\gtrsim 42.5\%$ (80%)	$\gtrsim 40.0\%$ (80%)	$\gtrsim 100.0\%$ (70%)	$\gtrsim 35.0\%$ (78%)	$\gtrsim 30.0\%$ (75%)	$\gtrsim 100.0\%$ (44%)
Type	$\Delta\text{BR}_{H_3 \tau^+ \tau^-}^{S_1}$	$\Delta\text{BR}_{H_3 \tau^+ \tau^-}^{S_2}$	$\Delta\text{BR}_{H_3 \tau^+ \tau^-}^{\text{MS}}$	$\Delta\text{BR}_{H_3 ZA}^{S_1}$	$\Delta\text{BR}_{H_3 ZA}^{S_2}$	$\Delta\text{BR}_{H_3 ZA}^{\text{MS}}$
I	$\lesssim 12.5\%$ (50%)	$\lesssim 12.5\%$ (51%)	$\lesssim 70.0\%$ (50%)	$\lesssim 7.5\%$ (35%)	$\lesssim 7.5\%$ (34%)	$\lesssim 90.0\%$ (44%)
	$\gtrsim 40.0\%$ (80%)	$\gtrsim 32.5\%$ (77%)	$\gtrsim 100.0\%$ (42%)	$\gtrsim 25.0\%$ (65%)	$\gtrsim 32.5\%$ (70%)	$\gtrsim 100.0\%$ (52%)
II	$\lesssim 10.0\%$ (49%)	$\lesssim 12.5\%$ (41%)	$\gtrsim 90.0\%$ (28%)	$\lesssim 10.0\%$ (36%)	$\lesssim 10.0\%$ (39%)	$\lesssim 90.0\%$ (39%)
	$\gtrsim 27.5\%$ (80%)	$\gtrsim 25.0\%$ (77%)	$\gtrsim 100.0\%$ (69%)	$\gtrsim 30.0\%$ (64%)	$\gtrsim 35.0\%$ (70%)	$\gtrsim 100.0\%$ (55%)
LS	$\lesssim 12.5\%$ (55%)	$\lesssim 10.0\%$ (33%)	$\gtrsim 80.0\%$ (35%)	$\lesssim 10.0\%$ (41%)	$\lesssim 10.0\%$ (41%)	$\lesssim 90.0\%$ (47%)
	$\gtrsim 32.5\%$ (80%)	$\gtrsim 30.0\%$ (79%)	$\gtrsim 100.0\%$ (60%)	$\gtrsim 35.0\%$ (70%)	$\gtrsim 35.0\%$ (70%)	$\gtrsim 100.0\%$ (49%)
FL	$\lesssim 10.0\%$ (48%)	$\lesssim 10.0\%$ (48%)	$\gtrsim 77.5\%$ (50%)	$\lesssim 10.0\%$ (36%)	$\lesssim 10.0\%$ (39%)	$\lesssim 90.0\%$ (38%)
	$\gtrsim 40.0\%$ (80%)	$\gtrsim 35.0\%$ (79%)	$\gtrsim 100.0\%$ (44%)	$\gtrsim 35.0\%$ (66%)	$\gtrsim 35.0\%$ (67%)	$\gtrsim 100.0\%$ (57%)
Type	$\Delta\text{BR}_{H_3 W^\pm H^\mp}^{S_1}$	$\Delta\text{BR}_{H_3 W^\pm H^\mp}^{S_2}$	$\Delta\text{BR}_{H_3 W^\pm H^\mp}^{\text{MS}}$	$\Delta\text{BR}_{H_3 ZZ}^{S_1}$	$\Delta\text{BR}_{H_3 ZZ}^{S_2}$	$\Delta\text{BR}_{H_3 ZZ}^{\text{MS}}$
I	$\lesssim 7.5\%$ (36%)	$\lesssim 7.5\%$ (35%)	$\lesssim 90.0\%$ (44%)	$\lesssim 7.5\%$ (43%)	$\lesssim 7.5\%$ (39%)	$\lesssim 52.5\%$ (50%)
	$\gtrsim 30.0\%$ (69%)	$\gtrsim 30.0\%$ (68%)	$\gtrsim 100.0\%$ (52%)	$\gtrsim 30.0\%$ (73%)	$\gtrsim 30.0\%$ (70%)	$\gtrsim 100.0\%$ (38%)
II	$\lesssim 7.5\%$ (30%)	$\lesssim 10.0\%$ (40%)	$\gtrsim 90.0\%$ (38%)	$\lesssim 7.5\%$ (41%)	$\lesssim 10.0\%$ (43%)	$\lesssim 70.0\%$ (50%)
	$\gtrsim 35.0\%$ (68%)	$\gtrsim 35.0\%$ (69%)	$\gtrsim 100.0\%$ (56%)	$\gtrsim 30.0\%$ (72%)	$\gtrsim 32.5\%$ (70%)	$\gtrsim 100.0\%$ (42%)
LS	$\lesssim 7.5\%$ (34%)	$\lesssim 7.5\%$ (34%)	$\lesssim 90.0\%$ (47%)	$\lesssim 7.5\%$ (43%)	$\lesssim 10.0\%$ (46%)	$\lesssim 47.5\%$ (50%)
	$\gtrsim 35.0\%$ (70%)	$\gtrsim 35.0\%$ (70%)	$\gtrsim 100.0\%$ (51%)	$\gtrsim 32.5\%$ (74%)	$\gtrsim 30.0\%$ (70%)	$\gtrsim 100.0\%$ (36%)
FL	$\lesssim 10.0\%$ (36%)	$\lesssim 10.0\%$ (38%)	$\gtrsim 95.0\%$ (38%)	$\lesssim 7.5\%$ (44%)	$\lesssim 7.5\%$ (41%)	$\lesssim 42.5\%$ (50%)
	$\gtrsim 40.0\%$ (69%)	$\gtrsim 40.0\%$ (70%)	$\gtrsim 100.0\%$ (58%)	$\gtrsim 25.0\%$ (70%)	$\gtrsim 27.5\%$ (70%)	$\gtrsim 100.0\%$ (34%)
Type	$\Delta\text{BR}_{H_3 H_1 H_1}^{S_1}$	$\Delta\text{BR}_{H_3 H_1 H_1}^{S_2}$	$\Delta\text{BR}_{H_3 H_1 H_1}^{\text{MS}}$	$\Delta\text{BR}_{H_3 H_1 H_2}^{S_1}$	$\Delta\text{BR}_{H_3 H_1 H_2}^{S_2}$	$\Delta\text{BR}_{H_3 H_1 H_2}^{\text{MS}}$
I	$\lesssim 35.0\%$ (50%)	$\lesssim 37.5\%$ (50%)	$\lesssim 85.0\%$ (45%)	$\lesssim 35.0\%$ (21%)	$\lesssim 32.5\%$ (20%)	$\lesssim 47.5\%$ (20%)
	$\gtrsim 100.0\%$ (32%)	$\gtrsim 100.0\%$ (32%)	$\gtrsim 100.0\%$ (52%)	$\gtrsim 100.0\%$ (62%)	$\gtrsim 100.0\%$ (62%)	$\gtrsim 100.0\%$ (68%)
II	$\lesssim 57.5\%$ (50%)	$\lesssim 57.5\%$ (50%)	$\lesssim 87.5\%$ (37%)	$\lesssim 50.0\%$ (10%)	$\lesssim 50.0\%$ (10%)	$\lesssim 35.0\%$ (10%)
	$\gtrsim 100.0\%$ (41%)	$\gtrsim 100.0\%$ (41%)	$\gtrsim 100.0\%$ (60%)	$\gtrsim 100.0\%$ (81%)	$\gtrsim 100.0\%$ (81%)	$\gtrsim 100.0\%$ (76%)
LS	$\lesssim 37.5\%$ (50%)	$\lesssim 37.5\%$ (50%)	$\lesssim 85.0\%$ (44%)	$\lesssim 50.0\%$ (20%)	$\lesssim 50.0\%$ (20%)	$\lesssim 10.0\%$ (20%)
	$\gtrsim 100.0\%$ (33%)	$\gtrsim 100.0\%$ (33%)	$\gtrsim 100.0\%$ (53%)	$\gtrsim 100.0\%$ (69%)	$\gtrsim 100.0\%$ (68%)	$\gtrsim 100.0\%$ (69%)
FL	$\lesssim 42.5\%$ (50%)	$\lesssim 42.5\%$ (50%)	$\lesssim 80.0\%$ (40%)	$\lesssim 10.0\%$ (10%)	$\lesssim 47.5\%$ (10%)	$\lesssim 30.0\%$ (11%)
	$\gtrsim 100.0\%$ (36%)	$\gtrsim 100.0\%$ (36%)	$\gtrsim 100.0\%$ (56%)	$\gtrsim 100.0\%$ (81%)	$\gtrsim 100.0\%$ (81%)	$\gtrsim 100.0\%$ (73%)
Type	$\Delta\text{BR}_{H_3 H_2 H_2}^{S_1}$	$\Delta\text{BR}_{H_3 H_2 H_2}^{S_2}$	$\Delta\text{BR}_{H_3 H_2 H_2}^{\text{MS}}$	$\Delta\text{BR}_{H_3 AA}^{S_1}$	$\Delta\text{BR}_{H_3 AA}^{S_2}$	$\Delta\text{BR}_{H_3 AA}^{\text{MS}}$
I	$\lesssim 35.0\%$ (40%)	$\lesssim 20.0\%$ (31%)	$\lesssim 27.5\%$ (20%)	$\lesssim 7.5\%$ (43%)	$\lesssim 7.5\%$ (43%)	$\lesssim 27.5\%$ (30%)
	$\gtrsim 100.0\%$ (42%)	$\gtrsim 100.0\%$ (43%)	$\gtrsim 100.0\%$ (63%)	$\gtrsim 30.0\%$ (75%)	$\gtrsim 30.0\%$ (76%)	$\gtrsim 100.0\%$ (41%)
II	$\lesssim 37.5\%$ (10%)	$\lesssim 35.0\%$ (10%)	$\lesssim 32.5\%$ (10%)	$\lesssim 25.0\%$ (42%)	$\lesssim 25.0\%$ (46%)	$\lesssim 20.0\%$ (30%)
	$\gtrsim 100.0\%$ (81%)	$\gtrsim 100.0\%$ (80%)	$\gtrsim 100.0\%$ (79%)	$\gtrsim 100.0\%$ (21%)	$\gtrsim 100.0\%$ (19%)	$\gtrsim 100.0\%$ (44%)
LS	$\lesssim 37.5\%$ (30%)	$\lesssim 20.0\%$ (21%)	$\lesssim 25.0\%$ (20%)	$\lesssim 10.0\%$ (40%)	$\lesssim 10.0\%$ (43%)	$\lesssim 25.0\%$ (37%)
	$\gtrsim 100.0\%$ (52%)	$\gtrsim 100.0\%$ (53%)	$\gtrsim 100.0\%$ (62%)	$\gtrsim 30.0\%$ (70%)	$\gtrsim 32.5\%$ (74%)	$\gtrsim 100.0\%$ (36%)
FL	$\lesssim 30.0\%$ (10%)	$\lesssim 30.0\%$ (10%)	$\lesssim 22.5\%$ (10%)	$\lesssim 30.0\%$ (42%)	$\lesssim 22.5\%$ (40%)	$\lesssim 35.0\%$ (37%)
	$\gtrsim 100.0\%$ (77%)	$\gtrsim 100.0\%$ (77%)	$\gtrsim 100.0\%$ (72%)	$\gtrsim 100.0\%$ (27%)	$\gtrsim 100.0\%$ (26%)	$\gtrsim 100.0\%$ (45%)

Table 20: Relative size of the EW corrections to the BRs of the non-SM-like N2HDM Higgs boson H_3 (H_1 is SM-like) into $b\bar{b}$, $t\bar{t}$, $\tau^+\tau^-$, ZA , $W^\pm H^\mp$, ZZ , $H_1 H_1$, $H_1 H_2$, $H_2 H_2$, and AA for the four N2HDM types I, II, LS and FL.

the total width the decay channels with typically more moderate corrections, inducing more significant ΔBR then.

Type	$\Delta\text{BR}_{H_1 b\bar{b}}^{\mathbf{S}_1}$	$\Delta\text{BR}_{H_1 b\bar{b}}^{\mathbf{S}_2}$	$\Delta\text{BR}_{H_1 b\bar{b}}^{\overline{\mathbf{MS}}}$	$\Delta\text{BR}_{H_1 \tau^+\tau^-}^{\mathbf{S}_1}$	$\Delta\text{BR}_{H_1 \tau^+\tau^-}^{\mathbf{S}_2}$	$\Delta\text{BR}_{H_1 \tau^+\tau^-}^{\overline{\mathbf{MS}}}$
I	$\lesssim 2.5\%$ (85%)	$\lesssim 2.5\%$ (85%)	$\lesssim 15.0\%$ (71%)	$\lesssim 2.5\%$ (73%)	$\lesssim 2.5\%$ (71%)	$\lesssim 15.0\%$ (70%)
II	$\lesssim 10.0\%$ (94%)	$\lesssim 10.0\%$ (93%)	$\gtrsim 100.0\%$ (6%)	$\lesssim 10.0\%$ (92%)	$\lesssim 10.0\%$ (91%)	$\gtrsim 100.0\%$ (6%)
LS	$\lesssim 2.5\%$ (95%)	$\lesssim 2.5\%$ (93%)	$\lesssim 20.0\%$ (60%)	$\lesssim 2.5\%$ (93%)	$\lesssim 2.5\%$ (94%)	$\lesssim 37.5\%$ (70%)
FL	$\lesssim 7.5\%$ (97%)	$\lesssim 7.5\%$ (96%)	$\gtrsim 100.0\%$ (18%)	$\lesssim 7.5\%$ (98%)	$\lesssim 7.5\%$ (97%)	$\gtrsim 100.0\%$ (18%)
LS	$\lesssim 2.5\%$ (77%)	$\lesssim 2.5\%$ (74%)	$\lesssim 45.0\%$ (50%)	$\lesssim 2.5\%$ (70%)	$\lesssim 2.5\%$ (60%)	$\lesssim 85.0\%$ (50%)
FL	$\lesssim 10.0\%$ (92%)	$\lesssim 10.0\%$ (92%)	$\gtrsim 100.0\%$ (35%)	$\lesssim 10.0\%$ (92%)	$\lesssim 10.0\%$ (92%)	$\gtrsim 100.0\%$ (47%)
FL	$\lesssim 2.5\%$ (93%)	$\lesssim 2.5\%$ (92%)	$\lesssim 17.5\%$ (60%)	$\lesssim 2.5\%$ (76%)	$\lesssim 2.5\%$ (67%)	$\lesssim 80.0\%$ (35%)
FL	$\lesssim 10.0\%$ (97%)	$\lesssim 10.0\%$ (96%)	$\gtrsim 100.0\%$ (20%)	$\lesssim 7.5\%$ (98%)	$\lesssim 7.5\%$ (97%)	$\gtrsim 100.0\%$ (61%)

Table 21: Relative size of the EW corrections to the BRs of the non-SM-like N2HDM Higgs boson H_1 into $b\bar{b}$ and $\tau^+\tau^-$, for the four N2HDM types I, II, LS and FL (H_2 is SM-like).

- We remark that the scheme sets \mathbf{S}_1 and \mathbf{S}_2 , *independently of the N2HDM type*, typically feature corrections larger than 100% for roughly 10% to 13% of the parameter points for *all decay channels* (of course, for the Higgs-to-Higgs decays, the amount of parameter points leading to large corrections is even larger)¹³. This is not a sign of numerical instability of the renormalization schemes though but instead this stems from small LO BRs and hence from a large sensitivity on the higher-order corrections. Moreover, BRs containing mixing angle CTs and off-diagonal scalar WFRCs become numerically enhanced in certain corners of parameter space and hence, ΔBR blows up there. Additionally, the counterterms are multiplied with coefficients containing couplings in the denominator that become small here and thereby lead to parametrically enhanced counterterm contributions.

4.7.2 H_2 is the SM-like Higgs Boson

We turn to the case where H_2 is SM-like so that we have an additional light CP-even Higgs boson in the spectrum, and investigate the decays of the non-SM-like Higgs bosons H_1 and H_3 . For this scenario the number of parameter points compatible with all constraints, and hence the statistics of the analysis, is significantly reduced, *cf.* Eq. (4.42).

H_1 Decays: Since the Higgs boson H_1 is rather light for this mass hierarchy, the only decay channels with important BRs (which are not loop-induced) are those into $b\bar{b}$ and $\tau^+\tau^-$ for which we show the relative EW corrections to the BRs in Tab. 21. The table shows that the relative corrections are small to moderate for the majority of all input parameter points for the two scheme sets \mathbf{S}_1 and \mathbf{S}_2 in all four N2HDM types.

H_3 Decays: For the heaviest Higgs boson H_3 , many more decay channels are kinematically open. Still, the requirement of OS decays reduces the original number of parameter points available, (*cf.* Eq. (4.42)), for the individual OS channels to the values listed in Tab. 22¹⁴. Note, in particular, that the statistics for the FL type in the ZA and $W^\pm H^\mp$ final states becomes very low in this scenario. The relative corrections ΔBR for the decays of H_3 are summarized in Tab. 23. We observe:

- The relative corrections for the Higgs-to-Higgs decays are very large for all N2HDM types and scheme sets. The reasons are small LO BRs and/or non-decoupling effects.

¹³This is not shown in the table in order not to blow up the presentation.

¹⁴Comparison with Eq. (4.42) shows that again some of the numbers are actually not reduced.

Type	$H_3 \rightarrow t\bar{t}$	$H_3 \rightarrow ZA$	$H_3 \rightarrow W^\pm H^\mp$	$H \rightarrow ZZ$
I	5856	2612	3330	8302
II	2381	74	28	2381
LS	2923	157	310	3203
FL	1562	12	8	1562

Type	$H_3 \rightarrow H_1 H_1$	$H_3 \rightarrow H_1 H_2$	$H_3 \rightarrow H_2 H_2$	$H_3 \rightarrow AA$
I	8205	7976	7609	1448
II	2381	2381	2381	0
LS	3065	2807	2173	66
FL	1562	1562	1562	0

Table 22: Number of parameter points available for the analysis in the individual OS decay channels of the non-SM-like Higgs boson H_3 (H_2 is SM-like).

- For the scheme sets \mathcal{S}_1 and \mathcal{S}_2 , the relative corrections to the other decays of H_3 are more moderate, but larger than for the scenarios where H_1 is the SM-like Higgs boson.
- For the N2HDM types I and LS, all decay channels typically feature huge corrections for a considerable amount of input parameters. This might stem from
 - * small LO BRs;
 - * relatively large EW corrections (also indirectly) in these two N2HDM types;
 - * parametrical enhancement of the mixing angle CTs and off-diagonal WFRCs for these two N2HDM types (since the CTs and WFRCs come in combination with the Yukawa couplings, their contribution strongly depends on the N2HDM type);
 - * enhanced uncanceled contributions from the singlet (through the off-diagonal WFRCs connected to H_3 and the mixing angle CTs $\delta\alpha_2$ and $\delta\alpha_3$).
- For the decays $H_3 \rightarrow ZA$, $W^\pm H^\mp$ and ZZ , the corrections can become very large. The reasons are small LO branching ratios due to suppressed couplings, counterterm contributions that are parametrically enhanced or large counterterms themselves.

4.8 Pseudoscalar N2HDM Decays

We finally turn to the decays of the pseudoscalar Higgs boson A in the N2HDM and again investigate the two cases where either H_1 or H_2 is the SM-like Higgs boson.

4.8.1 H_1 is the SM-like Higgs Boson

The requirement of the pseudoscalar Higgs boson decays to be OS reduces the originally available parameter points to those given in Tab. 24 for the individual channels¹⁵. In Tab. 25, we display the relative EW corrections to the BRs of the pseudoscalar Higgs boson for the case where H_1 is SM-like. The table allows for the following observations:

- The corrections for the decay $A \rightarrow t\bar{t}$ (which is typically the dominant one if it is kinematically allowed) are typically very small for the scheme sets \mathcal{S}_1 and \mathcal{S}_2 , indicating both low corrections for this decay in these schemes and numerical stability of the two scheme sets.

¹⁵As before, the amount of available input parameters for some N2HDM types is actually not reduced.

Type	$\Delta\text{BR}_{H_3 b\bar{b}}^{\mathbf{S}_1}$	$\Delta\text{BR}_{H_3 b\bar{b}}^{\mathbf{S}_2}$	$\Delta\text{BR}_{H_3 b\bar{b}}^{\overline{\text{MS}}}$	$\Delta\text{BR}_{H_3 t\bar{t}}^{\mathbf{S}_1}$	$\Delta\text{BR}_{H_3 t\bar{t}}^{\mathbf{S}_2}$	$\Delta\text{BR}_{H_3 t\bar{t}}^{\overline{\text{MS}}}$
I	$\lesssim 15.0\%$ (40%) $\gtrsim 100.0\%$ (21%)	$\lesssim 17.5\%$ (43%) $\gtrsim 100.0\%$ (22%)	$\lesssim 80.0\%$ (35%) $\gtrsim 100.0\%$ (59%)	$\lesssim 15.0\%$ (43%) $\gtrsim 100.0\%$ (23%)	$\lesssim 15.0\%$ (42%) $\gtrsim 100.0\%$ (24%)	$\lesssim 82.5\%$ (40%) $\gtrsim 100.0\%$ (55%)
II	$\lesssim 12.5\%$ (57%) $\gtrsim 20.0\%$ (91%)	$\lesssim 17.5\%$ (54%) $\gtrsim 25.0\%$ (91%)	$\lesssim 85.0\%$ (15%) $\gtrsim 100.0\%$ (83%)	$\lesssim 2.5\%$ (54%) $\gtrsim 12.5\%$ (92%)	$\lesssim 2.5\%$ (54%) $\gtrsim 10.0\%$ (90%)	$\lesssim 75.0\%$ (40%) $\gtrsim 100.0\%$ (55%)
LS	$\lesssim 10.0\%$ (51%) $\gtrsim 100.0\%$ (9%)	$\lesssim 10.0\%$ (51%) $\gtrsim 100.0\%$ (9%)	$\lesssim 77.5\%$ (30%) $\gtrsim 100.0\%$ (65%)	$\lesssim 12.5\%$ (70%) $\gtrsim 100.0\%$ (8%)	$\lesssim 12.5\%$ (70%) $\gtrsim 100.0\%$ (8%)	$\lesssim 80.0\%$ (33%) $\gtrsim 100.0\%$ (62%)
FL	$\lesssim 10.0\%$ (45%) $\gtrsim 20.0\%$ (86%)	$\lesssim 15.0\%$ (53%) $\gtrsim 27.5\%$ (88%)	$\lesssim 85.0\%$ (22%) $\gtrsim 100.0\%$ (75%)	$\lesssim 2.5\%$ (44%) $\gtrsim 20.0\%$ (87%)	$\lesssim 2.5\%$ (44%) $\lesssim 15.0\%$ (85%)	$\lesssim 87.5\%$ (30%) $\gtrsim 100.0\%$ (67%)
Type	$\Delta\text{BR}_{H_3 \tau^+ \tau^-}^{\mathbf{S}_1}$	$\Delta\text{BR}_{H_3 \tau^+ \tau^-}^{\mathbf{S}_2}$	$\Delta\text{BR}_{H_3 \tau^+ \tau^-}^{\overline{\text{MS}}}$	$\Delta\text{BR}_{H_3 ZA}^{\mathbf{S}_1}$	$\Delta\text{BR}_{H_3 ZA}^{\mathbf{S}_2}$	$\Delta\text{BR}_{H_3 ZA}^{\overline{\text{MS}}}$
I	$\lesssim 17.5\%$ (42%) $\gtrsim 100.0\%$ (20%)	$\lesssim 20.0\%$ (45%) $\gtrsim 100.0\%$ (21%)	$\lesssim 80.0\%$ (35%) $\gtrsim 100.0\%$ (59%)	$\lesssim 20.0\%$ (42%) $\gtrsim 100.0\%$ (31%)	$\lesssim 15.0\%$ (35%) $\gtrsim 100.0\%$ (31%)	$\lesssim 77.5\%$ (30%) $\gtrsim 100.0\%$ (62%)
II	$\lesssim 10.0\%$ (45%) $\gtrsim 17.5\%$ (89%)	$\lesssim 15.0\%$ (42%) $\gtrsim 22.5\%$ (89%)	$\lesssim 85.0\%$ (15%) $\gtrsim 100.0\%$ (83%)	$\lesssim 5.0\%$ (80%) $\gtrsim 10.0\%$ (93%)	$\lesssim 5.0\%$ (49%) $\gtrsim 12.5\%$ (93%)	$\lesssim 90.0\%$ (34%) $\gtrsim 100.0\%$ (38%)
LS	$\lesssim 15.0\%$ (58%) $\gtrsim 100.0\%$ (9%)	$\lesssim 15.0\%$ (47%) $\gtrsim 100.0\%$ (9%)	$\lesssim 80.0\%$ (30%) $\gtrsim 100.0\%$ (63%)	$\lesssim 12.5\%$ (30%) $\gtrsim 100.0\%$ (47%)	$\lesssim 15.0\%$ (30%) $\gtrsim 100.0\%$ (43%)	$\lesssim 90.0\%$ (32%) $\gtrsim 100.0\%$ (61%)
FL	$\lesssim 10.0\%$ (47%) $\gtrsim 25.0\%$ (88%)	$\lesssim 10.0\%$ (49%) $\gtrsim 20.0\%$ (86%)	$\lesssim 87.5\%$ (30%) $\gtrsim 100.0\%$ (67%)	$\lesssim 5.0\%$ (58%) $\gtrsim 100.0\%$ (33%)	$\lesssim 7.5\%$ (58%) $\gtrsim 100.0\%$ (33%)	$\lesssim 82.5\%$ (25%) $\gtrsim 100.0\%$ (58%)
Type	$\Delta\text{BR}_{H_3 W^\pm H^\mp}^{\mathbf{S}_1}$	$\Delta\text{BR}_{H_3 W^\pm H^\mp}^{\mathbf{S}_2}$	$\Delta\text{BR}_{H_3 W^\pm H^\mp}^{\overline{\text{MS}}}$	$\Delta\text{BR}_{H_3 ZZ}^{\mathbf{S}_1}$	$\Delta\text{BR}_{H_3 ZZ}^{\mathbf{S}_2}$	$\Delta\text{BR}_{H_3 ZZ}^{\overline{\text{MS}}}$
I	$\lesssim 17.5\%$ (37%) $\gtrsim 100.0\%$ (32%)	$\lesssim 15.0\%$ (33%) $\gtrsim 100.0\%$ (33%)	$\lesssim 75.0\%$ (30%) $\gtrsim 100.0\%$ (61%)	$\lesssim 15.0\%$ (30%) $\gtrsim 100.0\%$ (26%)	$\lesssim 20.0\%$ (30%) $\gtrsim 100.0\%$ (29%)	$\lesssim 60.0\%$ (30%) $\gtrsim 100.0\%$ (58%)
II	$\lesssim 2.5\%$ (41%) $\gtrsim 10.0\%$ (93%)	$\lesssim 2.5\%$ (50%) $\lesssim 12.5\%$ (93%)	$\lesssim 80.0\%$ (29%) $\gtrsim 100.0\%$ (36%)	$\lesssim 12.5\%$ (39%) $\gtrsim 100.0\%$ (12%)	$\lesssim 12.5\%$ (29%) $\gtrsim 100.0\%$ (19%)	$\lesssim 65.0\%$ (30%) $\gtrsim 100.0\%$ (60%)
LS	$\lesssim 22.5\%$ (29%) $\gtrsim 100.0\%$ (41%)	$\lesssim 22.5\%$ (30%) $\gtrsim 100.0\%$ (40%)	$\lesssim 72.5\%$ (30%) $\gtrsim 100.0\%$ (58%)	$\lesssim 15.0\%$ (31%) $\gtrsim 100.0\%$ (18%)	$\lesssim 20.0\%$ (28%) $\gtrsim 100.0\%$ (25%)	$\lesssim 70.0\%$ (30%) $\gtrsim 100.0\%$ (60%)
FL	$\lesssim 5.0\%$ (13%) $\gtrsim 100.0\%$ (50%)	$\lesssim 2.5\%$ (12.5%) $\gtrsim 100.0\%$ (50%)	$\lesssim 95.0\%$ (25%) $\gtrsim 100.0\%$ (63%)	$\lesssim 12.5\%$ (32%) $\gtrsim 100.0\%$ (17%)	$\lesssim 20.0\%$ (37%) $\gtrsim 100.0\%$ (20%)	$\lesssim 67.5\%$ (30%) $\gtrsim 100.0\%$ (57%)
Type	$\Delta\text{BR}_{H_3 H_1 H_1}^{\mathbf{S}_1}$	$\Delta\text{BR}_{H_3 H_1 H_1}^{\mathbf{S}_2}$	$\Delta\text{BR}_{H_3 H_1 H_1}^{\overline{\text{MS}}}$	$\Delta\text{BR}_{H_3 H_1 H_2}^{\mathbf{S}_1}$	$\Delta\text{BR}_{H_3 H_1 H_2}^{\mathbf{S}_2}$	$\Delta\text{BR}_{H_3 H_1 H_2}^{\overline{\text{MS}}}$
I	$\lesssim 17.5\%$ (30%) $\gtrsim 100.0\%$ (44%)	$\lesssim 20.0\%$ (31%) $\gtrsim 100.0\%$ (44%)	$\lesssim 57.5\%$ (10%) $\gtrsim 100.0\%$ (85%)	$\lesssim 37.5\%$ (30%) $\gtrsim 100.0\%$ (50%)	$\lesssim 37.5\%$ (30%) $\gtrsim 100.0\%$ (50%)	$\lesssim 85.0\%$ (8%) $\gtrsim 100.0\%$ (91%)
II	$\lesssim 40.0\%$ (10%) $\gtrsim 100.0\%$ (78%)	$\lesssim 40.0\%$ (10%) $\gtrsim 100.0\%$ (77%)	$\lesssim 95.0\%$ (2%) $\gtrsim 100.0\%$ (97%)	$\lesssim 62.5\%$ (10%) $\gtrsim 100.0\%$ (85%)	$\lesssim 60.0\%$ (10%) $\gtrsim 100.0\%$ (84%)	$\lesssim 90.0\%$ (1%) $\gtrsim 100.0\%$ (98%)
LS	$\lesssim 27.5\%$ (25%) $\gtrsim 100.0\%$ (53%)	$\lesssim 37.5\%$ (30%) $\gtrsim 100.0\%$ (52%)	$\lesssim 80.0\%$ (8%) $\gtrsim 100.0\%$ (90%)	$\lesssim 67.5\%$ (30%) $\gtrsim 100.0\%$ (62%)	$\lesssim 40.0\%$ (20%) $\gtrsim 100.0\%$ (62%)	$\lesssim 87.5\%$ (6%) $\gtrsim 100.0\%$ (93%)
FL	$\lesssim 32.5\%$ (10%) $\gtrsim 100.0\%$ (75%)	$\lesssim 32.5\%$ (10%) $\gtrsim 100.0\%$ (74%)	$\lesssim 90.0\%$ (3%) $\gtrsim 100.0\%$ (96%)	$\lesssim 47.5\%$ (10%) $\gtrsim 100.0\%$ (81%)	$\lesssim 45.0\%$ (10%) $\gtrsim 100.0\%$ (80%)	$\lesssim 82.5\%$ (2%) $\gtrsim 100.0\%$ (97%)
Type	$\Delta\text{BR}_{H_3 H_2 H_2}^{\mathbf{S}_1}$	$\Delta\text{BR}_{H_3 H_2 H_2}^{\mathbf{S}_2}$	$\Delta\text{BR}_{H_3 H_2 H_2}^{\overline{\text{MS}}}$	$\Delta\text{BR}_{H_3 AA}^{\mathbf{S}_1}$	$\Delta\text{BR}_{H_3 AA}^{\mathbf{S}_2}$	$\Delta\text{BR}_{H_3 AA}^{\overline{\text{MS}}}$
I	$\lesssim 32.5\%$ (30%) $\gtrsim 100.0\%$ (43%)	$\lesssim 20.0\%$ (20%) $\gtrsim 100.0\%$ (44%)	$\lesssim 67.5\%$ (10%) $\gtrsim 100.0\%$ (87%)	$\lesssim 10.0\%$ (43%) $\gtrsim 100.0\%$ (22%)	$\lesssim 12.5\%$ (45%) $\gtrsim 100.0\%$ (23%)	$\lesssim 30.0\%$ (20%) $\gtrsim 100.0\%$ (56%)
II	$\lesssim 45.0\%$ (10%) $\gtrsim 100.0\%$ (79%)	$\lesssim 42.5\%$ (10%) $\gtrsim 100.0\%$ (80%)	$\lesssim 90.0\%$ (4%) $\gtrsim 100.0\%$ (95%)	-	-	-
LS	$\lesssim 32.5\%$ (21%) $\gtrsim 100.0\%$ (52%)	$\lesssim 37.5\%$ (21%) $\gtrsim 100.0\%$ (54%)	$\lesssim 92.5\%$ (10%) $\gtrsim 100.0\%$ (89%)	$\lesssim 7.5\%$ (44%) $\gtrsim 100.0\%$ (30%)	$\lesssim 10.0\%$ (44%) $\gtrsim 100.0\%$ (30%)	$\lesssim 32.5\%$ (30%) $\gtrsim 100.0\%$ (47%)
FL	$\lesssim 37.5\%$ (10%) $\gtrsim 100.0\%$ (71%)	$\lesssim 40.0\%$ (10%) $\gtrsim 100.0\%$ (72%)	$\lesssim 90.0\%$ (4%) $\gtrsim 100.0\%$ (95%)	-	-	-

Table 23: Relative size of the EW corrections to the BRs of the non-SM-like N2HDM Higgs boson H_3 into $b\bar{b}$, $t\bar{t}$, $\tau^+\tau^-$, ZA , $W^\pm H^\mp$, ZZ , $H_1 H_1$, $H_1 H_2$, $H_2 H_2$, and AA , for the four N2HDM types I, II, LS and FL (H_2 is SM-like).

- For the other fermionic decay channels as well as for $A \rightarrow ZH_2$, the corrections in the two schemesets \mathbf{S}_1 and \mathbf{S}_2 are small to moderate for all four types of the N2HDM.

Type	$A \rightarrow t\bar{t}$	$A \rightarrow ZH_1$	$A \rightarrow ZH_2$	$A \rightarrow ZH_3$
I	245 233	257 182	127 677	17 786
II	299 959	299 959	155 270	14 149
LS	281 965	282 998	145 633	18 419
FL	292 634	292 634	150 051	14 481

Table 24: Number of parameter points available for the analysis in the individual OS decay channels of A (H_1 is SM-like).

Type	$\Delta\text{BR}_{Abb}^{S_1}$	$\Delta\text{BR}_{Abb}^{S_2}$	$\Delta\text{BR}_{Abb}^{\text{MS}}$	$\Delta\text{BR}_{At\bar{t}}^{S_1}$	$\Delta\text{BR}_{At\bar{t}}^{S_2}$	$\Delta\text{BR}_{At\bar{t}}^{\text{MS}}$
I	$\gtrsim 5.0\%$ (52%)	$\gtrsim 5.0\%$ (96%)	$\lesssim 35.0\%$ (50%)	$\gtrsim 2.5\%$ (94%)	$\lesssim 2.5\%$ (95%)	$\lesssim 32.5\%$ (50%)
	$\gtrsim 12.5\%$ (96%)	$\gtrsim 12.5\%$ (97%)	$\gtrsim 100.0\%$ (29%)	$\gtrsim 7.5\%$ (99%)	$\gtrsim 7.5\%$ (99%)	$\gtrsim 100.0\%$ (27%)
II	$\gtrsim 7.5\%$ (49%)	$\gtrsim 12.5\%$ (43%)	$\gtrsim 90.0\%$ (8%)	$\gtrsim 2.5\%$ (98%)	$\gtrsim 2.5\%$ (98%)	$\gtrsim 12.5\%$ (50%)
	$\gtrsim 17.5\%$ (94%)	$\gtrsim 22.5\%$ (94%)	$\gtrsim 100.0\%$ (90%)	$\gtrsim 5.0\%$ (99%)	$\gtrsim 5.0\%$ (99%)	$\gtrsim 100.0\%$ (12%)
LS	$\gtrsim 5.0\%$ (52%)	$\gtrsim 5.0\%$ (56%)	$\gtrsim 27.5\%$ (50%)	$\gtrsim 2.5\%$ (98%)	$\gtrsim 2.5\%$ (98%)	$\gtrsim 25.0\%$ (50%)
	$\gtrsim 12.5\%$ (97%)	$\gtrsim 10.0\%$ (93%)	$\gtrsim 100.0\%$ (24%)	$\gtrsim 5.0\%$ (99%)	$\gtrsim 5.0\%$ (99%)	$\gtrsim 100.0\%$ (24%)
FL	$\gtrsim 7.5\%$ (56%)	$\gtrsim 12.5\%$ (60%)	$\gtrsim 90.0\%$ (10%)	$\gtrsim 2.5\%$ (98%)	$\gtrsim 2.5\%$ (98%)	$\gtrsim 22.5\%$ (50%)
	$\gtrsim 17.5\%$ (96%)	$\gtrsim 20.0\%$ (94%)	$\gtrsim 100.0\%$ (89%)	$\gtrsim 5.0\%$ (99%)	$\gtrsim 5.0\%$ (99%)	$\gtrsim 100.0\%$ (19%)

Type	$\Delta\text{BR}_{A\tau^+\tau^-}^{S_1}$	$\Delta\text{BR}_{A\tau^+\tau^-}^{S_2}$	$\Delta\text{BR}_{A\tau^+\tau^-}^{\text{MS}}$	$\Delta\text{BR}_{AZH_1}^{S_1}$	$\Delta\text{BR}_{AZH_1}^{S_2}$	$\Delta\text{BR}_{AZH_1}^{\text{MS}}$
I	$\gtrsim 7.5\%$ (49%)	$\gtrsim 7.5\%$ (54%)	$\lesssim 37.5\%$ (50%)	$\lesssim 12.5\%$ (48%)	$\lesssim 12.5\%$ (51%)	$\lesssim 85.0\%$ (25%)
	$\gtrsim 15.0\%$ (98%)	$\gtrsim 12.5\%$ (95%)	$\gtrsim 100.0\%$ (29%)	$\gtrsim 100.0\%$ (10%)	$\gtrsim 100.0\%$ (9%)	$\gtrsim 100.0\%$ (73%)
II	$\gtrsim 7.5\%$ (57%)	$\gtrsim 12.5\%$ (49%)	$\gtrsim 90.0\%$ (8%)	$\gtrsim 17.5\%$ (48%)	$\gtrsim 12.5\%$ (47%)	$\gtrsim 82.5\%$ (16%)
	$\gtrsim 15.0\%$ (97%)	$\gtrsim 20.0\%$ (96%)	$\gtrsim 100.0\%$ (90%)	$\gtrsim 100.0\%$ (14%)	$\gtrsim 100.0\%$ (10%)	$\gtrsim 100.0\%$ (81%)
LS	$\gtrsim 7.5\%$ (55%)	$\gtrsim 12.5\%$ (61%)	$\gtrsim 90.0\%$ (15%)	$\gtrsim 17.5\%$ (47%)	$\gtrsim 15.0\%$ (49%)	$\gtrsim 77.5\%$ (18%)
	$\gtrsim 15.0\%$ (98%)	$\gtrsim 17.5\%$ (95%)	$\gtrsim 100.0\%$ (82%)	$\gtrsim 100.0\%$ (13%)	$\gtrsim 100.0\%$ (11%)	$\gtrsim 100.0\%$ (79%)
FL	$\gtrsim 7.5\%$ (61%)	$\gtrsim 7.5\%$ (66%)	$\gtrsim 25.0\%$ (50%)	$\gtrsim 15.0\%$ (47%)	$\gtrsim 15.0\%$ (52%)	$\gtrsim 90.0\%$ (19%)
	$\gtrsim 12.5\%$ (94%)	$\gtrsim 12.5\%$ (96%)	$\gtrsim 100.0\%$ (19%)	$\gtrsim 100.0\%$ (13%)	$\gtrsim 100.0\%$ (12%)	$\gtrsim 100.0\%$ (80%)

Type	$\Delta\text{BR}_{AZH_2}^{S_1}$	$\Delta\text{BR}_{AZH_2}^{S_2}$	$\Delta\text{BR}_{AZH_2}^{\text{MS}}$	$\Delta\text{BR}_{AZH_3}^{S_1}$	$\Delta\text{BR}_{AZH_3}^{S_2}$	$\Delta\text{BR}_{AZH_3}^{\text{MS}}$
I	$\gtrsim 2.5\%$ (60%)	$\gtrsim 2.5\%$ (70%)	$\lesssim 92.5\%$ (30%)	$\lesssim 20.0\%$ (7%)	$\lesssim 27.5\%$ (11%)	$\lesssim 75.0\%$ (10%)
	$\gtrsim 10.0\%$ (97%)	$\gtrsim 7.5\%$ (95%)	$\gtrsim 100.0\%$ (67%)	$\lesssim 70.0\%$ (42%)	$\lesssim 60.0\%$ (33%)	$\gtrsim 100.0\%$ (53%)
II	$\gtrsim 2.5\%$ (52%)	$\gtrsim 2.5\%$ (55%)	$\lesssim 90.0\%$ (23%)	$\lesssim 22.5\%$ (10%)	$\lesssim 25.0\%$ (11%)	$\lesssim 75.0\%$ (10%)
	$\gtrsim 10.0\%$ (96%)	$\gtrsim 10.0\%$ (97%)	$\gtrsim 100.0\%$ (72%)	$\gtrsim 50.0\%$ (63%)	$\gtrsim 55.0\%$ (77%)	$\gtrsim 100.0\%$ (70%)
LS	$\gtrsim 2.5\%$ (58%)	$\gtrsim 2.5\%$ (69%)	$\lesssim 85.0\%$ (25%)	$\gtrsim 22.5\%$ (9%)	$\gtrsim 25.0\%$ (10%)	$\gtrsim 75.0\%$ (10%)
	$\gtrsim 10.0\%$ (96%)	$\gtrsim 7.5\%$ (96%)	$\gtrsim 100.0\%$ (69%)	$\gtrsim 67.5\%$ (50%)	$\gtrsim 67.5\%$ (50%)	$\gtrsim 100.0\%$ (57%)
FL	$\gtrsim 2.5\%$ (56%)	$\gtrsim 2.5\%$ (67%)	$\lesssim 87.5\%$ (25%)	$\gtrsim 22.5\%$ (12%)	$\gtrsim 22.5\%$ (10%)	$\gtrsim 80.0\%$ (10%)
	$\gtrsim 10.0\%$ (96%)	$\gtrsim 7.5\%$ (96%)	$\gtrsim 100.0\%$ (69%)	$\gtrsim 60.0\%$ (70%)	$\gtrsim 60.0\%$ (69%)	$\gtrsim 100.0\%$ (73%)

Table 25: Relative size of the EW corrections to the BRs of the pseudoscalar A into $b\bar{b}$, $t\bar{t}$, $\tau^+\tau^-$, ZH_1 , ZH_2 , and ZH_3 , for the four N2HDM types I, II, LS and FL (H_1 is SM-like).

- On the other hand, the decay channels $A \rightarrow ZH_1$ and $A \rightarrow ZH_3$ typically feature very large EW corrections for all N2HDM types and for all scheme sets. This is due to suppressed BRs at leading order. For an SM-like H_1 the coupling AZH_1 is very suppressed due to sum rules. The coupling of the H_3 , which is rather singlet-like, is also suppressed but less strongly, so that the resulting decays widths and BRs for $A \rightarrow ZH_1$ become very small and also those for $A \rightarrow ZH_3$, which are less suppressed however. Apart from small coupling constants, also parametrically enhanced counterterm contributions or uncanceled counterterms that blow up in this parameter region can be responsible for the large corrections. The coupling AZH_2 on the other hand is close to its maximum value so that the decay $A \rightarrow ZH_2$ can become significant, resulting in small relative corrections.

Type	$A \rightarrow t\bar{t}$	$A \rightarrow ZH_1$	$A \rightarrow ZH_2$	$A \rightarrow ZH_3$
I	4737	7566	7040	1632
II	2381	2381	2381	342
LS	3122	3303	3203	961
FL	1562	1562	1562	304

Table 26: Number of parameter points available for the analysis in the individual OS decay channels of A (H_2 is SM-like).

Type	$\Delta\text{BR}_{Abb}^{\mathcal{S}_1}$	$\Delta\text{BR}_{Abb}^{\mathcal{S}_2}$	$\Delta\text{BR}_{Abb}^{\overline{\text{MS}}}$	$\Delta\text{BR}_{At\bar{t}}^{\mathcal{S}_1}$	$\Delta\text{BR}_{At\bar{t}}^{\mathcal{S}_2}$	$\Delta\text{BR}_{At\bar{t}}^{\overline{\text{MS}}}$
I	$\gtrsim 5.0\%$ (47%)	$\gtrsim 5.0\%$ (51%)	$\gtrsim 80.0\%$ (50%)	$\gtrsim 2.5\%$ (74%)	$\gtrsim 2.5\%$ (73%)	$\gtrsim 67.5\%$ (50%)
	$\gtrsim 15.0\%$ (90%)	$\gtrsim 15.0\%$ (90%)	$\gtrsim 100.0\%$ (43%)	$\gtrsim 15.0\%$ (91%)	$\gtrsim 12.5\%$ (91%)	$\gtrsim 100.0\%$ (41%)
II	$\gtrsim 10.0\%$ (64%)	$\gtrsim 15.0\%$ (53%)	$\gtrsim 82.5\%$ (5%)	$\gtrsim 2.5\%$ (98%)	$\gtrsim 2.5\%$ (98%)	$\gtrsim 77.5\%$ (50%)
	$\gtrsim 17.5\%$ (92%)	$\gtrsim 22.5\%$ (90%)	$\gtrsim 100.0\%$ (94%)	$\gtrsim 5.0\%$ (99%)	$\gtrsim 5.0\%$ (99%)	$\gtrsim 100.0\%$ (44%)
LS	$\gtrsim 7.5\%$ (75%)	$\gtrsim 5.0\%$ (46%)	$\gtrsim 75.0\%$ (50%)	$\gtrsim 2.5\%$ (90%)	$\gtrsim 2.5\%$ (90%)	$\gtrsim 70.0\%$ (50%)
	$\gtrsim 12.5\%$ (95%)	$\gtrsim 12.5\%$ (96%)	$\gtrsim 100.0\%$ (44%)	$\gtrsim 7.5\%$ (96%)	$\gtrsim 5.0\%$ (95%)	$\gtrsim 100.0\%$ (58%)
FL	$\gtrsim 7.5\%$ (48%)	$\gtrsim 12.5\%$ (51%)	$\gtrsim 92.5\%$ (8%)	$\gtrsim 2.5\%$ (97%)	$\gtrsim 2.5\%$ (97%)	$\gtrsim 77.5\%$ (40%)
	$\gtrsim 17.5\%$ (94%)	$\gtrsim 20.0\%$ (91%)	$\gtrsim 100.0\%$ (91%)	$\gtrsim 7.5\%$ (99%)	$\gtrsim 5.0\%$ (98%)	$\gtrsim 100.0\%$ (55%)
Type	$\Delta\text{BR}_{A\tau^+\tau^-}^{\mathcal{S}_1}$	$\Delta\text{BR}_{A\tau^+\tau^-}^{\mathcal{S}_2}$	$\Delta\text{BR}_{A\tau^+\tau^-}^{\overline{\text{MS}}}$	$\Delta\text{BR}_{AZH_1}^{\mathcal{S}_1}$	$\Delta\text{BR}_{AZH_1}^{\mathcal{S}_2}$	$\Delta\text{BR}_{AZH_1}^{\overline{\text{MS}}}$
I	$\gtrsim 7.5\%$ (43%)	$\gtrsim 7.5\%$ (48%)	$\gtrsim 80.0\%$ (50%)	$\gtrsim 2.5\%$ (73%)	$\gtrsim 2.5\%$ (71%)	$\gtrsim 92.5\%$ (25%)
	$\gtrsim 15.0\%$ (89%)	$\gtrsim 15.0\%$ (90%)	$\gtrsim 100.0\%$ (43%)	$\gtrsim 10.0\%$ (93%)	$\gtrsim 7.5\%$ (91%)	$\gtrsim 100.0\%$ (74%)
II	$\gtrsim 7.5\%$ (45%)	$\gtrsim 15.0\%$ (60%)	$\gtrsim 80.0\%$ (5%)	$\gtrsim 5.0\%$ (56%)	$\gtrsim 5.0\%$ (47%)	$\gtrsim 90.0\%$ (3%)
	$\gtrsim 15.0\%$ (95%)	$\gtrsim 20.0\%$ (93%)	$\gtrsim 100.0\%$ (94%)	$\gtrsim 17.5\%$ (89%)	$\gtrsim 15.0\%$ (91%)	$\gtrsim 100.0\%$ (96%)
LS	$\gtrsim 10.0\%$ (67%)	$\gtrsim 12.5\%$ (61%)	$\gtrsim 87.5\%$ (16%)	$\gtrsim 2.5\%$ (53%)	$\gtrsim 2.5\%$ (47%)	$\gtrsim 87.5\%$ (11%)
	$\gtrsim 15.0\%$ (95%)	$\gtrsim 17.5\%$ (93%)	$\gtrsim 100.0\%$ (82%)	$\gtrsim 15.0\%$ (92%)	$\gtrsim 12.5\%$ (92%)	$\gtrsim 100.0\%$ (88%)
FL	$\gtrsim 7.5\%$ (46%)	$\gtrsim 7.5\%$ (52%)	$\gtrsim 77.5\%$ (40%)	$\gtrsim 2.5\%$ (42%)	$\gtrsim 5.0\%$ (57%)	$\gtrsim 90.0\%$ (3%)
	$\gtrsim 15.0\%$ (97%)	$\gtrsim 15.0\%$ (98%)	$\gtrsim 100.0\%$ (55%)	$\gtrsim 15.0\%$ (89%)	$\gtrsim 15.0\%$ (91%)	$\gtrsim 100.0\%$ (96%)
Type	$\Delta\text{BR}_{AZH_2}^{\mathcal{S}_1}$	$\Delta\text{BR}_{AZH_2}^{\mathcal{S}_2}$	$\Delta\text{BR}_{AZH_2}^{\overline{\text{MS}}}$	$\Delta\text{BR}_{AZH_3}^{\mathcal{S}_1}$	$\Delta\text{BR}_{AZH_3}^{\mathcal{S}_2}$	$\Delta\text{BR}_{AZH_3}^{\overline{\text{MS}}}$
I	$\gtrsim 15.0\%$ (49%)	$\gtrsim 12.5\%$ (47%)	$\gtrsim 85.0\%$ (10%)	$\gtrsim 50.0\%$ (10%)	$\gtrsim 50.0\%$ (10%)	$\gtrsim 82.5\%$ (10%)
	$\gtrsim 100.0\%$ (13%)	$\gtrsim 100.0\%$ (13%)	$\gtrsim 100.0\%$ (89%)	$\gtrsim 95.0\%$ (53%)	$\gtrsim 90.0\%$ (40%)	$\gtrsim 100.0\%$ (49%)
II	$\gtrsim 17.5\%$ (41%)	$\gtrsim 15.0\%$ (50%)	$\gtrsim 90.0\%$ (3%)	$\gtrsim 27.5\%$ (20%)	$\gtrsim 35.0\%$ (30%)	$\gtrsim 92.5\%$ (20%)
	$\gtrsim 100.0\%$ (15%)	$\gtrsim 100.0\%$ (10%)	$\gtrsim 100.0\%$ (96%)	$\gtrsim 55.0\%$ (78%)	$\gtrsim 57.5\%$ (81%)	$\gtrsim 100.0\%$ (65%)
LS	$\gtrsim 20.0\%$ (38%)	$\gtrsim 15.0\%$ (38%)	$\gtrsim 87.5\%$ (7%)	$\gtrsim 35.0\%$ (10%)	$\gtrsim 60.0\%$ (21%)	$\gtrsim 85.0\%$ (10%)
	$\gtrsim 100.0\%$ (20%)	$\gtrsim 100.0\%$ (18%)	$\gtrsim 100.0\%$ (92%)	$\gtrsim 80.0\%$ (39%)	$\gtrsim 90.0\%$ (51%)	$\gtrsim 100.0\%$ (58%)
FL	$\gtrsim 20.0\%$ (49%)	$\gtrsim 15.0\%$ (48%)	$\gtrsim 85.0\%$ (3%)	$\gtrsim 37.5\%$ (32%)	$\gtrsim 37.5\%$ (29%)	$\gtrsim 85.0\%$ (10%)
	$\gtrsim 100.0\%$ (15%)	$\gtrsim 100.0\%$ (13%)	$\gtrsim 100.0\%$ (96%)	$\gtrsim 67.5\%$ (81%)	$\gtrsim 72.5\%$ (88%)	$\gtrsim 100.0\%$ (77%)

Table 27: Relative size of the EW corrections to the BRs of the pseudoscalar A into $b\bar{b}$, $t\bar{t}$, $\tau^+\tau^-$, ZH_1 , ZH_2 , and ZH_3 , for the four N2HDM types I, II, LS and FL (H_2 is SM-like).

4.8.2 H_2 is the SM-like Higgs Boson

In case that H_2 is the SM-like Higgs boson, the additional OS requirement for all pseudoscalar Higgs decays to be OS reduces the amount of available parameter points in some channels as shown in Tab. 26¹⁶. The results for the relative corrections ΔBR of the pseudoscalar decays for the scenarios where H_2 is SM-like are displayed in Tab. 27. We make the following observations:

- The corrections for the fermionic decays and for $A \rightarrow ZH_1$ are typically small to moderate for the scheme sets \mathcal{S}_1 and \mathcal{S}_2 and for all N2HDM types, indicating again both moderate

¹⁶As before, some of the numbers are actually not reduced.

corrections for these channels in these schemes and numerical stability of the two scheme sets. Overall the corrections are slightly larger than in the case where H_1 is SM-like.

- On the other hand, the decay channels $A \rightarrow ZH_2$ and $A \rightarrow ZH_3$ typically feature very large EW corrections for all N2HDM types and for all scheme sets. Again the reason are suppressed tree-level decays and BRs. With H_2 being SM-like, the sum rules lead to suppressed AZH_2 and AZH_3 couplings with the former being more suppressed so that the LO decays for $A \rightarrow ZH_{2,3}$ are very small, with $A \rightarrow ZH_3$ in general being a bit less suppressed. Again, also parametrically enhanced counterterm contributions or large uncanceled counterterms themselves can lead to large EW corrections in this corner of the parameter space. The coupling involving the singlet-like H_1 , AZH_1 , on the other hand is not suppressed, apart from the singlet admixture suppression, so that the LO BR for the decay $A \rightarrow ZH_1$ can be moderate to large, inducing small relative corrections.

5 Conclusions

In this paper, we presented an overview over the size of the EW corrections to the decays of the neutral Higgs bosons of the 2HDM and the N2HDM for different renormalization schemes. Our aim was to quantify the EW corrections that typically appear in beyond-the-SM models with non-minimal Higgs sectors, to identify decays and parameter regions that lead to large corrections and require further treatment, and finally to classify renormalization schemes with respect to the size of EW corrections they produce in order to filter for suitable renormalization schemes that do not induce unnaturally large corrections. For our analysis, we only considered parameter scenarios that fulfill theoretical and experimental constraints and that are obtained from a scan in the parameter ranges of the two considered models. Furthermore, EW corrections were only computed for OS and non-loop induced decays.

Our thus obtained results show that the corrections are in general well-behaving for renormalization schemes that are not process-dependent. For these schemes, the relative corrections to the SM-like Higgs bosons into SM final states are typically small, with the bulk of the corrections being situated below 5%. For some scenarios, they can go up to 7.5%. For the case in the N2HDM where the second-lightest Higgs boson H_2 is SM-like, also decays into a lighter H_1H_1 pair are possible, and the corrections to these decays can become very large for some parameter scenarios. This is due to small tree-level BRs or non-decoupling effects. For the decays of the non-SM-like Higgs bosons, the corrections are in general more important and can become significant. Also here, some parameter scenarios feature very large corrections which can be traced back to suppressed tree-level decays, parametrically enhanced corrections or uncanceled large counterterm contributions. Large counterterms can appear *e.g.* in certain regions of the parameter space with small parameter values (namely small couplings because of sum rule constraints) in the denominator. The large corrections require further investigation and call for an improvement of the fixed-order calculation, such as inclusion of higher-orders or the resummation of the corrections to all orders.

Concerning the renormalization schemes, we found that the process-dependent schemes typically lead to larger corrections that can even become unphysically large with corrections beyond 100% that may also be negative. The $\overline{\text{MS}}$ scheme throughout leads to huge corrections in the decays and hence turns out to be unsuitable.

Acknowledgments

We thank Ansgar Denner and Stefan Dittmaier for fruitful discussion on renormalization issues, we thank Michael Spira for discussions on combining electroweak and QCD corrections. We are grateful to Philipp Basler for providing us with valid data samples. MK and MM acknowledge financial support from the DFG project “Precision Calculations in the Higgs Sector - Paving the Way to the New Physics Landscape” (ID: MU 3138/1-1).

References

- [1] ATLAS, G. Aad *et al.*, Phys. Lett. **B716**, 1 (2012), 1207.7214.
- [2] CMS, S. Chatrchyan *et al.*, Phys. Lett. **B716**, 30 (2012), 1207.7235.
- [3] T. D. Lee, Phys. Rev. **D8**, 1226 (1973).
- [4] G. C. Branco *et al.*, Phys. Rept. **516**, 1 (2012), 1106.0034.
- [5] C.-Y. Chen, M. Freid, and M. Sher, Phys. Rev. **D89**, 075009 (2014), 1312.3949.
- [6] M. Muhlleitner, M. O. P. Sampaio, R. Santos, and J. Wittbrodt, JHEP **03**, 094 (2017), 1612.01309.
- [7] F. Bojarski, G. Chalons, D. Lopez-Val, and T. Robens, JHEP **02**, 147 (2016), 1511.08120.
- [8] M. D. Goodsell, S. Liebler, and F. Staub, Eur. Phys. J. **C77**, 758 (2017), 1703.09237.
- [9] S. Kanemura, M. Kikuchi, K. Mawatari, K. Sakurai, and K. Yagyu, Phys. Lett. **B783**, 140 (2018), 1803.01456.
- [10] S. Kanemura, M. Kikuchi, K. Mawatari, K. Sakurai, and K. Yagyu, Nucl. Phys. **B949**, 114791 (2019), 1906.10070.
- [11] G. Bélanger, V. Bizouard, F. Boudjema, and G. Chalons, Phys. Rev. **D93**, 115031 (2016), 1602.05495.
- [12] G. Bélanger, V. Bizouard, F. Boudjema, and G. Chalons, Phys. Rev. **D96**, 015040 (2017), 1705.02209.
- [13] D. T. Nhung, M. Mühlleitner, J. Streicher, and K. Walz, JHEP **1311**, 181 (2013), 1306.3926.
- [14] M. Mühlleitner, D. T. Nhung, and H. Ziesche, JHEP **12**, 034 (2015), 1506.03321.
- [15] J. Baglio, C. O. Krauss, M. Mühlleitner, and K. Walz, JHEP **10**, 024 (2015), 1505.07125.
- [16] F. Domingo, S. Heinemeyer, S. Paßehr, and G. Weiglein, Eur. Phys. J. **C78**, 942 (2018), 1807.06322.
- [17] J. Baglio, T. N. Dao, and M. Muhlleitner, (2019), 1907.12060.
- [18] F. Domingo and S. Paßehr, Eur. Phys. J. **C79**, 905 (2019), 1907.05468.
- [19] T. N. Dao, L. Fritz, M. Krause, M. Mühlleitner, and S. Patel, (2019), 1911.07197.

- [20] J. Baglio *et al.*, *Comput. Phys. Commun.* **185**, 3372 (2014), 1312.4788.
- [21] M. Krause, R. Lorenz, M. Muhlleitner, R. Santos, and H. Ziesche, *JHEP* **09**, 143 (2016), 1605.04853.
- [22] M. Krause, M. Muhlleitner, R. Santos, and H. Ziesche, *Phys. Rev.* **D95**, 075019 (2017), 1609.04185.
- [23] A. Denner, L. Jenniches, J.-N. Lang, and C. Sturm, *JHEP* **09**, 115 (2016), 1607.07352.
- [24] L. Altenkamp, S. Dittmaier, and H. Rzehak, *JHEP* **09**, 134 (2017), 1704.02645.
- [25] L. Altenkamp, S. Dittmaier, and H. Rzehak, *JHEP* **03**, 110 (2018), 1710.07598.
- [26] M. Krause, D. Lopez-Val, M. Muhlleitner, and R. Santos, *JHEP* **12**, 077 (2017), 1708.01578.
- [27] S. Kanemura, M. Kikuchi, K. Sakurai, and K. Yagyu, *Phys. Rev.* **D96**, 035014 (2017), 1705.05399.
- [28] A. Denner, S. Dittmaier, and J.-N. Lang, *Journal of High Energy Physics* **2018**, 104 (2018).
- [29] A. Denner, S. Dittmaier, and J.-N. Lang, *Renormalization schemes for mixing angles in extended Higgs sectors*, 2019, 1912.02425.
- [30] M. Fox, W. Grimus, and M. Löschner, *Int. J. Mod. Phys.* **A33**, 1850019 (2018), 1705.09589.
- [31] W. Grimus and M. Löschner, *JHEP* **11**, 087 (2018), 1807.00725.
- [32] S. Kanemura, S. Kiyoura, Y. Okada, E. Senaha, and C. P. Yuan, *Phys. Lett.* **B558**, 157 (2003), hep-ph/0211308.
- [33] S. Kanemura, Y. Okada, E. Senaha, and C. P. Yuan, *Phys. Rev.* **D70**, 115002 (2004), hep-ph/0408364.
- [34] M. Krause, M. Muhlleitner, and M. Spira, *Comput. Phys. Commun.* **246** (2020), 1810.00768.
- [35] M. Krause and M. Muhlleitner, *Comput. Phys. Commun.* **247** (2020), 1904.02103.
- [36] A. Djouadi, J. Kalinowski, and M. Spira, *Computer Physics Communications* **108**, 56 (1998).
- [37] A. Djouadi, J. Kalinowski, M. Muehleitner, and M. Spira, *Comput. Phys. Commun.* **238**, 214 (2019), 1801.09506.
- [38] S. Kanemura, M. Kikuchi, K. Sakurai, and K. Yagyu, *Comput. Phys. Commun.* **233**, 134 (2018), 1710.04603.
- [39] S. Kanemura, M. Kikuchi, K. Mawatari, K. Sakurai, and K. Yagyu, (2019), 1910.12769.
- [40] A. Denner, S. Dittmaier, and A. Mück, (2019), 1912.02010.
- [41] M. Muhlleitner, M. O. P. Sampaio, R. Santos, and J. Wittbrodt, *JHEP* **08**, 132 (2017), 1703.07750.

- [42] D. Azevedo, P. Ferreira, M. M. Mühlleitner, R. Santos, and J. Wittbrodt, *Phys. Rev.* **D99**, 055013 (2019), 1808.00755.
- [43] I. Engeln, M. Muhlleitner, and J. Wittbrodt, *Comput. Phys. Commun.* **234**, 256 (2019), 1805.00966.
- [44] P. M. Ferreira, M. Muhlleitner, R. Santos, G. Weiglein, and J. Wittbrodt, *JHEP* **09**, 006 (2019), 1905.10234.
- [45] M. Krause, Master thesis, Karlsruhe Institute of Technology (KIT), Institute for Theoretical Physics (ITP), Karlsruhe, May, 2016.
- [46] M. Krause, PhD thesis, Karlsruhe Institute of Technology (KIT), Institute for Theoretical Physics (ITP), Karlsruhe, July, 2019, DOI: 10.5445/IR/1000096645.
- [47] A. Denner, *Fortsch. Phys.* **41**, 307 (1993), 0709.1075.
- [48] S. Kanemura, M. Kikuchi, and K. Yagyu, *Nucl. Phys.* **B896**, 80 (2015), 1502.07716.
- [49] J. Fleischer and F. Jegerlehner, *Phys. Rev.* **D23**, 2001 (1981).
- [50] D. Binosi, *J. Phys.* **G30**, 1021 (2004), hep-ph/0401182.
- [51] D. Binosi and J. Papavassiliou, *Phys. Rept.* **479**, 1 (2009), 0909.2536.
- [52] J. M. Cornwall and J. Papavassiliou, *Phys. Rev.* **D40**, 3474 (1989).
- [53] J. Papavassiliou, *Phys. Rev.* **D41**, 3179 (1990).
- [54] G. Degrossi and A. Sirlin, *Phys. Rev.* **D46**, 3104 (1992).
- [55] J. Papavassiliou, *Phys. Rev.* **D50**, 5958 (1994), hep-ph/9406258.
- [56] N. J. Watson, *Phys. Lett.* **B349**, 155 (1995), hep-ph/9412319.
- [57] J. Papavassiliou and A. Pilaftsis, *Phys. Rev. Lett.* **75**, 3060 (1995), hep-ph/9506417.
- [58] H. Kluberg-Stern and J. B. Zuber, *Phys. Rev.* **D12**, 482 (1975).
- [59] H. Kluberg-Stern and J. B. Zuber, *Phys. Rev.* **D12**, 3159 (1975).
- [60] D. G. Boulware, *Phys. Rev.* **D23**, 389 (1981).
- [61] L. F. Abbott, *Nucl. Phys.* **B185**, 189 (1981).
- [62] L. F. Abbott, *Acta Phys. Polon.* **B13**, 33 (1982).
- [63] C. F. Hart, *Phys. Rev.* **D28**, 1993 (1983).
- [64] A. Denner, G. Weiglein, and S. Dittmaier, *Nucl. Phys.* **B440**, 95 (1995), hep-ph/9410338.
- [65] R. Lorenz, Master's thesis, Karlsruher Institut für Technologie (KIT), Institut für theoretische Physik (ITP), Karlsruhe, 2015.
- [66] M. Spira, *Prog. Part. Nucl. Phys.* **95**, 98 (2017), 1612.07651.

- [67] R. Harlander, M. Muhlleitner, J. Rathsmann, M. Spira, and O. Stål, (2013), 1312.5571.
- [68] ATLAS, CMS, G. Aad *et al.*, Phys. Rev. Lett. **114**, 191803 (2015), 1503.07589.
- [69] S. Actis, G. Passarino, C. Sturm, and S. Uccirati, Phys. Lett. **B670**, 12 (2008), 0809.1301.
- [70] S. Actis, G. Passarino, C. Sturm, and S. Uccirati, Nucl. Phys. **B811**, 182 (2009), 0809.3667.
- [71] S. Actis, G. Passarino, C. Sturm, and S. Uccirati, Phys. Lett. **B669**, 62 (2008), 0809.1302.
- [72] M. Spira, Fortsch. Phys. **46**, 203 (1998), hep-ph/9705337.
- [73] A. Djouadi, P. Gambino, and B. A. Kniehl, Nucl. Phys. **B523**, 17 (1998), hep-ph/9712330.
- [74] G. Degrossi and F. Maltoni, Nucl. Phys. **B724**, 183 (2005), hep-ph/0504137.
- [75] G. Passarino, C. Sturm, and S. Uccirati, Phys. Lett. **B655**, 298 (2007), 0707.1401.
- [76] A. Bredenstein, A. Denner, S. Dittmaier, and M. M. Weber, Phys. Rev. **D74**, 013004 (2006), hep-ph/0604011.
- [77] A. Bredenstein, A. Denner, S. Dittmaier, and M. M. Weber, JHEP **02**, 080 (2007), hep-ph/0611234.
- [78] S. Boselli, C. M. Carloni Calame, G. Montagna, O. Nicrosini, and F. Piccinini, JHEP **06**, 023 (2015), 1503.07394.
- [79] J. Braathen and S. Kanemura, Phys. Lett. **B796**, 38 (2019), 1903.05417.
- [80] J. Braathen and S. Kanemura, (2019), 1911.11507.